

Measuring extended Higgs sectors as a consistent free couplings model

David López-Val,^{a,*} Tilman Plehn,^a Michael Rauch^b

^a*Institut für Theoretische Physik, Universität Heidelberg, Germany*

^b*Institute for Theoretical Physics, Karlsruhe Institute of Technology (KIT), Germany*

E-mail: lopez@thphys.uni-heidelberg.de, plehn@uni-heidelberg.de,
michael.rauch@kit.edu

ABSTRACT: Extended Higgs sectors appear in many models for physics beyond the Standard Model. Current Higgs measurements at the LHC are starting to significantly constrain them. We study their Higgs coupling patterns at tree level as well as including quantum corrections. Our benchmarks include a dark singlet-doublet extension and several two-doublet setups. Using SFitter we translate the current Higgs coupling measurements for one light Higgs state into their respective parameter spaces. Finally, we show how two-Higgs-doublet models can serve as a consistent ultraviolet completion of an assumed single Standard-Model-like Higgs boson with free couplings.

*Corresponding author.

Contents

1	Introduction	2
2	Extended Higgs sectors	3
2.1	Adding one singlet	4
2.2	Adding one doublet	5
2.3	Adding one doublet and one singlet	9
2.4	Adding one triplet	10
2.5	Degenerate spectrum	10
2.6	Ultraviolet structure	11
3	Coupling patterns	12
3.1	Tree-level couplings	12
3.2	Quantum effects: Higgs and gauge sector	16
3.3	Quantum effects: fermions	20
4	LHC data	22
4.1	Free Standard Model couplings	22
4.2	Dark singlet	24
4.3	Hierarchical 2HDM	24
4.4	General 2HDM	26
4.5	Yukawa-aligned 2HDM	29
4.6	Degenerate spectrum	31
5	Summary	35
A	Parameterizations	37
A.1	Additional singlet	37
A.2	Additional doublet	37
B	Hierarchical 2HDM	39

1 Introduction

In the Standard Model of particle physics electroweak symmetry breaking is described by the Higgs mechanism [1]. It assumes the existence of a CP-even scalar field whose non-vanishing expectation value breaks the $SU(2)_L \times U(1)_Y$ gauge group down to the electromagnetic $U(1)$ gauge group. The Standard Model predicts all properties of the Higgs boson, except for its mass [2]. Recently, a Higgs boson with mass around 126 GeV has been discovered by ATLAS [3] and CMS [4]. Its decays to $\gamma\gamma$, ZZ^* , WW^* , and $\tau\tau$ [5] have been established and the observed event numbers in each of these final states agree with the Standard Model predictions [6–10].

While some alternative theoretical descriptions of such a scalar, linked to electroweak symmetry breaking or not, predict significant deviations from the Standard Model operator structure and coupling strengths, many perturbative extensions of the Standard Model also predict a light Higgs boson with very similar properties as in the Standard Model. Reasons for this tendency are general decoupling patterns as well as experimental constraints in the electroweak precision and flavor sectors. This defines two ways to look at extended Higgs sectors including a light Higgs state with a mass of 126 GeV: on the one hand we might interpret the recently discovered Higgs boson as just one of several Higgs states. On the other hand, we can use extended Higgs sectors as possible ultraviolet completions of a light Higgs boson with couplings deviating from the Standard Model predictions.

Higgs couplings are defined as prefactors of the respective Lagrangian terms coupling the Higgs field to other particles. To leading order in perturbation theory this is obvious, while including higher orders we need to add a proper definition of the counter terms. Defining a set of couplings to be compared to experimental measurements always relies on a hypothetical Lagrangian. Given the current experimental knowledge we start from the renormalizable Lagrangian of the Standard Model and measure each coupling to a Standard Model particle x [6, 11, 12],

$$g_{xxH} \equiv g_x = (1 + \Delta_x) g_x^{\text{SM}}. \quad (1.1)$$

The loop-induced Higgs coupling to photons then reads

$$g_{\gamma\gamma H} \equiv g_\gamma = (1 + \Delta_\gamma^{\text{SM}} + \Delta_\gamma) g_\gamma^{\text{SM}}. \quad (1.2)$$

Any modification of the underlying tree-level couplings to Standard Model particles inside the loop induces $\Delta_\gamma^{\text{SM}}$. The remaining Δ_γ characterizes genuine non-Standard Model contributions. The total coupling shift, for example appearing in the measured signal strength, reads $\Delta_\gamma^{\text{tot}} \equiv \Delta_\gamma^{\text{SM}} + \Delta_\gamma$. The same setup applies to the loop-induced Higgs coupling to gluons. Equivalent parameters $\kappa_x \equiv 1 + \Delta_x$ are used in Ref. [13].

The one problem with this model independent approach is that such a theory with free Higgs couplings has poor ultraviolet properties. It may violate unitarity just above LHC energy scales and is not renormalizable. This means that once LHC observables reach a precision where electroweak corrections become relevant the approach of Eq.(1.1) is not well defined [14]. We need to also define an ultraviolet completion which at low energies reduces to a single light Higgs boson and which is renormalizable. This limitation becomes particularly important when one quantifies the potential of a linear collider for probing new physics effects in the Higgs sector [15].

A prime candidate for such a theory is a perturbative extended Higgs sector, which includes additional singlet, doublet, or triplet fields. It clearly allows for precision calculations in electroweak perturbation theory. One of the key questions which we will answer in this paper is if such models give us enough freedom for a full set of independent Higgs couplings differing from the Standard Model.

In addition to modified Higgs couplings to all the Standard Model particles, extended Higgs sectors provide candidate particles that may induce invisible Higgs decays.

Extended Higgs sectors have attractive features. Adding for instance a singlet to the minimal Higgs sector of the Standard Model is one of the few ways to link the Standard Model to a new physics sector in a renormalizable way. Such a Higgs portal makes distinctive predictions for the LHC, including Higgs decays to invisible states [16, 17].

Adding a second Higgs doublet to the Standard Model is a natural extension of the very minimal Higgs sector of the Standard Model, where one is no longer forced to rely on Φ and Φ^\dagger to give masses to up-type and down-type fermions. For example in supersymmetric models the appearance of the conjugate Higgs field is not allowed, so we need two Higgs doublets to give mass to up-type and down-type fermions. With two vacuum expectation values this setup can lead to key signatures at the LHC as well as to new effects in flavor physics.

The Glashow–Weinberg–Salam group can be embedded in different grand unified theories, like the Pati–Salam group [18], E_6 [19], $SO(10)$ [20], or the trinification group [21, 22]. The subgroups relevant for the Higgs sector can be $SU(3)_L \times SU(3)_R$ or $SU(2)_L \times SU(2)_R$, which means they include two or more doublet representations of scalar fields. One of them can have couplings to gauge bosons and fermions proportional to the Standard Model couplings while the other misses Yukawa couplings completely [23]. The LHC could then see two Higgs fields with suppressed coupling patterns. It can even occur that the Higgs resonance is a nearly degenerate state composed of two orthogonal states of this type [22, 24].

As we will see, each of these extensions predicts distinct features in the set of light Higgs couplings observed at the LHC. This allows us to significantly constrain the available parameter space in the more constrained extended Higgs sectors. Obviously, the most general extended models essentially allow for a free variation of all measured couplings of the lightest discovered Higgs state.

This paper consists of two main parts. First, we introduce different extensions of the Standard Model Higgs sector and study their impact on the light Higgs couplings to leading order and to next-to-leading order. The latter includes a multitude of new qualitative and quantitative results. In the second part we define a set of benchmark models for extended Higgs sectors and determine their parameters from current ATLAS and CMS results. This includes an update of the SFITTER [6] coupling measurement of the Standard Model Higgs boson, including the Moriond/Aspen results from the 2012 run. In both parts we will comment on how suitable extended Higgs sectors are as renormalizable, ultraviolet-consistent extensions of a Standard Model Higgs Lagrangian with free couplings. Many details about the benchmark parameterizations we give in the appendices.

2 Extended Higgs sectors

A brief overview of extended Higgs sector models in this section serves two purposes: first, we determine which of these models give us enough flexibility to be considered as an ultraviolet completion of a model with a single light Higgs boson and variable couplings differing from the Standard Model at the 20% – 50% level. Second, we need to define benchmark models which we can compare to current ATLAS and CMS data.

Deviations in the Higgs couplings in a consistent framework can occur in two ways: first, new particles with direct or indirect couplings to the Higgs can contribute to the loop-induced hgg and $h\gamma\gamma$ vertices. Second, new scalar multiplets can give rise to additional neutral and charged states, in turn leading to mixing effects [25]. Beyond leading order, the two avenues are no longer separated; the

new scalar degrees of freedom will contribute to quantum effects and may exhibit a non-decoupling behavior discussed in Section 3.2.

In the mixing approach we consider models with complex $SU(2)$ doublets Φ_i and singlets S_j ,

$$\Phi_i = \begin{pmatrix} h_i^+ \\ \frac{v_i + h_i^0 + ia_i^0}{\sqrt{2}} \end{pmatrix} \quad S_j = \frac{v_j + s_j}{\sqrt{2}}. \quad (2.1)$$

The relation between the fields appearing in the Lagrangian and the physical mass eigenstates is spelled out in the appendix. The weak doublets couple to the gauge bosons via the $SU(2)_L \times U(1)_Y$ covariant derivatives. Fermion masses can be related to the Yukawa couplings through a VEV of the respective Higgs field, $m_f = y_f v_f / \sqrt{2}$. The extension to more general flavor patterns is straightforward.

Any extension of the electroweak sector of the Standard Model is severely constrained by electroweak precision data. The ρ or T parameter constraints point to a global custodial symmetry protecting tree-level relations. For example, a number of Higgs fields with weak isospins T_i , hypercharge Y_i , and vacuum expectation values v_i gives [26]

$$\frac{m_W^2}{m_Z^2 c_w^2} = \frac{\sum_i \left[T_i(T_i + 1) - \frac{1}{4} Y_i^2 \right] v_i^2}{\frac{1}{2} \sum_i Y_i^2 v_i^2} \stackrel{\text{doublets}}{=} \frac{\sum_i \left[\frac{3}{4} - \frac{1}{4} \right] v_i^2}{\frac{1}{2} \sum_i v_i^2} = 1. \quad (2.2)$$

Any number of singlets and doublets respects custodial symmetry at tree level; loop-induced contributions naturally remain small. In contrast, higher isospin representations violate custodial symmetry at tree level. This means that phenomenologically viable extensions beyond singlets and doublets must either [27]

1. obey stringent tree-level constraints, like type-II see-saw models with one additional Higgs triplet. Its VEV is strongly constrained, as described in Section 2.4,
2. carefully align different Higgs fields, like in the Georgi-Machacek model [28],
3. or combine exotic representations, like a Higgs doublet combined with a septet [29], such that custodial symmetry is accidentally preserved.

None of these options is particularly appealing if we are looking for a simple extension of the Standard Model Higgs sector. Thus, we limit ourselves to singlet and doublet extensions whenever possible.

2.1 Adding one singlet

An additional real $SU(2)_L$ singlet field S_i is the simplest extension of the minimal Higgs sector. For example, a Higgs unparticle or a Randall–Sundrum radion can mix with the Standard Model Higgs boson, leading to a universal depletion of all Higgs couplings. All branching ratios of the lightest Higgs mass eigenstate stay the same as in the Standard Model while all production rates are reduced by the universal mixing factor. If the new scalar is light, $m_S < m_H/2 \simeq 63$ GeV, and not coupled to any other Standard Model particle, it will lead to invisible Higgs decays [17]. Implications of LHC data on singlet extensions of the Standard Model have been analyzed thoroughly in Ref. [30]. In our search for a consistent model of a light Higgs with variable couplings an additional singlet will be a first step towards a more general layout.

The scalar potential of the minimal doublet-plus-singlet model can be written as [31, 32]

$$V(\Phi, S) = \mu_1^2 (\Phi^\dagger \Phi) + \lambda_1 |\Phi^\dagger \Phi|^2 + \mu_2^2 S^2 + \kappa S^3 + \lambda_2 S^4 + \lambda_3 |\Phi^\dagger \Phi| S^2, \quad (2.3)$$

where μ_1^2 and λ_1 form the Standard Model potential. Doublet-singlet mixing is induced by λ_3 and gives rise to a light and a heavy Higgs boson mass-eigenstate, h^0 and H^0 , and a mixing angle θ defined in Appendix A. Strong mixing with one singlet or equivalently mixing with a large number of additional fields translates into a too large depletion factor, inconsistent with the experimental limit $\cos \theta \lesssim 0.7$ [6, 9]. Additional theoretical (electroweak precision, perturbativity and unitarity) and experimental constraints (mainly direct exclusion) turn out to be special cases of the doublet extension and will be discussed in Section 2.2.

An interesting setup avoiding a second VEV introduces a global Z_2 parity under which S is odd. This predicts a SM-like Higgs sector alongside with a dark matter candidate whose decays are precluded by this Z_2 parity [16]. Following Eq.(2.3) this WIMP singlet model is defined in terms of the singlet mass term μ_2^2 , its portal coupling to the doublet λ_3 , and the singlet self-interactions λ_2 .

Interactions of the singlet with Standard Model fields are mediated by Higgs exchange. This way the quartic coupling λ_3 determines both WIMP-nucleon scattering and WIMP-WIMP annihilation and can be constrained experimentally. Depending on its mass the singlet annihilates into Standard Model fermions, gauge bosons and Higgs bosons via an s -channel Higgs propagator. For $m_S \lesssim 1$ TeV the present cosmic abundance constrains the quartic coupling to $\lambda_3 = \mathcal{O}(0.01 - 1)$, irrespective of the singlet self-interactions. WIMP-nucleon scattering is sensitive to the singlet mass and the singlet-doublet mixing. Values of λ_3 giving the correct relic density yield direct detection rates around $\sigma_{\text{NS}} = \mathcal{O}(10^{-43}) \text{ cm}^2$, within reach of ongoing experiments. Last but not least, indirect searches in gamma rays test the model through singlet annihilation into photon pairs via an s -channel Higgs subsequently decaying into $\gamma\gamma$.

A light singlet with $m_S < m_H/2$ contributes to an invisible Higgs width [33]. While first direct searches for invisible decays have recently been performed in the Higgs-strahlung processes at the LHC [34], model dependent indirect limits can also be derived and yield stronger constraints [35]. They rule out wide domains in the $\lambda_3 - \mu_2$ plane corresponding to light $\mathcal{O}(10)$ GeV WIMPs which otherwise agree with astrophysical observations. A global fit including the WMAP results [36], XENON-100 direct detection data [37], the FERMI-LAT di-photon spectrum [38], and LHC constraints singles out a best-fit point. It lies close to the resonance $m_S = 63$ GeV, and is correlated with a small quartic coupling $\lambda_3 = \mathcal{O}(10^{-2})$ to reconcile a large annihilation rate with the observed relic density [39]. A comprehensive update has been made available very recently [40].

The real singlet model can be extended to a complex singlet, with largely unchanged phenomenological patterns. If the complex singlet remains inert we obtain a two-component dark matter model. When the scalar potential is expanded by a soft $U(1)$ -breaking term the imaginary part of S gives rise to a massive pseudo-Goldstone boson. In the presence of additional vector-like matter, models with a complex singlet are capable to describe the current LHC search results [41]. Interesting implications have also been highlighted in models with multiple singlet fields [42].

2.2 Adding one doublet

The two Higgs doublet model (2HDM) [43] adds a second $SU(2)$ doublet with weak hypercharge one. It provides a low-energy description for a broad ensemble of TeV-scale models, such as the Minimal Supersymmetric Standard Model (MSSM) [44], GUTs [18–22], composite Higgs models [45], and little Higgs models [46]. It allows for CP violation as well as a complex vacuum structure [47] and addresses

problems like neutrino mass generation [48], electroweak baryogenesis [49], or dark matter [50]. Because the 2HDM includes two fields which can couple to fermions and gauge bosons independently, it is a candidate for an ultraviolet completion of a light Higgs model with variable couplings. The main question is how strongly such variable couplings are correlated by construction or through experimental constraints.

Numerous studies have explored signatures of the 2HDM at the LHC [51] and attempted to interpret the LHC Higgs discovery in this framework. Owing to the SM-like Higgs observation any 2HDM explanation tends to translate into parameter constraints. Early attempts ascribed the new resonance to either the lighter [52] or the heavier [53] neutral CP-even states, as well as to their CP-odd companion [54]. Updates cover all major requirements for flavor structures: natural flavor conservation [55–57], Yukawa alignment [58, 59], and minimal flavor violation [60].

The 2HDM Higgs sector contains four complex scalar fields defined in Eq.(2.1). The most general gauge and CP-invariant renormalizable potential reads

$$\begin{aligned} V(\Phi_1, \Phi_2) = & m_{11}^2 \Phi_1^\dagger \Phi_1 + m_{22}^2 \Phi_2^\dagger \Phi_2 - \left[m_{12}^2 \Phi_1^\dagger \Phi_2 + \text{h.c.} \right] \\ & + \frac{\lambda_1}{2} (\Phi_1^\dagger \Phi_1)^2 + \frac{\lambda_2}{2} (\Phi_2^\dagger \Phi_2)^2 + \lambda_3 (\Phi_1^\dagger \Phi_1) (\Phi_2^\dagger \Phi_2) + \lambda_4 |\Phi_1^\dagger \Phi_2|^2 \\ & + \left[\frac{\lambda_5}{2} (\Phi_1^\dagger \Phi_2)^2 + \lambda_6 (\Phi_1^\dagger \Phi_1) (\Phi_1^\dagger \Phi_2) + \lambda_7 (\Phi_2^\dagger \Phi_2) (\Phi_1^\dagger \Phi_2) + \text{h.c.} \right], \end{aligned} \quad (2.4)$$

where the mass terms m_{ij}^2 and the dimensionless self-couplings λ_i are real parameters and $v_j = \sqrt{2} \langle \Phi_j^0 \rangle$. Their ratio we denote as $\tan \beta = v_2/v_1$. Electroweak symmetry breaking requires $v_1^2 + v_2^2 = (246 \text{ GeV})^2$. The physical spectrum entails five mass-eigenstates: two neutral CP-even scalars h^0, H^0 , one neutral CP-odd scalar A^0 , and a set of charged scalars H^\pm . As described in Appendix A the two mass eigenstates H^0 and h^0 arise from a rotation by the angle α . Throughout this study we interpret the observed Higgs scalar as the lighter h^0 state. At tree level, custodial symmetry ensures that the couplings to the weak gauge bosons $V = W, Z$ scale with the same factor

$$g_V = \sin(\beta - \alpha) g_V^{\text{SM}}. \quad (2.5)$$

The pattern of the Yukawa couplings depends on the 2HDM setup. In general, two of them can be modified independently in terms of α and β , correlated with g_{VVh^0} . Quantum corrections may change this picture and lead to non-universal coupling shifts $\Delta g_Z \neq \Delta g_W$ or coupling enhancements $\Delta_V > 0$. We will discuss them in Secs. 3.2 and 3.3.

A fully flexible spectrum described by Eq.(2.4) allows for different patterns:

1. compressed masses $m_{h^0} \simeq m_{H^0}$,
2. twisted masses $m_{A^0} < m_{h^0, H^0}$,
3. single mass hierarchy $m_{h^0} \ll m_{H^0, A^0, H^\pm}$,
4. or multiple mass hierarchies $m_{h^0} \ll m_{H^0} \ll m_{A^0, H^\pm}$.

The Higgs sector of the MSSM is one example of a constrained 2HDM Higgs sector descending from a more general UV completion [44]. Another example are dark portal or inert doublet models [48, 61, 62]. They follow when we enforce a Z_2 symmetry in Eq.(2.4) and require one of the Higgs doublets to transform as $\Phi_1 \rightarrow -\Phi_1$, such that $\langle \Phi_1 \rangle = 0$. This doublet does not participate in electroweak

symmetry breaking, and therefore it does not interact with weak gauge bosons or fermions. Because the SM-like Higgs field is exclusively linked to Φ_2 , without any admixture of Φ_1 , the resulting Higgs couplings do not depart from the Standard Model, except for charged Higgs contributions to g_γ .

An extensive set of bounds restricts the phenomenologically viable regions of the 2HDM parameter space [7, 55, 57, 63, 64]. Accidental tree-level symmetries in the Higgs sector play a big role facing these constraints. We need a novel class of possible symmetries which relate the different potential terms. They can be classified as Higgs family (HF) symmetries, linking Φ_1 and Φ_2 via a unitary transformation, and generalized CP (GCP) transformations [65], linking Φ_1 and Φ_2^* via a unitary transformation [43]. No matter what combination of HF and/or GCP symmetries are enforced one always ends up with one out of six distinct classes of Higgs potentials described in Refs. [43, 66]. We will focus on the flavor sector, while keeping the general potential of Eq.(2.4). Three types of symmetries allow us to write down 2HDM potentials in agreement with experimental constraints:

Custodial symmetry: an accidental global $SU(2)_{L+R}$ symmetry in the Standard Model protects the relation $m_W = m_Z c_w$. It is broken by different up-type and down-type fermion masses and by virtual Higgs exchange at one loop [67]. Correspondingly, mass terms involving the additional 2HDM fields are strongly constrained. This effectively reduces the number of free parameters and leads to a larger predictive power. Barring fine-tuned mixing angle choices we distinguish two scenarios for a phenomenologically viable 2HDM: a compressed mass spectrum with only moderately split Higgs masses or a light SM-like Higgs with mass-degenerate heavy companions H^0, A^0, H^\pm . In the latter all Higgs states fall into the singlet and triplet representations of $SU(2)_{L+R}$

$$\Phi_1 \supset \begin{pmatrix} H^+ \\ A^0 \\ H^- \end{pmatrix} \oplus H^0 \quad \text{or} \quad \Phi_1 \supset \begin{pmatrix} H^+ \\ H^0 \\ H^- \end{pmatrix} \oplus A^0 \quad \Phi_2 \supset \begin{pmatrix} G^+ \\ G^0 \\ G^- \end{pmatrix} \oplus \frac{v + h^0}{\sqrt{2}}. \quad (2.6)$$

This structure nicely illustrates the mechanism that protects the custodial symmetry: while Φ_2 accommodates a light, SM-like Higgs boson all other mass eigenstates belong to Φ_1 . We can integrate them out simultaneously and retrieve an effective field theory description in terms of Φ_2 only.

With $m_H = 126$ GeV electroweak precision data [68, 69] requires $S = 0.03 \pm 0.01$, $T = 0.05 \pm 0.12$, and $U = 0.03 \pm 0.10$ [70, 71]. The genuine 2HDM contributions to the dominant constraint read

$$T = -\frac{\sqrt{2}G_F}{16\pi^2\alpha_{em}} \left[m_{H^\pm}^2 \left(1 - \frac{m_{A^0}^2}{m_{H^\pm}^2 - m_{A^0}^2} \log \frac{m_{H^\pm}^2}{m_{A^0}^2} \right) + \cos^2(\beta - \alpha) m_{h^0}^2 \left(\frac{m_{A^0}^2}{m_{A^0}^2 - m_{h^0}^2} \log \frac{m_{A^0}^2}{m_{h^0}^2} - \frac{m_{H^\pm}^2}{m_{H^\pm}^2 - m_{h^0}^2} \log \frac{m_{H^\pm}^2}{m_{h^0}^2} \right) + \sin^2(\beta - \alpha) m_{H^0}^2 \left(\frac{m_{A^0}^2}{m_{A^0}^2 - m_{H^0}^2} \log \frac{m_{A^0}^2}{m_{H^0}^2} - \frac{m_{H^\pm}^2}{m_{H^\pm}^2 - m_{H^0}^2} \log \frac{m_{H^\pm}^2}{m_{H^0}^2} \right) \right], \quad (2.7)$$

For degenerate masses $m_{H^0} \simeq m_{A^0} \simeq m_{H^\pm}$ we find $S = T = 0$. In contrast, in the decoupling limit $\sin(\beta - \alpha) \simeq 1$ with $m_{H^0} \simeq m_{A^0}$, the corrections read

$$S \simeq -\frac{1}{12\pi} \log \frac{m_{H^\pm}^2}{m_{A^0}^2} \quad T \simeq \frac{\sqrt{2}G_F}{16\pi^2\alpha_{ew}} (m_{H^\pm}^2 - m_{A^0}^2). \quad (2.8)$$

Moderate mass splittings are hence directly related to custodial symmetry. This is a key ingredient to understanding the deviations in the W and Z interactions to the light Higgs boson.

Flavor symmetry: the symmetry group $U(3)_{Q_L} \times U(3)_{U_R} \times U(3)_{D_R}$ acting on three different types of quarks leaves the CKM matrix invariant and guarantees the absence of tree-level FCNCs through GIM suppression. It is broken by large Yukawas which give rise to loop-induced FCNC interactions. This picture does not hold in the presence of a second Higgs doublet. Traditionally, natural flavor conservation imposes a global, flavor-blind, Z_2 discrete symmetry $\Phi_{1,2} \rightarrow \mp \Phi_{1,2}$ and demands any fermion family to couple to only one Higgs doublet. It satisfies the Glashow-Weinberg theorem [72] and defines the canonical 2HDM setups:

- type-I, where all fermions couple to just one Higgs doublet, namely Φ_2 ;
- type-II, where up-type (down-type) fermions couple exclusively to Φ_2 (Φ_1);
- lepton-specific, with a type-I quark sector and a type-II lepton sector;
- flipped, with a type-II quark sector and a type-I lepton sector.

The formulas for all these couplings are provided in Appendix A. The discrete Z_2 symmetry $\Phi_{1,2} \rightarrow \mp \Phi_{1,2}$ can be understood as a single-parameter HF symmetry. It forbids the mass term m_{12}^2 and the self interactions $\lambda_{6,7}$. If extended to the Yukawa sector it automatically removes all sources of tree-level FCNC interactions. The continuous $U(1)$ transformation is $\Phi_{1,2} \rightarrow \Phi_{1,2} \exp(\mp i\theta)$ with a real phase θ . It is a genuine Peccei-Quinn (PQ) symmetry. The field combination $h_j^0 + ia_j^0$ has a non-vanishing PQ charge, explaining why the mass splitting between the mass eigenstates H^0, A^0 is controlled by the size of the PQ-breaking terms m_{12}^2 and $\lambda_{6,7}$.

Yukawa structures featuring natural flavor conservation constitute one case of a broader class of models, in which tree-level FCNCs are largely suppressed, albeit not fully absent. This is ensured via minimal flavor violation [73, 74]. This mechanism is based on promoting the Yukawa couplings to auxiliary fields or spurions, and imposes a link between the (3×3) Yukawa matrices y_1, y_2 which couple to the corresponding Higgs doublets. All flavor transitions are controlled by CKM matrix elements, so that they become naturally small.

One implementation of minimal flavor violation are aligned models [75]. There, the fermions couple to both Higgs doublets with *aligned* Yukawa matrices, *i.e.* linked to one another by linear shifts ϵ_f ,

$$y_{u1} = \epsilon_u y_{u2} \quad y_{d2} = \epsilon_d y_{d1} \quad y_{l2} = \epsilon_\tau y_{l1} , \quad (2.9)$$

with $y_{f,i} = \sqrt{2}m_{f,i}/v_i$. This way the fermion masses and Yukawa matrices diagonalize simultaneously. The construction of the aligned 2HDM relies on basis invariance properties [76] to absorb the ϵ_f into a field re-definition and rotate one of them away (usually ϵ_u). In practice, we parameterize the dependence on the different doublets by introducing angles $\gamma_{b,\tau}$, by which we may write the bottom and tau Yukawas

$$\frac{m_{b,\tau}}{v} = y_{b,\tau} \langle \Phi_1 \rangle \cos \gamma_{b,\tau} + y_{b,\tau} \langle \Phi_2 \rangle \sin \gamma_{b,\tau} \quad \Rightarrow \quad y_{b,\tau} \cos(\beta - \gamma_{b,\tau}) = \frac{\sqrt{2}m_{b,\tau}}{v} . \quad (2.10)$$

The aligned setup includes natural flavor conservation, but covers all regimes with absent tree-level FCNC interactions.

CP invariance: while hermiticity of the Higgs potential Eq.(2.4) requires m_{11}^2, m_{22}^2 and $\lambda_{1,2,3,4}$ to be real, the parameters $m_{12}^2, \lambda_{5,6,7}$ may be complex. In that case not only the CP-even but also the CP-odd neutral Higgs fields will mix and define physical fields which are no longer CP-eigenstates. New CP-violating phases can also appear in the Higgs Yukawa matrices. We will omit CP-violating terms in the Higgs potential.

Additional experimental constraints from B -mesons and taus [64, 77] we account for assuming no cancellation of 2HDM effects and for example other supersymmetric contributions. The new heavy scalars may also contribute to the muon anomalous magnetic moment $(g-2)_\mu$ [78], even though their effect gives rise to mass constraints which are milder than those from custodial symmetry. Last but not least, any Higgs mass spectrum ought to satisfy all current limits from direct searches at LEP, Tevatron and LHC [79]. Notice that systematic searches for heavy Higgs bosons at the LHC have been so far restricted mainly to the MSSM, *e.g.* ruling out $\tan\beta \gtrsim 7.58$ for $m_{A^0} \simeq 300$ GeV. We implement all the above mentioned constraints using 2HDMC [80], HIGGSBOUNDS [81] and SUPERISO [82] together with a number of in-house routines.

2.3 Adding one doublet and one singlet

Adding singlets to the 2HDM setup hardly changes its main features. Following Eq.(2.2) such models respect custodial symmetry at tree level, which means that the Higgs couplings to the W and Z bosons are linked. In the light of an ultraviolet completion of a model with variable Higgs couplings the main advantage of the additional singlet is a consistent modelling of invisible Higgs decays.

Usually, the main interest in these scenarios comes from a less strict upper limit on the lightest Higgs mass in its supersymmetric version, the NMSSM [83]. The main virtue of the NMSSM is that it explains the mass term $\mu\Phi_u\Phi_d$ of the order of the soft SUSY-breaking scale M_{SUSY} by generating it through a singlet VEV and adding

$$W_{\text{NMSSM}} \supset \lambda S \hat{H}_u \hat{H}_d + \frac{k}{3} \hat{S}^3 \quad (2.11)$$

to the Higgs superpotential. The particle spectrum now includes three neutral CP-even states, all linear combinations of \hat{H}_u, \hat{H}_d and \hat{S} , and two neutral CP-odd scalars. The higgsinos mix with the usual neutralinos. A 126 GeV SM-like Higgs boson with slightly enhanced g_γ can be realized for large λ and small $\tan\beta$ values. In these instances, the two lightest mass eigenstates $h_{1,2}^0$ typically have nearby masses and very weak doublet mixing.

If, in the spirit of the NMSSM we assume that the additional singlet develops a VEV, we find a light Higgs state $h^0 = \cos\theta (\cos\alpha h_2^0 - \sin\alpha h_1^0) + \sin\theta s$ with couplings

$$\frac{g_{VVh^0}}{g_V^{\text{SM}}} = \cos\theta \sin(\beta - \alpha) \quad \frac{g_{ffh^0}}{g_f^{\text{SM}}} = \cos\theta \frac{\cos\alpha}{\sin\beta}, \quad (2.12)$$

where we assume a type-I 2HDM structure. The 2HDM interaction pattern is therefore simply rescaled.

Given that an additional singlet with a VEV does not structurally enhance our ability to describe a light Higgs state with free couplings we can focus on an additional inert Higgs singlet as a source of invisible Higgs decays. The mixing parameter η is defined by

$$\mathcal{L} \supset \eta \left(\Phi_1^\dagger \Phi_1 + \Phi_2^\dagger \Phi_2 \right) S^2. \quad (2.13)$$

The corresponding invisible width for the SM-like Higgs boson $\Gamma_{h^0}^{\text{inv}}$ reads

$$\eta^2 = \frac{32\pi m_{h^0}}{v^2 \sin^2(\beta - \alpha)} \left(1 - \frac{4m_s^2}{m_{h^0}^2} \right)^{-1/2} \Gamma_{h^0}^{\text{inv}}. \quad (2.14)$$

2.4 Adding one triplet

Adding a triplet to the Standard Model Higgs sector allows to separately vary the light Higgs couplings to the W and Z bosons. The model has enough degrees of freedom to accommodate a wide range of independent variations in all Higgs couplings. The phenomenological motivations for Higgs triplet models are based, among others, on left-right symmetries [84] or type-II see-saw models for neutrino mass generation. Interesting implications have been highlighted in the context of non-minimal SUSY extensions [85]. A study of the model at the quantum level is available in Ref. [86].

The Higgs sector consists of an isospin doublet Φ with hypercharge $+1$ and an $SU(2)_L$ triplet $\Delta = (\vec{T} \cdot \vec{\tau})$, also with hypercharge $+1$. In terms of the doublet and triplet VEVs the tree-level gauge boson masses are

$$m_W^2 = \frac{g^2}{4} (v_\Phi^2 + 2v_\Delta^2) \qquad m_Z^2 = \frac{g^2}{4c_w^2} (v_\Phi^2 + 4v_\Delta^2) , \quad (2.15)$$

manifesting the breaking of the custodial symmetry already at the tree-level. The physical spectrum includes two CP-even scalars h^0, H^0 , one CP-odd scalar A^0 , one singly charged scalar H^\pm , and one doubly-charged state $H^{\pm\pm}$. Barring marginal corners of the parameter space, one of the CP-even scalars will behave like a Standard Model Higgs boson. All remaining states can be described by an almost-decoupled $SU(2)$ triplet – minimizing the tree-level breaking of the custodial symmetry.

As alluded to above, adding a triplet is the obvious choice when we look for an extended Higgs sector with maximum flexibility in the couplings of the lightest state. However, because of the phenomenological problems of these models we will stick to additional singlets and doublets and enhance their flexibility by fully exploiting not only tree-level but also loop effects.

2.5 Degenerate spectrum

In extensions of the Standard Model often two or more representations of scalar fields are necessary. It can happen that fields in one representation have couplings to gauge bosons and fermions similar to the Standard Model couplings, while fields in the other representation only couple to gauge bosons. Such models can arise in generalizations of the Glashow–Weinberg–Salam group to left-right symmetric groups like E_6 , its subgroup $SU(3)_L \times SU(3)_R \times SU(3)_C$ [22, 23, 87], or even smaller subgroups.

In these cases the first representation can account for all fermion couplings. Nonetheless, the corresponding fields are not sufficient to provide the correct low-scale chirality properties of the Standard Model. For instance, when the left-right symmetry is not broken by the VEVs one needs fields of a second representation performing this task. Such fields will then not directly couple to fermions, but only via the gauge vector bosons.

Interestingly, in such models, the Higgs candidate found at the LHC might no longer be a single resonance. Instead, it can be a mass degenerate state, consisting of two orthogonal components; each of them is an admixture of a conventional, SM-like scalar with the new fermiophobic counterparts [24]. Mass degenerate scalar states of a different type have been considered in connection with singlet extensions [88], the NMSSM approach [89] and also within conventional 2HDM [90]. In order to discover or disprove such near degeneracies with mass separations smaller than the experimental mass resolution, dedicated strategies are necessary [91]. Although such models in general contain more $SU(2)_L$ doublets, in Section 4.6 we concentrate on the case where the observed 126 GeV resonance is composed of two scalar fields, with only one of them giving masses to all of the fermions in a type-I Yukawa structure.

2.6 Ultraviolet structure

If we want to establish extended Higgs sectors as a consistent perturbative framework for a light Higgs boson with variable couplings we need to carefully study the high energy behavior of our theory. The Standard Model Higgs sector with the observed mass of $m_H = 126$ GeV navigates between two strong high-scale constraints: first, the triviality bound forbids a significant enhancement of the relevant Higgs self-couplings [92, 93]. Second, for $m_H \lesssim 130$ GeV the electroweak vacuum may become metastable and eventually decay into the global low-lying vacuum via thermal or quantum-induced tunneling [94–96]. While these constraints might be avoidable through an appropriate ultraviolet embedding, we still consider them for the study of these effective extended models.

At high energy scales the running Higgs self-coupling develops a Landau pole, which has to lie outside the range of validity of our fundamental theory. In the same spirit, but numerically more relevant, the size of the Higgs self-couplings is limited by unitarity [97]. To avoid this the partial waves of the scalar–scalar, gauge boson–gauge boson and scalar–gauge boson scattering processes must be limited from above. Following the Goldstone equivalence theorem the high energy behavior of all these processes is determined by the scalar sector. The leading contributions are governed by the scalar self-couplings λ_i in the Higgs potential in Eq.(2.4). We can in general apply unitarity bounds for an additional singlet, doublet and triplet. In the 2HDM the different channels force the absolute value of each combination of scalar self-couplings [32, 98–100]

$$\begin{aligned}
a_{\pm} &= \frac{1}{16\pi} \left[3(\lambda_1 + \lambda_2) \pm \sqrt{9(\lambda_1 - \lambda_2)^2 + 4(2\lambda_3 + \lambda_4)^2} \right] & f_1 &= f_2 = \frac{1}{8\pi} (\lambda_3 + \lambda_4) \\
b_{\pm} &= \frac{1}{16\pi} \left[(\lambda_1 + \lambda_2) \pm \sqrt{(\lambda_1 - \lambda_2)^2 + 4\lambda_4^2} \right] & f_+ &= \frac{1}{8\pi} (\lambda_3 + 2\lambda_4 + 3\lambda_5) \\
c_{\pm} &= \frac{1}{16\pi} \left[(\lambda_1 + \lambda_2) \pm \sqrt{(\lambda_1 - \lambda_2)^2 + 4\lambda_5^2} \right] & f_- &= \frac{1}{8\pi} (\lambda_3 + \lambda_5) \\
e_1 &= \frac{1}{8\pi} (\lambda_3 + 2\lambda_4 - 3\lambda_5) & p_1 &= \frac{1}{8\pi} (\lambda_3 - \lambda_4) \\
e_2 &= \frac{1}{8\pi} (\lambda_3 - \lambda_5); & &
\end{aligned} \tag{2.16}$$

to be smaller than unity. In addition, tree-level unitarity in the usual 2HDM-like mixing pattern imposes a set of sum rules for the Higgs couplings to Standard Model particles [101]

$$\begin{aligned}
g_{VVh^0}^2 + g_{VH^0}^2 &= (g_V^{\text{SM}})^2 & g_{ffh^0}^2 + g_{ffH^0}^2 + g_{ffA^0}^2 &= \frac{m_f^2}{v^2} \equiv (g_f^{\text{SM}})^2 \\
g_{h^0A^0Z^0}^2 + g_{H^0A^0Z^0}^2 &= \frac{g^2}{4c_w^2} & g_{\phi ZZ}^2 + 4m_Z^2 g_{\phi A^0 Z^0}^2 &= \frac{g^2 m_Z^2}{c_w^2} \\
g_{ffh^0} g_{VVh^0} + g_{ffH^0} g_{VH^0} &= g_f^{\text{SM}} g_V^{\text{SM}}, & &
\end{aligned} \tag{2.17}$$

with $\phi = h^0, H^0$ and $V = W, Z$. The weak coupling is $g = e/s_w$. These tree-level sum rules have obvious implications: first, the Higgs couplings to massive gauge bosons can be at most as strong as in the Standard Model; second, the related sum rules for W and Z bosons suggest a universal modification to both couplings $\Delta_W \simeq \Delta_Z$, reflecting custodial invariance; third, and owing to the structure of the gauge derivative, all vertices containing at least one gauge boson and exactly one non-standard Higgs field (H^0, A^0, H^{\pm}) will be proportional to $\cos(\beta - \alpha)$. Consequently, these heavy fields will decouple from the Standard Model dynamics in the limit $\alpha \rightarrow \beta - \pi/2$ [100].

The second condition on ultraviolet models is the stability of the vacuum. For a 2HDM with the most general potential the non-linear nature of the vacuum conditions $\partial V / \partial \Phi = 0$ as a function of the

VEVs may lead to different vacua featuring spontaneous CP or $U(1)$ breaking. Vacuum stability can be ensured by requiring [94, 100, 102]

$$\lambda_1 > 0 \quad \lambda_2 > 0 \quad \sqrt{\lambda_1 \lambda_2} + \lambda_3 + \min(0, \lambda_4 - |\lambda_5|) > 0. \quad (2.18)$$

Using the renormalization group equations for the 2HDM [103] we can demand these conditions to hold for running self-couplings up to any arbitrarily high scale [102, 104]. A few generic properties govern the outcome: very small weak-scale self-couplings typically lead to unbounded high-scale potentials; very large weak-scale self-coupling values would hit a low-lying Landau pole; all constraints are very sensitive to additional symmetries in the 2HDM potential like a global Z_2 parity [43]. In practice, we envision our 2HDM setup as an effective Higgs sector parameterization of a generic TeV-scale UV-completion. We thus allow for new physics entering around $\mathcal{O}(1 - 10)$ TeV. Therefore tree-level bounds provide a suitable vacuum stability prescription.

Finally, to ensure that the entire modified Higgs sector remains weakly interacting all Yukawas should be sufficiently small at the weak scale, $y_f/\sqrt{2} < \sqrt{4\pi}$. This translates into $\tan\beta > 0.28$ for all natural flavor conservation 2HDM models, $\tan\beta < 140$ for type-II and the flipped models, and $\tan\beta < 350$ in the lepton-specific case [57].

3 Coupling patterns

If we assume that the observed light Higgs resonance is part of an extended Higgs sector the key question is what we can say about the structure of such an extended Higgs sector when looking at patterns in the light Higgs couplings. The challenge in this section is to identify model features which allow light Higgs particles with flexible couplings $\Delta_x = (g_x - g_x^{\text{SM}})/g_x^{\text{SM}}$ [6] and an invisible decay width.

Turning this argument around we can ask if a sufficiently general extended Higgs sector can serve as a consistent renormalizable framework to describe free Higgs couplings in the Standard Model Higgs Lagrangian. We will attempt to build such models based on the extended Higgs sectors summarized in Section 2. For these models we can compute electroweak quantum corrections to Higgs observables without assuming a Standard Model structure [14]. After largely reviewing the tree-level patterns of extended Higgs sectors we will give a comprehensive discussion of quantum effects from this perspective.

3.1 Tree-level couplings

In models with additional singlets and doublets the light Higgs interactions to massive gauge bosons show a systematic suppression

$$\frac{g_V}{g_V^{\text{SM}}} \stackrel{\text{singlet}}{=} \cos\theta \quad \text{and} \quad \frac{g_V}{g_V^{\text{SM}}} \stackrel{2\text{HDM}}{=} \sin(\beta - \alpha), \quad (3.1)$$

arising from tree-level mixing in the light Higgs mass eigenstate. The Standard Model coupling g_V^{SM} is fixed by unitarity and renormalizability. Assuming the singlets and doublets all develop a non-zero VEV, it is composed of the different CP-even scalar components. In the 2HDM the mixing factors $\cos(\beta - \alpha)$ and $\sin(\beta - \alpha)$ realize the unitarity sum rule in Eq.(2.17). These couplings appear in the covariant derivative, so the suppression is universal for g_Z and g_W , unless we introduce a Higgs triplet. As we will see in Sections 3.2 and 3.3 quantum effects modify this coupling pattern slightly. We document this simple structure of the couplings of the lightest Higgs boson in Table 1. The notation $\mathcal{O}(y_f, \lambda_H)$ stands for fermion-mediated or Higgs-mediated loop contributions which we will discuss below.

		hVV	
extension	model	universal rescaling	non-universal rescaling
singlet	inert ($v_S = 0$)		
	EWSB ($v_S \neq 0$)	$\theta \quad \Delta_V < 0$	
doublet	inert ($v_d = 0$)		
	type-I	$\alpha - \beta \quad \Delta_V < 0$	$\mathcal{O}(y_f, \lambda_H) \quad \Delta_V \gtrless 0$
	type-II-IV	$\alpha - \beta \quad \Delta_V < 0$	$\mathcal{O}(y_f, \lambda_H) \quad \Delta_V \gtrless 0$
	aligned, MFV	$\alpha - \beta \quad \Delta_V < 0$	$\mathcal{O}(y_f, \lambda_H) \quad \Delta_V \gtrless 0$
singlet+doublet		$\alpha - \beta, \theta \quad \Delta_V < 0$	$\mathcal{O}(y_f, \lambda_H) \quad \Delta_V \gtrless 0$
triplet			$\alpha, \beta_n, \beta_c \quad \Delta_V \gtrless 0$

Table 1. Interaction patterns for a light Higgs boson to weak gauge bosons ($V = W^\pm, Z$), allowing for universal or non-universal departures from the Standard Model interactions. We indicate the relevant model parameters defined in Appendix A and the possibility of coupling enhancement vs suppression.

Departures from the Standard Model Higgs couplings to fermions can have two origins: first, the fermionic 2HDM mixing structure includes a CP-odd gauge boson A^0 . This coupling comes with an additional factor $i\gamma_5$, which means that $g_{ffA^0}^2 < 0$ in the sum rule quoted in Eq.(2.17) allows for at least one of the CP-even couplings to lie above g_f^{SM} . Second, multi-doublet structures typically allow for independent variations for the up-type and down-type fermions. Combining both effects, positive and negative tree-level non-universal shifts Δ_f are attainable, as shown in Table 2. A serious limitation of the 2HDM setup is that we only have two parameters to describe the leading tree-level effects in g_V and $g_{t,b,\tau}$. If $(\beta - \alpha)$ is fixed by g_V all three Yukawas are described by $\tan \beta$. Only Yukawa alignment gives rise to a more flexible pattern, unlinking the bottom and tau Yukawas via the independent angles $\gamma_{b,\tau}$.

Higgs interactions to photons and gluons are generated by loops of all relevant particles in a given model. For the gluon case this requires colored states, so we can immediately apply the modified quark Yukawa patterns of an extended Higgs sector. In the Standard Model the bottom contribution to these Higgs coupling loops is negligible, so we can generate a non-trivial scaling of g_g with respect to g_t by significantly increasing the bottom Yukawa, as we will see later. The photon coupling depends on the

		$hf\bar{f}$	
extension	model	universal rescaling	non-universal rescaling
singlet	inert ($v_S = 0$)		
	EWSB ($v_S \neq 0$)	$\theta \quad \Delta_f < 0$	
doublet	inert ($v_d = 0$)		
	type-I	$\alpha - \beta \quad \Delta_f \gtrless 0$	$\mathcal{O}(y_f, \lambda_H) \quad \Delta_f \gtrless 0$
	type-II		$\alpha - \beta, \mathcal{O}(y_f, \lambda_H) \quad \Delta_f \gtrless 0$
	aligned/MFV	$y_f, \quad \Delta_f \gtrless 0$	$y_f, \mathcal{O}(y_f, \lambda_H) \quad \Delta_f \gtrless 0$
singlet+doublet		$y_f, \theta \quad \Delta_f \gtrless 0$	$y_f, \mathcal{O}(y_f, \lambda_H) \quad \Delta_f \gtrless 0$
triplet		$\beta_n \quad \Delta_f \gtrless 0$	$\mathcal{O}(y_f, \lambda_H) \quad \Delta_f \gtrless 0$

Table 2. Interaction patterns for a light Higgs boson to fermions, allowing for universal or non-universal departures from the Standard Model interactions. We indicate the relevant model parameters defined in Appendix A and the possibility of coupling enhancement vs suppression.

		$h\gamma\gamma$		hgg	Γ_{inv}
extension	model				
singlet	inert ($v_S = 0$)				λ_{hSS}
	EWSB ($v_S \neq 0$)	θ	$\Delta_\gamma^{\text{tot}} < 0$	θ	$\Delta_g^{\text{tot}} < 0$
doublet	inert ($v_d = 0$)	$\lambda_{hH^+H^-}$	$\Delta_\gamma^{\text{tot}} \geq 0$		λ_H
	type-I	$\alpha - \beta, \lambda_{hH^+H^-}$	$\Delta_\gamma^{\text{tot}} \geq 0$	$\alpha - \beta$	$\Delta_g^{\text{tot}} \geq 0$
	type-II-IV	$\alpha - \beta, \lambda_{hH^+H^-}$	$\Delta_\gamma^{\text{tot}} \geq 0$	$\alpha - \beta$	$\Delta_g^{\text{tot}} \geq 0$
	aligned, MFV	$\alpha - \beta, \lambda_{hH^+H^-}$	$\Delta_\gamma^{\text{tot}} \geq 0$	y_f	$\Delta_g^{\text{tot}} \geq 0$
singlet + doublet		$\alpha - \beta, \theta, \lambda_{hH^+H^-}$	$\Delta_\gamma^{\text{tot}} \geq 0$	y_f, θ	$\Delta_g^{\text{tot}} \geq 0$
triplet		$\alpha, \beta_n, \beta_c,$ $\lambda_{hH^+H^-},$ $\lambda_{hH^{++}H^{--}}$	$\Delta_\gamma^{\text{tot}} \geq 0$	β_n	$\Delta_g^{\text{tot}} \geq 0$

Table 3. Interaction patterns for a light Higgs boson to photons, gluons and invisible states, allowing for universal or non-universal departures from the Standard Model interactions. We indicate the relevant model parameters defined in Appendix A and the possibility of coupling enhancement vs suppression.

three heavy Yukawas and on g_W , but will also receive corrections due to new charged scalars in the Higgs sector. The effect of additional states is relatively enhanced as it overlays to the destructive interference between the leading top and W contributions in the Standard Model [105]. Electroweak corrections to the two channels can have similarly enhanced effects. A charged Higgs loop is governed by the Higgs potential [106]. Deviations from g_γ^{SM} can manifest themselves both as an increase and a reduction, depending on the size and sign of the $h^0 H^+ H^-$ coupling.

Finally, if one of the extra Higgs multiplets does not develop a VEV the Higgs boson can decay into a pair of inert light scalars. This will be observed as an invisible Higgs width Γ_{inv} . Again, this decay will depend on the self-coupling structure of the potential. The patterns of such modifications are illustrated in Table 3.

We can then easily summarize the general Higgs coupling structure at tree level: in the absence of a Higgs triplet any modification of $g_{W,Z}$ will be negative and fully correlated. Changes in the Yukawas $g_{b,t,\tau}$ can follow a wide range of model-specific patterns. The effective coupling g_g will only be affected through the modified Yukawas, while g_γ as well as invisible Higgs decays can be generated through self-couplings in the Higgs potential. Adding a singlet will always give a further universal reduction of all Higgs couplings, as shown in Eq.(2.12), so we only resort to such a singlet to describe invisible Higgs decays.

Each panel in Figure 1 shows different Higgs interactions as a function of $\tan \beta$ for a fixed value of $\sin(\beta - \alpha) = 0.85\dots 1$, i.e. implying a reduction of g_V by up to 15%. To soften the impact of the large- $\tan \beta$ constraints by unitarity and vacuum stability we allow for a moderate Z_2 -breaking term $m_{12} = 50\dots 60$ GeV in Eq.(2.4). If we ignore these constraints we find that towards small values of $\tan \beta$ the top Yukawa is no longer perturbative. Note that we do not attempt to fully account for all constraints because extended Higgs sectors as consistent descriptions of single-Higgs models with variable Higgs couplings are not meant to be realistic models describing all available data in high energy physics.

By definition, in a type-I 2HDM all Yukawa couplings vary simultaneously, as shown in the upper panels of Figure 1. As long as we remain close to the Standard Model limit $\alpha - \beta = -\pi/2 + \delta$ the largest deviations are found at small $\tan \beta$. Following Eq.(2.12) the corrections then scale like

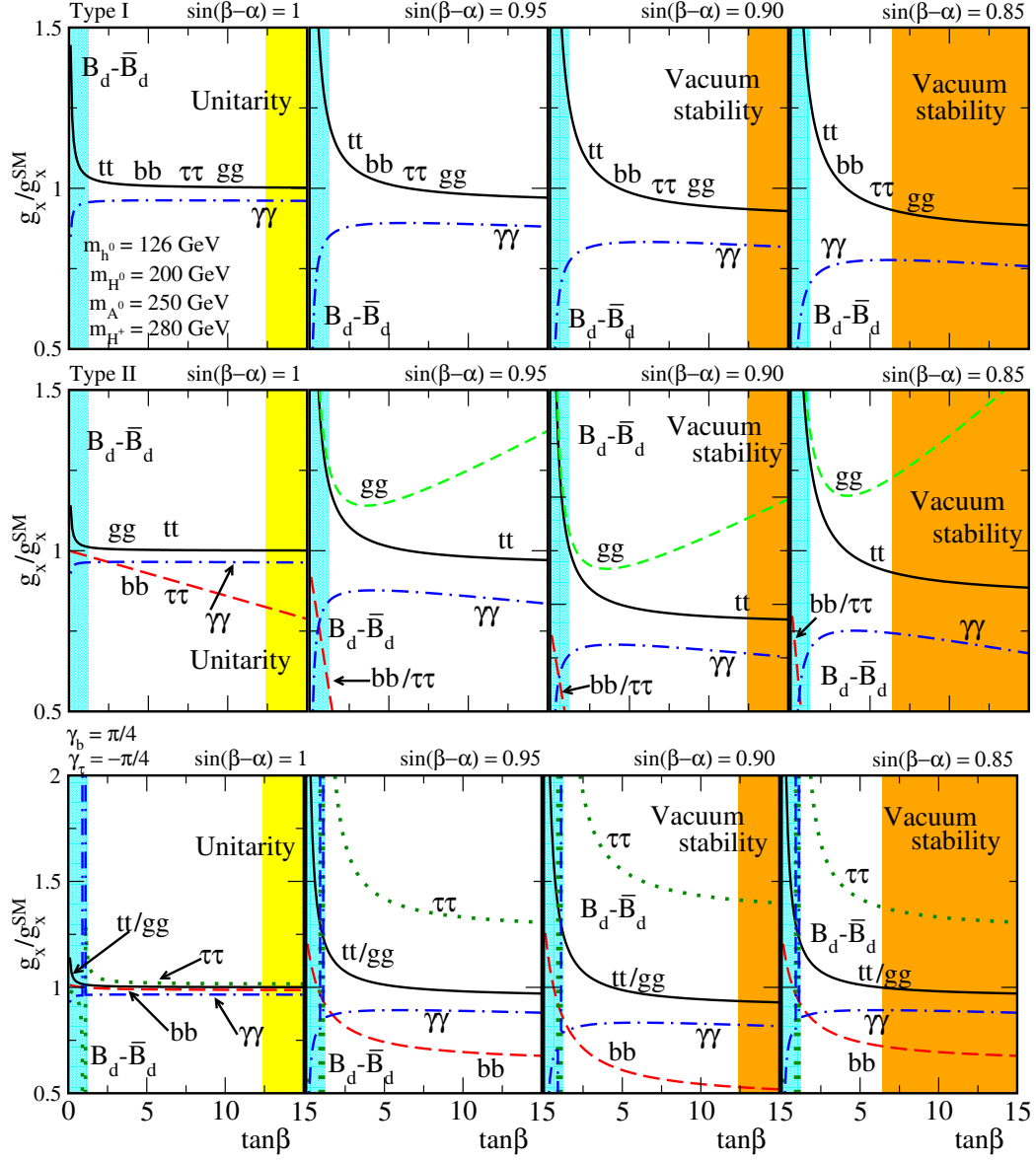


Figure 1. Dependence of the Higgs couplings $g_x/g_x^{\text{SM}} = 1 + \Delta_x$ on $\tan \beta$. The couplings to weak gauge bosons are fixed by the values of $\sin(\beta - \alpha)$. For type-I (top), type-II (center) and one specific aligned configuration with $\gamma_{b,\tau} = \pm\pi/4$ (bottom) we illustrate four choices of mixing angles $\sin(\beta - \alpha)$. The shaded regions are excluded by the leading constraints.

$\cos \alpha / \sin \beta \simeq 1 + \sin \delta / \tan \beta$. This means that for all 2HDM setups the couplings barely deviate from the Standard Model for $\sin(\beta - \alpha) \simeq 1$. Once we allow for a stronger suppression of g_V we find sizeable modifications in the Yukawa couplings. Shifts in g_g and g_γ are inherited from the tree-level couplings, with an additional contribution to g_γ from new charged Higgs states in the loop.

In a type-II model up-type and down-type Yukawas can vary separately, scaling like

$$\begin{aligned} \frac{g_{b,\tau}}{g_{b,\tau}^{\text{SM}}} &= 1 + \Delta_{b,\tau} = -\frac{\sin \alpha}{\cos \beta} = \cos \delta - \sin \delta \tan \beta = 1 - \delta \tan \beta - \frac{\delta^2}{2} + \mathcal{O}(\delta^3) \\ \frac{g_t}{g_t^{\text{SM}}} &= 1 + \Delta_t = +\frac{\cos \alpha}{\sin \beta} = 1 + \frac{\sin \delta}{\tan \beta} = 1 + \frac{\delta}{\tan \beta} - \frac{\delta^2}{2} + \mathcal{O}(\delta^3). \end{aligned} \quad (3.2)$$

If $\sin \delta \simeq \delta > 0$ the down-type couplings decrease with large $\tan \beta$ while the top Yukawa shows an increase at small $\tan \beta$ values, and vice versa. The lepton-specific and flipped setups combine a type-I pattern for the quark Yukawas with a type-II pattern for the lepton Yukawas, and vice versa.

Once we depart from natural flavor conservation more possibilities arise. Aligned models allow for an independent variation of the three Yukawa interactions and accommodate enhancements, suppressions and even sign flips [59]. The lower panels of Figure 1 illustrate this for $\gamma_{b,\tau} = \pm\pi/4$, as defined in Eq.(2.9) and in Appendix A. We identify two distinct patterns for g_b and g_τ . The bottom Yukawa is suppressed with respect to the Standard Model, with growing deviations for larger $\tan \beta$. Instead, the tau lepton is increasingly enhanced as we lower $\tan \beta$. Coupling shifts of $\mathcal{O}(\pm 30\%)$ are possible within the allowed $\tan \beta$ range.

Building on these tree-level patterns we can construct a model which gives us maximal flexibility in the light Higgs coupling variations. We consider an aligned 2HDM with one additional inert singlet. The relevant light Higgs couplings g_x are determined by six model parameters, with the only constraint $\Delta_W = \Delta_Z = \Delta_V$ due to custodial symmetry,

$$\begin{aligned} \frac{g_V}{g_V^{\text{SM}}} &= 1 + \Delta_V(\alpha, \tan \beta) \\ \frac{g_t}{g_t^{\text{SM}}} &= 1 + \Delta_t(\alpha, \tan \beta) & \frac{g_{b,\tau}}{g_{b,\tau}^{\text{SM}}} &= 1 + \Delta_{b,\tau}(\alpha, \tan \beta, \gamma_{b,\tau}) \\ \frac{g_\gamma}{g_\gamma^{\text{SM}}} &= 1 + \Delta_\gamma^{\text{SM}}(\alpha, \tan \beta, \gamma_{b,\tau}) + \Delta_\gamma(\alpha, \tan \beta, m_{12}^2, m_{H^\pm}^2) & \frac{g_g}{g_g^{\text{SM}}} &= 1 + \Delta_g^{\text{SM}}(\Delta_t, \Delta_b). \end{aligned} \quad (3.3)$$

The loop-induced Higgs coupling to photons receives a contribution from a charged Higgs loop, which means it depends on the trilinear self-interactions. This self-interaction we can trade for the Higgs boson masses and the PQ-breaking scale m_{12} . Additional non-minimal doublet mixing can be introduced through non-vanishing Z_2 -breaking quartic couplings $\lambda_{6,7}$.

In the case of an inert or purely dark singlet, none of the above couplings carries information on the singlet-doublet portal interaction $\lambda_3(\Phi^\dagger \Phi) S^2$ of Eq.(2.3). It can only be determined from invisible Higgs decays. With the exception of $\Delta_W = \Delta_Z < 0$ and the parametric dependence of Δ_g the setup in Eq.(3.3) indeed describes a set of completely independent Higgs couplings [6].

3.2 Quantum effects: Higgs and gauge sector

Beyond the simple tree-level patterns described in the last section an extended Higgs sector will affect all Higgs couplings at the quantum level. These loop effects do not have as simple patterns and depend on the heavy Standard Model states as well as on the entire Higgs spectrum. They significantly increase the number of degrees of freedom which we can use to for example modify the couplings of the lightest Higgs state to all Standard Model particles. Typical weak corrections are too small to account for experimentally relevant coupling shifts in the 20% range. However, non-decoupling effects can have the desired strength. Such effects can be linked to the Higgs self couplings or to very large values of $\tan \beta$ or $\cot \beta$. In this section we discuss the first kind, the latter will follow in Section 3.3.

One source of decoupling effects is the mass of a new state unrelated to the Higgs mechanism. For example in the singlet extension of Eq.(2.3) the heavier neutral CP-even state obtains its mass $m_{H^0}^2 \simeq \mu_2^2 + \lambda_3 v_1^2/2$ from the singlet dimension-2 operator μ_2^2 as well as from the Higgs VEV via the quartic interaction λ_3 . The first term is unrelated to electroweak symmetry breaking and decouples. The second term cannot be detached from the light Higgs dynamics and leads to non-decoupling. This is in agreement with the Appelquist-Carrazzone theorem [107] which is based on three conditions:

renormalizability, no Yukawa couplings, and no spontaneous symmetry breaking. If $\lambda_3^2 v_1^2 \gg \mu_2^2$, heavy Higgs effects can be large and for example useful in stabilizing the vacuum through a large shift in the Higgs quartic coupling from threshold corrections [108].

The same effects occur in the 2HDM. The decoupling of the heavy states can be described in terms of the small parameter $\cos(\beta - \alpha)$, as shown in Appendix B. Just like in the singlet case we can relate the heavy masses $M_{\text{heavy}}^2 = m_{H^0, A^0, H^\pm}^2$ to the mass terms and self-couplings in the potential of Eq.(2.4). This gives us

$$m_{H^0, A^0, H^\pm}^2 = \frac{m_{12}^2}{\sin \beta \cos \beta} + \mathcal{O}(\lambda_i v^2) + \mathcal{O}\left(\frac{\lambda_i v^4}{M_{\text{heavy}}^2}\right). \quad (3.4)$$

A non-decoupling behavior manifests itself as power-like contributions from the heavy masses and may shift the light Higgs couplings to weak gauge bosons and heavy quarks by up to 10% [109]. For the trilinear Higgs self-interaction such effects can reach $\mathcal{O}(100\%)$.

Independent of the origin of the heavy Higgs masses the self-interactions in the 2HDM potential Eq.(2.4) can induce sizeable quantum effects. We show the corresponding Feynman diagrams in Figure 2. This is because $\mathcal{O}(\lambda_i v^2)$ contributions are not limited by any underlying symmetry and only a subset of them is related to physical masses and constrained indirectly. While large self-interactions are often identified with heavy masses this does not hold in the general 2HDM [106, 110]. Usually, we select m_{12} and $\lambda_{6,7}$ as model parameters which are only related to independent self-couplings. From Section 2.6 we know that perturbativity, vacuum stability and unitarity slightly tame these effects in realistic scenarios.

In Figure 3 we show the electroweak corrections to the light Higgs couplings to heavy quarks and to massive gauge bosons as a function of the PQ soft-breaking scale m_{12}^2 . We consider type-I, type-II, and aligned setups, just like for the tree-level analysis in Figure 1. The difference is that we now fix $\tan \beta = 1.4$ and vary m_{12}^2 . The values for m_{12}^2 are constrained by unitarity and vacuum stability. The calculation is based on FEYNARTS, FORMCALC and LOOPTOOLS [111] with an appropriate renormalization [110]. Technically, we relate the relative coupling shift to the corresponding loop-corrected decay rate, $\Delta g_x/g_x = 1/2 \Delta \Gamma(H \rightarrow xx)/\Gamma(H \rightarrow xx)$.

Some basic features are common to all couplings, with the exception of the more model dependent case of the bottom quark. Quantum effects give rise to a systematic $\mathcal{O}(10\%)$ depletion, mostly stemming from the Higgs-mediated finite wave-function corrections to the light Higgs boson. The leading contributions are governed by two trilinear Higgs self-interactions, shown in Figure 2. In combination they scale as $|m_{12}^2|^2$. The key question is if such corrections can either separate Δ_W from Δ_Z or lead to positive corrections $\Delta_V > 0$. From the leading Feynman diagram we know that this is unlikely to happen: large corrections induced by Higgs self-couplings will affect the wave function renormalization

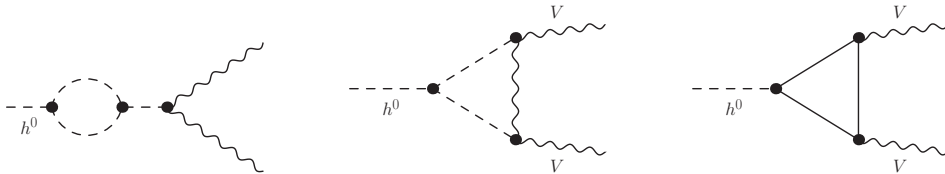


Figure 2. Sample Feynman diagrams accounting for the electroweak corrections to the Higgs couplings. In terms of self-couplings they scale with the square (left), linearly (center) and flat (right).

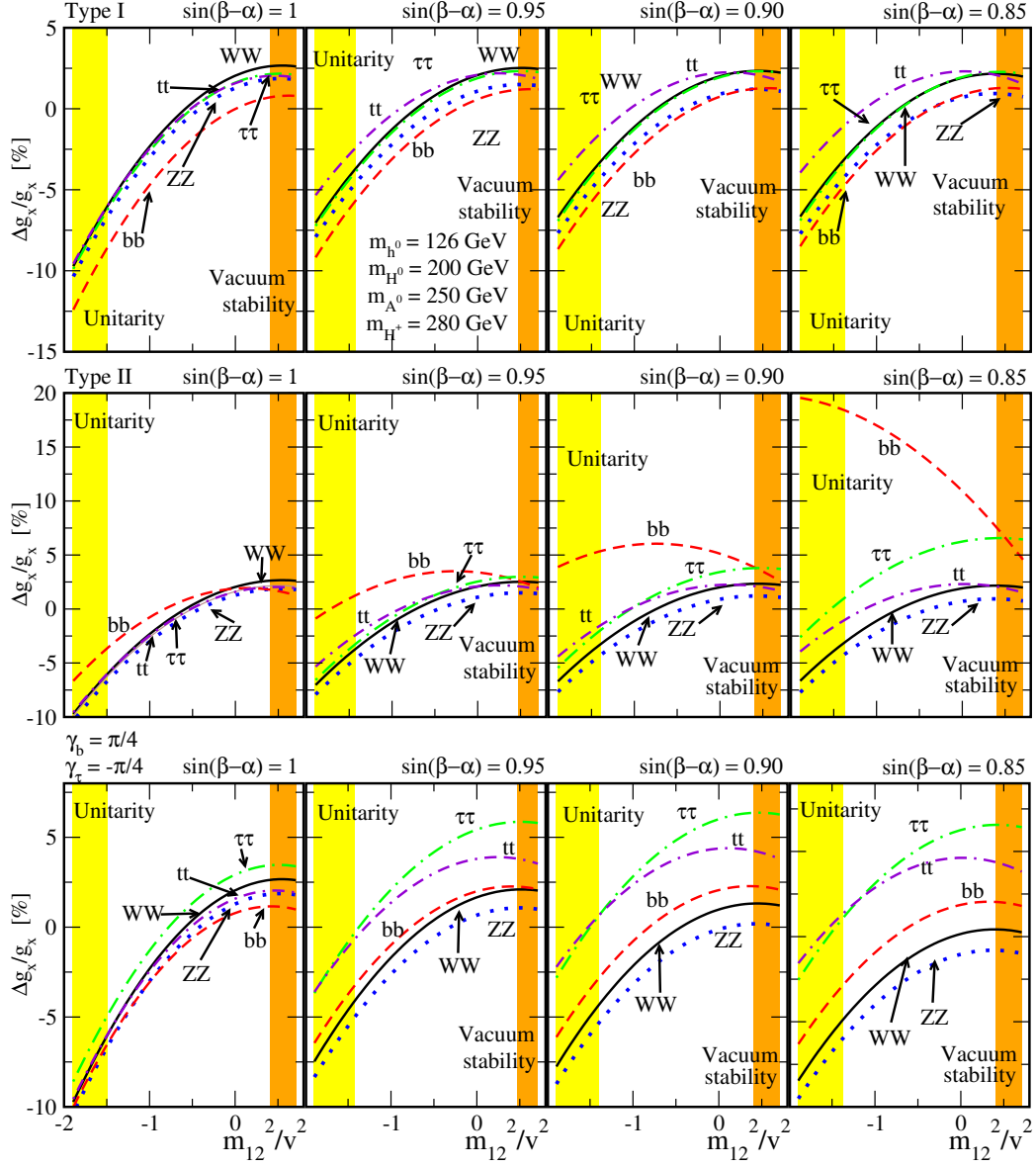


Figure 3. Loop corrections to the light Higgs couplings $\Delta g_x/g_x$ (in %) for type-I (top), type-II (center), and aligned configurations (bottom) as a function of m_{12}^2 . Just like in Figure 1 the latter model is defined with $\gamma_{b,\tau} = \pm\pi/4$. The shaded regions are excluded by unitarity and vacuum stability as discussed in Section 2.6.

of the light Higgs and the renormalization of mixing angles in the Higgs sector. Both are negative and universal. Because the leading corrections to the Higgs wave function renormalization are proportional to the self coupling squared, signs or phases in the Higgs potential do not affect this conclusion.

It turns out that the situation is even worse: from Eq.(2.7) we know that custodial symmetry can be broken by non-degenerate masses in the Higgs sector. This effect we can trace through the asymmetry

$$x_m = \frac{m_{H^\pm} - m_{A^0}}{m_{H^\pm} + m_{A^0}} \quad \text{and} \quad A_{W/Z}(x_m) = \frac{|\Delta_W| - |\Delta_Z|}{|\Delta_W| + |\Delta_Z|}. \quad (3.5)$$

Note that $A_{W/Z}$ is defined on the loop-induced shift in the W and Z couplings, not on their coupling values. Effects of this kind arise for example from the central Higgs vertex diagram in Figure 2. However, these mass-induced corrections are tied to the gauge couplings and unrelated to potentially

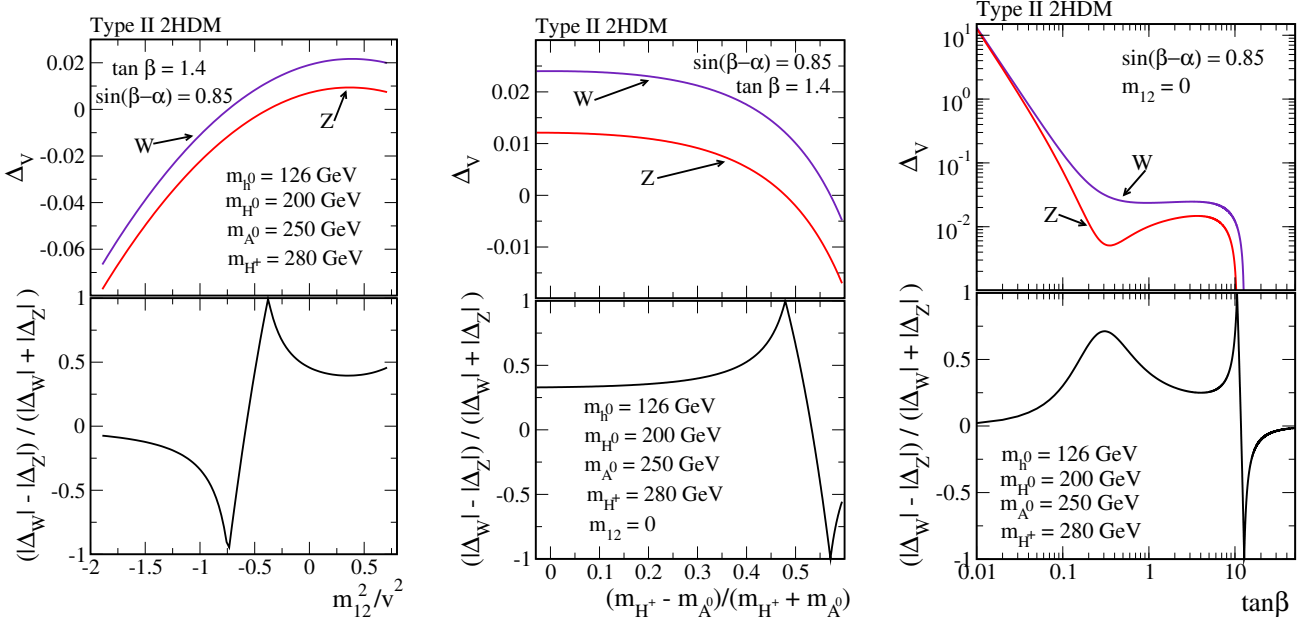


Figure 4. Loop corrections to $\Delta_{W,Z}$ and to the asymmetry $A_{W/Z}$ as a function of m_{12}^2/v^2 (left), x_m (middle), and $\tan \beta$ (right). We only show typical results for a type-II 2HDM with light additional Higgs states. All curves include the full set of Higgs/gauge and fermion loops.

enhanced scalar self-interactions. In practice, the $A_{W/Z}$ variation due to universal non-decoupling effects is reduced.

In the left panel of Figure 4 we show the behavior of the loop corrections to the Higgs couplings to massive gauge bosons as a function of m_{12}^2 . As expected, the weak loop corrections can be large. For negative values $m_{12}^2 \simeq -2v^2$ they shift $\Delta_W \simeq \Delta_Z$ down by 6-7%. On the other hand, positive contributions to the W and Z couplings are at the per-cent level and cannot compensate the tree-level reduction by 15% for our assumed parameter point. Similarly, the split $A_{W/Z}$ is small wherever the absolute size of the loop corrections is large, reflecting again the universal character of the leading loop-induced deviations. Around $m_{12}^2 = -v^2/2$ the loop corrections both cross zero. The large value of $A_{W/Z}$ at large positive values of m_{12}^2 is due to vanishing loop-induced Δ_Z .

In the central panel of Figure 4 we show the size of the coupling shifts as a function of x_m defined in Eq.(3.5). Wherever the second diagram in Figure 2 dominates the asymmetry roughly scales like

$$A_{W/Z} \sim \frac{\left| \frac{m_{H^\pm}^2}{m_{h^0}^2 - m_{H^\pm}^2} \log \frac{m_{h^0}^2}{m_{H^\pm}^2} \right| - \left| \frac{m_{A^0}^2}{m_{h^0}^2 - m_{A^0}^2} \log \frac{m_{h^0}^2}{m_{A^0}^2} \right|}{\left| \frac{m_{H^\pm}^2}{m_{h^0}^2 - m_{H^\pm}^2} \log \frac{m_{h^0}^2}{m_{H^\pm}^2} \right| + \left| \frac{m_{A^0}^2}{m_{h^0}^2 - m_{A^0}^2} \log \frac{m_{h^0}^2}{m_{A^0}^2} \right|}. \quad (3.6)$$

Comparing to the T contributions shown in Eq.(2.7) the asymmetry $A_{W/Z}$ will indeed behave similarly and therefore be strongly constrained by electroweak precision data. Numerically, the corrections to $\Delta_{W,Z}$ are indeed small and degenerate.

A richer range of patterns only appears for the bottom Yukawa. There, quantum effects are strongly model dependent and may eventually yield large (and positive) 20% corrections, including sizable $m_t/\tan \beta$ pieces from charged Higgs corrections, which can be further boosted by the trilinear $h^0 H^+ H^-$ coupling.

However, to overcome the tree-level limitations of Eq.(3.3) loop effects from the gauge and Higgs sector are generally of limited use. They hardly predict structurally new positive or non-degenerate $\Delta_{W,Z}$ contributions. The question is if fermion-induced loops lead to the desired effects.

3.3 Quantum effects: fermions

At tree level, Figure 1 shows that the variation of the modified light Higgs couplings in the aligned model the range of patterns is rich and non-universal. However, the couplings to weak gauge bosons show no dependence on $\tan\beta$ for fixed $(\alpha - \beta)$. Obviously, this simple picture will not hold once we include fermion loop effects.

The trademark feature for top-mediated effects in all conventional 2HDMs with natural flavor conservation is a modified Yukawa coupling scaling like $m_t/\tan\beta$ for $\tan\beta \ll 1$. For type-II models a complementary $\tan\beta$ enhancement of down-type Yukawas is given in Eq.(3.2). In Figure 1 we see that small $\tan\beta$ enhances the top Yukawa enough to overshoot perturbativity constraints. Experimentally, this low $\tan\beta$ region is in strong tension with the $B_d^0-\bar{B}_d^0$ mixing rate data, a constraint we will ignore for the structural argument in this section. The question is then how this richer Higgs coupling pattern to fermions may be imprinted on the loop-induced effects.

For small $\tan\beta$ the right panel of Figure 4 indicates for the first time sizeable and non-universal quantum contributions to Δ_W and Δ_Z . They arise because towards small $\tan\beta$ the fermionic and the Higgs-mediated contributions to the wave function renormalization shown in Figure 2 become similar in size and carry opposite signs. As long as this partial compensation holds, the one-loop contributions are dominated by the $1/\tan\beta$ -enhanced top-mediated vertex corrections. For $\tan\beta \simeq 0.1$ the positive contributions to $\Delta_{W,Z}$ exceed 10% and become of similar size as the tree level contributions. Because the top and bottom couplings are different for W and Z bosons this induces a violation of custodial symmetry $\Delta_Z \neq \Delta_W$ with an asymmetry $A_{WZ} \simeq 0.5$. This scan over $\tan\beta$ we extend to the full set of relevant couplings in Figure 5, similar to the Higgs and gauge-induced loop corrections in Figure 3. We examine type-I (top), type-II (center) and aligned (bottom) 2HDM configurations. The different $(\alpha - \beta)$ choices cover tree level g_V/g_V^{SM} suppressions to -15% .

Once we continue beyond $\tan\beta \simeq 0.1$ the top Yukawa grows much faster than the scalar self-interactions. This gives rise to strongly enhanced but universal shifts in $g_{W,Z}$. Moreover, in this regime the top Yukawa is extremely large already at the weak scale.

We see that parameter regions with positive non-universal $\Delta_{W,Z}$ values are severely limited by many constraints on the low- $\tan\beta$ regime. On the other hand, this structural pattern is attainable within the 2HDM, as long as we assume that experimental constraints should only be placed on the full and unknown ultraviolet model. The only structural constraint is a perturbative top Yukawa coupling.

An alternative model inducing the desired effects on $\Delta_{W,Z}$ is based on new vector-like fermions coupling to the Higgs and eventually to weak gauge bosons. Their contribution to the Higgs wave-function and to the Higgs-gauge boson vertex corrections yield coupling shifts $\Delta_W \neq \Delta_Z > 0$. The relevant interactions we can model as Higgs and vector portal-like operators [112]

$$\mathcal{L} \supset c_{HF} \frac{\psi^c \Phi \psi (\Phi^\dagger \Phi)}{\Lambda^2} + c_{WF} \frac{\bar{\psi} \sigma^{\mu\nu} W_{\mu\nu} \psi}{\Lambda} + c_{BF} \frac{\bar{\psi} \sigma^{\mu\nu} B_{\mu\nu} \psi}{\Lambda}, \quad (3.7)$$

with the usual definition for the field-strength tensors and $\sigma^{\mu\nu} \equiv i[\gamma^\mu, \gamma^\nu]/2$. The scale Λ determines the mass range for a specific ultraviolet completion. Realizations of these nature have been proposed in the literature [113]. As long as the new fermions do not carry color they do not affect the Higgs-gluon coupling and are therefore not constrained by the experimental limits on a chiral 4th generation [114].

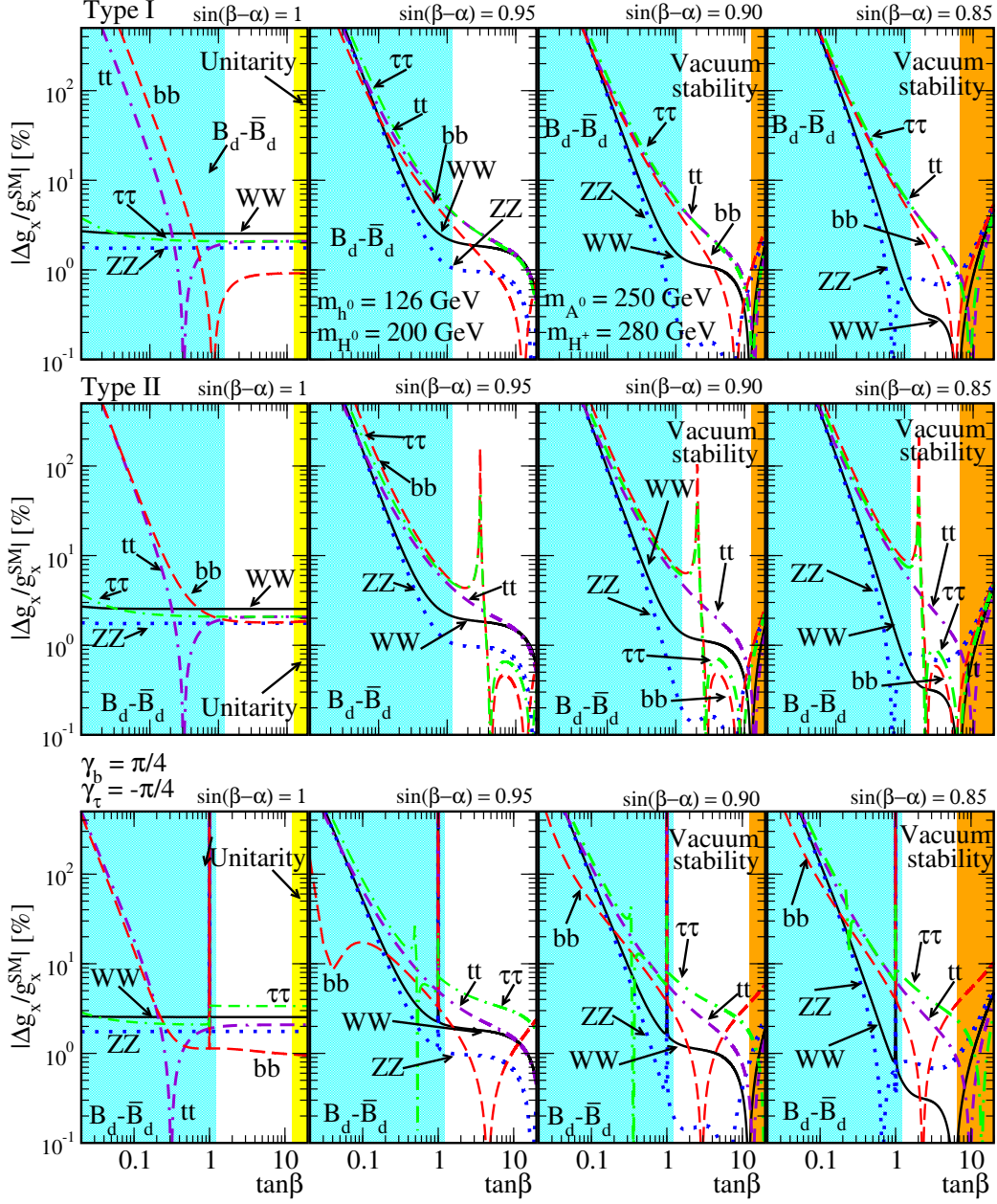


Figure 5. Loop corrections to the light Higgs couplings for type-I (top), type-II(center), and aligned configurations (bottom) as a function of $\tan\beta$. Just like in Figure 1 the latter is defined with $\gamma_{b,\tau} = \pm\pi/4$. The shaded regions are excluded by unitarity and vacuum stability as discussed in Section 2.6. The dashed area at low $\tan\beta$ is ruled out by the flavor bounds from $B_d^0 - \bar{B}_d^0$ mixing.

In passing we remark that in the supersymmetric 2HDM the situation is very different. There, the self-couplings are gauge couplings and scale like $g^2 v^2$. Consequently, heavy MSSM Higgs bosons decouple. Non-decoupling effects may arise when we break the strict type-II structure of the Yukawa couplings via enhanced quantum effects at large $\tan\beta$ [115, 116]. In the non-supersymmetric 2HDM such $\tan\beta$ -enhanced couplings appear as well, but are numerically not as relevant.

4 LHC data

In this second part of the paper we compare some of the extended Higgs sectors discussed in Section 2 to the available ATLAS and CMS measurements. For details on the corresponding Standard Model analysis and the channels included we refer to Ref. [6]. The coupling extraction is performed in the fully correlated SFITTER framework [6, 15, 117] which gives us two-dimensional correlations in the log-likelihood distributions. The difference to the best fit value defined as $-2(\log \mathcal{L} - \log \mathcal{L}_{\text{best}}) < \{1, 4, 9\}$ would in the Gaussian approximation mark the $\{1, 2, 3\}\sigma$ confidence level regions. Note that in computing error bars on the model parameters SFITTER does not use a Gaussian approximation. Correlations between the theory uncertainties are not included because the analyses in the different channels are hardly comparable and because theory errors are sub-leading at this point in time. First SFITTER studies show that the 2011-2012 coupling fit will not significantly change when we fully correlate the theory uncertainties on the production and decay sides.

After very briefly reviewing and updating the fully general Higgs coupling fit we will turn to a set of extended Higgs sectors defined according to Eq.(3.3). Quantum corrections to the Higgs couplings are not taken into account, with the exception of a charged Higgs loop in the effective Higgs–photon coupling. For all 2HDM scenarios considered this ansatz differs from the most general Higgs fit only in that $\Delta_W = \Delta_Z \equiv \Delta_V$, *i.e.* we only consider extended Higgs sectors with negligible violation of custodial symmetry. The quantum corrections analyzed in Sections 3.2 and 3.3 are not included in the fit because the current LHC data is not sensitive to such small effects. This has to be kept in mind when the naive tree-level constraints $\Delta_W = \Delta_Z$ and $\Delta_W < 0$ are reflected in the results. Moreover, when deriving Higgs couplings from extended sectors we do not enforce the usual SFITTER condition $\Delta_W > -1$ and deal with ambiguities from over-all re-rotations of the Higgs field individually.

Because the full parameter space for extended models is vast and the number of measurements is limited we adopt a number of assumptions: the lightest Higgs mass is fixed at $m_{h^0} = 126$ GeV, possibly accompanied by a single heavy mass scale for additional Higgs states $m_{H^0} \simeq m_{A^0} \simeq m_{H^\pm} \equiv M_{\text{heavy}}$. In the Higgs potential of Eq.(2.4) we assume vanishing quartic couplings $\lambda_{6,7} = 0$ and limit PQ soft-breaking contributions to the bilinear term m_{12} . For notational convenience we trade m_{12} for the self-coupling it induces after minimizing the potential,

$$\tilde{\lambda} = \frac{2m_{12}^2}{\sin \beta \cos \beta v^2}. \quad (4.1)$$

We define a few representative benchmark points with the parameter ranges given in Table 4. Electroweak and flavor physics constraints, unitarity, and vacuum stability will be discussed separately.

4.1 Free Standard Model couplings

Before we study different extended Higgs sectors we review the Higgs coupling extraction in the Standard Model. In Figure 6 we show all Higgs couplings to Standard Model particles with their best-fit central values as well as their non-Gaussian error bars. The red points indicate what we would expect using the current data sets with the given experimental and theoretical errors, but with all rate measurements fixed to the Standard Model predictions. The dark blue points assume that the dimension-5 Higgs coupling to photons, g_γ , is fully determined by Standard Model loops. Finally, for the light blue dots we allow for additional states contributing to g_γ . In this case, the quantity Δ_γ defined in Eq. (1.2) enters the fit as an additional free parameter. The dimension-5 Higgs coupling to gluons is identified with the Standard Model top contribution because there is no independent measurement of the top Yukawa available yet.

	parameters	
dark singlet	$m_s = (0 \rightarrow 65) \text{ GeV}$	$\lambda_3 = 0 \rightarrow 1$
hierarchical 2HDM	$\tan \beta = 1 \rightarrow 50$	$\xi = 0.0 \rightarrow 1.0$
general 2HDM	$\tan \beta = 0.01 \rightarrow 50$	$\sin \alpha = -1.0 \rightarrow 1.0$
	$M_{\text{heavy}} = (200 \rightarrow 1000) \text{ GeV}$	$\tilde{\lambda} = -10 \rightarrow 5$
Yukawa-aligned 2HDM	$\tan \beta = 0.01 \rightarrow 50$	$\sin \alpha = -1.0 \rightarrow 1.0$
	$M_{\text{heavy}} = (200 \rightarrow 1000) \text{ GeV}$	$\tilde{\lambda} = -10 \rightarrow 5$
degenerate spectrum	$\gamma_{b,\tau} = 0 \rightarrow 2\pi$	
	$\tan \beta = 0.01 \rightarrow 50$	$\sin \alpha = -1.0 \rightarrow 1.0$
	$M_{\text{heavy}} = (200 \rightarrow 1000) \text{ GeV}$	$\tilde{\lambda} = -10 \rightarrow 5$
	$\gamma_{b,\tau} = 0 \rightarrow 2\pi$	

Table 4. Free parameters for each benchmark fit to LHC data. Details on the model parameterizations are provided in Appendix A. For all of the benchmarks we fix the light (or twin) Higgs mass to $m_{h^0, H^0} = 126 \text{ GeV}$.

We see that there is no visible tension between the Higgs measurements and a purely Standard Model explanation. However, this outcome is not at all unexpected. The precision on the individual couplings still ranges around 20 to 50%, while typical models for physics beyond the Standard Model predict significantly smaller deviations once all other model constraints are taken into account [118]. Only strongly constrained models, like a universal Higgs coupling modification Δ_H or universal fermion and gauge coupling modifications $\Delta_{V,f}$ are restricted at a level which significantly limits their underlying toy models. As a matter of fact, for a single modification $\Delta_H = 0 \pm \mathcal{O}(10\%)$ the LHC constraints are in a similar range as electroweak precision data constraints on the weakly interacting underlying models [118].

In the following, we will discuss constraints on extended Higgs sectors, which represent consistent perturbative new physics scenarios in between the most general and extremely simplified scenarios shown in Figure 6. Eventually, the question is how close the results in the most general Yukawa-aligned 2HDM without loop corrections will be to the general fit including all Standard Model Higgs operators.

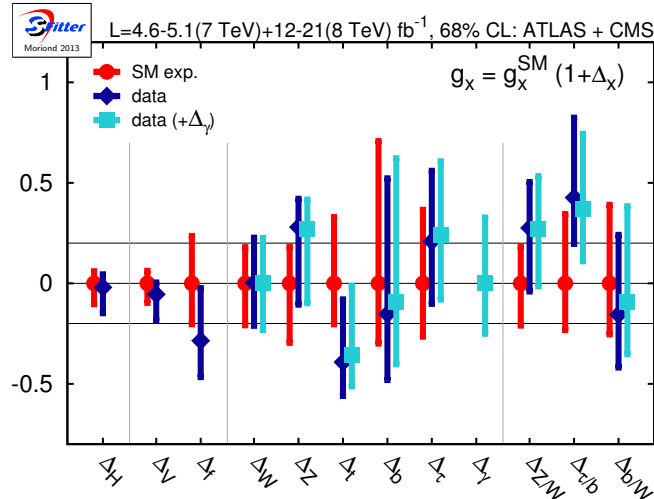


Figure 6. Higgs coupling extraction based on all ATLAS and CMS results presented until the Winter conferences 2013 in Moriond and Aspen. The results shown are a yet unpublished update of the analyses published in Ref. [6].

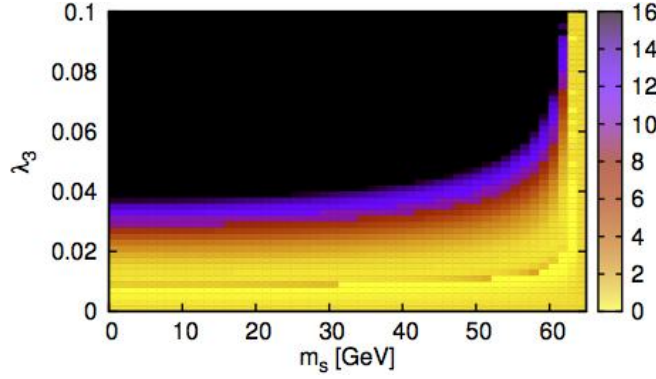


Figure 7. Correlated relative log-likelihood $-2\Delta \log \mathcal{L}$ for the dark scalar mass m_s vs the portal interaction λ_3 assuming an additional dark singlet.

4.2 Dark singlet

The lowest-dimension Lorentz and gauge invariant field combination in the Standard Model is $\Phi^\dagger \Phi$. In a minimal setup it can couple to an $SU(2)$ singlet from a hidden sector [119]. In that case the Higgs self-interactions form the only link, or portal, between the visible and the hidden domains. For an additional singlet the corresponding potential is given in Eq.(2.3). If it does not develop a second VEV it does not contribute to electroweak symmetry breaking and hence does not mix with the Higgs doublet. Nevertheless, the portal interaction $\mathcal{L} \supset \lambda_3 (\Phi^\dagger \Phi) S^2$ defined in Eq.(2.3) triggers a new triple scalar coupling. If kinematically allowed it gives rise to an invisible decay mode

$$\Gamma_{\text{inv}} \equiv \Gamma(h \rightarrow ss) = \frac{1}{32\pi m_h} \sqrt{1 - \frac{4m_s^2}{m_h^2}} \lambda_3^2 v^2. \quad (4.2)$$

It depends only on two new model parameters, the dark singlet mass and the strength of the portal interaction. In Figure 7 we show the m_s vs λ_3 correlation after confronting the model with the most recent LHC Higgs measurements. Because there are no significant LHC analyses directly probing invisible Higgs decays, we only obtain an indirect limit from the assumption that the sum of the visible and invisible partial widths forms the total Higgs width. The total Higgs width can be extracted as a common normalization factor to all predicted event rates. As expected in the absence of a signal for invisible Higgs decays, a light inert scalar is only allowed with weak portal interactions. A stronger singlet-doublet coupling $\lambda_3 \gtrsim 0.03$ is only compatible with LHC data when the invisible decay is suppressed by phase space effects.

4.3 Hierarchical 2HDM

The simplest two Higgs doublet model includes one light Higgs scalar and an approximately degenerate set of heavy states. From Eq.(2.6) we know that for $m_{H^\pm} \simeq m_{A^0}$ the custodial symmetry is protected. In the absence of significant non-decoupling effects a large mass hierarchy is trivially in agreement with the stringent B -physics bounds [64], which disfavor charged Higgs masses $m_{H^\pm} \leq 300$ GeV for a wide $\tan \beta$ range. For extended Higgs sectors such indirect flavor physics constraints are presently much stronger than constraints from direct searches.

A hierarchical 2HDM can be described by the effective field theory described in Appendix B. Its expansion parameter is $v/M_{\text{heavy}} \ll 1$ or equivalently $\xi \equiv \cos(\beta - \alpha) \simeq v^2/M_{\text{heavy}}^2$. The consistency condition $\xi < 1$ needs to be taken into account in the discussion of the results. It immediately forbids sign changes in Higgs couplings $\Delta_x \simeq -2$. We assume natural flavor conservation and separately examine

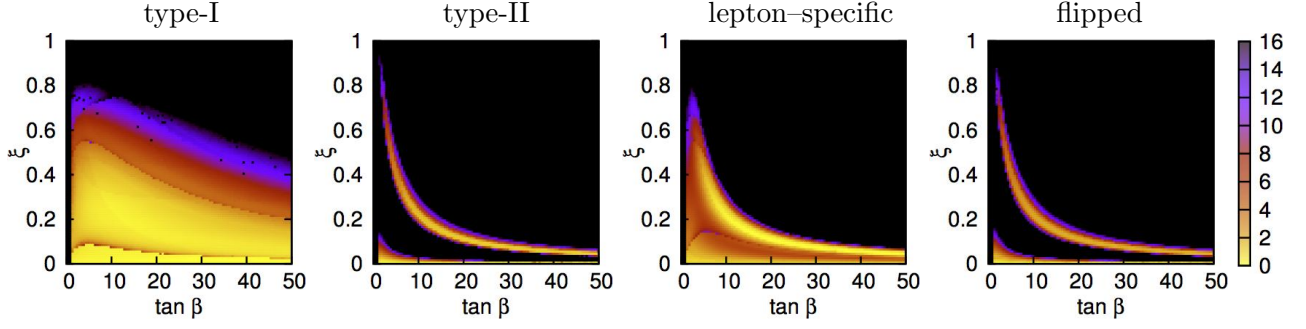


Figure 8. Correlated relative log-likelihood $-2\Delta \log \mathcal{L}$ for $\tan \beta$ vs ξ , assuming a hierarchical 2HDM with natural flavor conservation.

the type-I, type-II, lepton-specific, and flipped setups discussed in Section 2.2. They are initially characterized by four parameters, leading to coupling shifts

$$\Delta_f(\tan \beta, \xi) \quad \Delta_V(\tan \beta, \xi) \quad \Delta_\gamma(\tan \beta, \xi, m_{H^\pm}^2(\xi), \tilde{\lambda}(\xi)) . \quad (4.3)$$

Only two of them turn out to be independent, which we take to be the VEV ratio $\tan \beta$ and the decoupling parameter ξ . By construction, the heavy Higgs mass and the self-coupling $\tilde{\lambda}$ are fixed at

$$M_{\text{heavy}}^2 = \frac{v^2}{\xi} \quad \text{and} \quad \tilde{\lambda} v^2 \simeq m_{h^0}^2 + 2M_{\text{heavy}}^2 . \quad (4.4)$$

This guarantees that the light Higgs boson self-interactions to the heavy fields exhibit a consistent $\mathcal{O}(\xi)$ behavior in the decoupling limit, as discussed in Appendix B. The parameter ranges are defined in Table 4.

In Figure 8 we show the likelihood correlations for the hierarchical 2HDM fit to LHC data. The favored regions are particularly clear for type-II and flipped 2HDM models, where the top and bottom Yukawas are largely independent when we vary $\tan \beta$ and ξ . This enhanced flexibility allows for an easier convergence to parameter regions preferred by the LHC results.

As derived in Appendix B the correlation between $\tan \beta$ and ξ follows the line $\xi \sim \tan \beta / (1 + \tan^2 \beta)$ for $\tan \beta \gg 1$. For the Yukawa couplings in type-II and flipped models large deviations in ξ only occur at relatively small $\tan \beta$, because simultaneously large $|\xi|$ and $\tan \beta$ values would lead to too large shifts in the bottom and tau Yukawas. The gauge boson couplings scale as $\Delta_V \sim -\xi^2/2$, which means that typical allowed deviations $|\Delta_V| \lesssim 0.2$ correspond to $\xi \lesssim 0.63$.

Type-I models are less efficient in profiling the LHC measurements, so their parameters are less clearly constrained. We will come back to this kind of effect when comparing the fits to the different models. In all setups of the hierarchical 2HDM the LHC measurements broadly prefer $\xi \lesssim 0.4$, possibly correlated with $\tan \beta$ and entirely consistent with the original assumption $\xi < 1$ underlying our effective theory.

The sub-leading charged Higgs parameters can be tested by computing the correlated Δ_γ and Δ_W ranges. We find that we are limited to $\Delta_\gamma = 0 \dots 0.1$ with preferred $\Delta_W < 0$, except for type-I models. There, the scan over the model parameters fills the generally allowed range $\Delta_\gamma = -0.3 \dots 0.3$ shown in Figure 6. This is in line with the also broader $\Delta_\gamma^{\text{SM}}$ range which results from the wider shifts in the top Yukawas.

In Table 5 we show the single best-fit parameter points for the hierarchical 2HDM. We do not quote error bars on the individual parameters because of the strong correlations shown in Figure 8.

	unconstrained				constrained			
	type-I	type-II	lepton	flipped	type-I	type-II	lepton	flipped
$\tan \beta$	24.0	19.9	16.4	36.9	10.6	9.2	14.2	13.9
ξ	0.000	0.000	0.134	0.000	0.000	0.000	0.002	0.000
Δ_V	0.000	0.000	-0.009	0.000	0.000	0.000	0.000	0.000
Δ_t	0.000	0.000	-0.001	0.000	0.000	0.000	0.000	0.000
Δ_b	0.000	0.000	-0.001	0.000	0.000	0.000	0.000	0.000
Δ_τ	0.000	0.000	-2.208	0.000	0.000	0.000	-0.030	0.000
Δ_γ	0.000	0.000	-0.055	0.000	0.000	0.000	-0.001	0.000
$\Delta_\gamma^{\text{tot}}$	0.000	0.000	-0.074	0.000	0.000	0.000	-0.001	0.000
$-2 \log \mathcal{L}$	31.7	31.7	30.8	31.7	31.7	31.7	31.6	31.7

Table 5. Best-fit parameter points for the hierarchical 2HDM. Separate results are shown for a fully unconstrained fit (left columns) and after we include the theoretical and experimental bounds as fit priors (right columns).

Not surprisingly, the best log-likelihood is reached in the $\xi \rightarrow 0$ limit. The results highlight a clear preference for a SM-like pattern with vanishing coupling deviations within numerical precision. A slightly improved log-likelihood value we can only achieve for the lepton-specific setup. Here, the tau Yukawa can be adjusted independently of the quark Yukawas, which allows us to accommodate the central values $\Delta_\tau > 0$ and $\Delta_{b,t} \lesssim 0$ in the general couplings fit — at the expense of a simultaneously larger deviation from $\Delta_V \simeq -\xi^2/2 \rightarrow 0$. Nevertheless, the general agreement of the LHC measurements with the hierarchical 2HDM is satisfactory.

In practice, vacuum stability precludes $\tan \beta \gtrsim 15$ for a hierarchical spectrum in the $\xi \rightarrow 0$ limit. Similar constraints follow from self-coupling perturbativity. This explains the downward shift in the favored $\tan \beta$ values, once the model constraints are included in the fit. A consistent $\tan \beta \gg 1$ limit can only be reached in this benchmark if $\lambda_7 \neq 0$ [100].

4.4 General 2HDM

In the next step we release the assumption of decoupled heavy Higgs states and instead vary their common single mass parameter as $M_{\text{heavy}} = 200 \dots 1000$ GeV. By the same token, we no longer impose the decoupling condition $\cos(\beta - \alpha) \rightarrow 0$ and allow for an independent variation of both mixing angles. The individual coupling shifts are based on four independent model parameters,

$$\Delta_f(\tan \beta, \sin \alpha) \quad \Delta_V(\tan \beta, \sin \alpha) \quad \Delta_\gamma(\tan \beta, \sin \alpha, m_{H^\pm}^2, \tilde{\lambda}) . \quad (4.5)$$

The $\sin \alpha$ and $\tan \beta$ ranges given in Table 4 cover the whole range of modified Yukawas, including sign flips. The range of $\tan \beta$ is severely constrained by flavor physics, disfavoring $\tan \lesssim 1$ as well as large $\tan \beta$ values. Barring the type-I models, charged Higgs bosons below 300 GeV tend to be also ruled out. As for the $\tilde{\lambda}$ range, large (negative) values are excluded by unitarity, while the upper (positive) edge is constrained by vacuum stability.

In Figure 9 we show how a 2HDM with a single variable heavy Higgs mass describes the current LHC data. The preferred regions in the $\tan \beta$ vs $\sin \alpha$ plane are similar to those for the hierarchical spectrum displayed in Figure 8. They cover the entire $\tan \beta$ range with some preference for moderately small values. The second mixing angle $\sin \alpha$ spans a correlated symmetric range $\sin^2 \alpha \sim 1/(1 + \tan^2 \beta)$, reflecting the decoupling condition $\cos(\beta - \alpha) \rightarrow 0$ discussed in Appendix B.

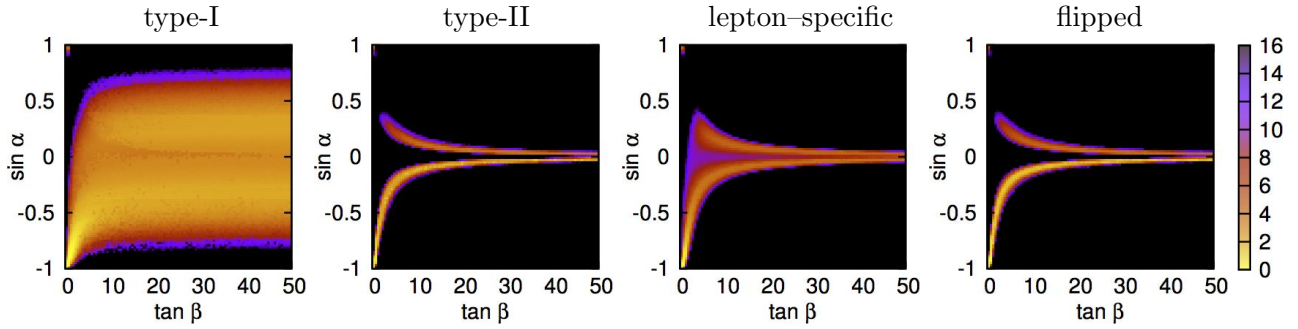


Figure 9. Correlated relative log-likelihood $-2\Delta \log \mathcal{L}$ for $\tan \beta$ vs $\sin \alpha$ ranges assuming a general 2HDM with a common heavy Higgs mass scale and natural flavor conservation.

The best-fit parameter points for $\tan \beta < 1$ and $\tan \beta > 1$ are separately quoted in Table 6. First, we focus on the results for the unconstrained fit. The absolute best-fit point lies at $\sin \alpha \simeq -1$ and, with the exception of the type-I setup, $\tan \beta < 1$. The sign of the mixing angle α is linked to the sign of the Yukawa couplings, which for the bottom quark and the tau lepton is not determined by LHC data. Only for the top Yukawa the destructive interference in the effective Higgs-photon coupling resolves this sign ambiguity. The larger best-fit value of $\tan \beta$ in type-I models can be traced to competing effects in this strongly constrained setup: in all fits data prefers tiny deviations of $\Delta_V \ll 0.1$. In type-I models the central value is pulled down to $\Delta_V = -0.037$. At the same time the shift in the top Yukawa, scaling like $\Delta_t \sim \cos(\beta - \alpha)/\tan \beta$, prefers to be negative and small. This moves the very small $\tan \beta$ values towards unity. Conversely, for the type-II 2HDM the value $\Delta_V \simeq 0$ pulls towards $\tan \beta = \mathcal{O}(0.1)$. The preference for small finite coupling shifts to the top-quark and the other heavy fermions also explains the preference for $\tan \beta \simeq 1$ for all models when we focus on the $\tan \beta > 1$ range.

It is useful to translate the favored 2HDM configurations into the associated coupling strength deviations, illustrated in Figure 10. We see that in the fermion sector type-II and flipped realizations show a slight preference for enhanced couplings to the bottom quarks, staying either way in the SM-like region $\Delta_b \sim 0$. All of the remaining cases favor a mild suppression, and neatly peak around the decoupling limit $\Delta_V \simeq 0$. The largest deviation from the decoupling limit we find for type-I and lepton-specific models. This reflects the more constrained nature of their correlated top and bottom Yukawa couplings. This is also the reason for a tendency towards a slightly larger negative Δ_t in the same models.

When the tau Yukawa can be shifted independently, like in the lepton-specific setup, the data prefers a slight positive deviation $\Delta_\tau \gtrsim 0$. This is in line with the general Standard Model fit from Figure 6 and stems from the mild CMS excess in the $\tau\tau$ search channel. Correspondingly, an independent tau Yukawa turns out to be key to improve the overall fit quality. As seen in Table 6 the lepton-specific 2HDM yields a best-fit log-likelihood value $-2\log \mathcal{L} \simeq 27.2$, which is roughly as good as the values for a general Yukawa alignment, as will be discussed next.

In addition to the best fit regions centered around the SM-like solution $\Delta_x \simeq 0$ our results also spotlight additional solutions including a sign-flipped bottom Yukawa $\Delta_b \lesssim -2$ at $\Delta_W > 0$ in Figure 10 or $\Delta_{b,W} \lesssim -2$ corresponding to SM-like coupling strengths with opposite signs relative to the top Yukawa. All these observations are in agreement with the literature [57].

Aside from the two key parameters which affect all coupling shifts we also examine the impact of the charged Higgs mass $m_{H^\pm} = M_{\text{heavy}}$ and the self-coupling $\tilde{\lambda}$ corresponding to the PQ-breaking scale m_{12}^2 , Eq.(4.1). They determine the charged Higgs contribution Δ_γ , which can be sizable for $m_{H^\pm} \lesssim 300$ GeV and/or $|\tilde{\lambda}| \gtrsim \mathcal{O}(5)$. The bulk of the scanned m_{H^\pm} - $\tilde{\lambda}$ plane is allowed and carries

	unconstrained				constrained			
	type-I	type-II	lepton	flipped	type-I	type-II	lepton	flipped
$\tan \beta < 1$	0.920	0.115	0.594	0.270	0.999	0.816	0.976	0.857
$\sin \alpha$	-0.891	-0.996	-0.950	-0.975	-0.859	-0.826	-0.866	-0.814
M_{heavy}	614.7	202.3	220.2	243.5	608.0	624.0	627.8	607.0
$\tilde{\lambda}$	-8.19	4.49	-2.31	4.63	3.14	2.17	4.11	1.50
Δ_V	-0.037	0.000	-0.024	-0.001	-0.031	-0.003	-0.031	-0.004
Δ_t	-0.328	-0.213	-0.387	-0.150	-0.276	-0.108	-0.284	-0.107
Δ_b	-0.328	0.003	-0.387	0.010	-0.276	0.066	-0.284	0.072
Δ_τ	-0.328	0.003	0.105	-0.150	-0.276	0.066	0.210	-0.107
Δ_γ	-0.082	0.098	-0.124	0.057	-0.038	-0.043	-0.035	-0.046
$\Delta_\gamma^{\text{tot}}$	-0.043	0.155	-0.052	0.096	-0.005	-0.019	0.002	-0.022
$-2 \log \mathcal{L}$	28.8	28.7	26.6	29.2	28.9	30.5	27.1	30.8
$\tan \beta > 1$	1.000	1.051	1.000	1.000	1.324	1.491	1.093	2.918
$\sin \alpha$	-0.878	-0.746	-0.862	-0.756	-0.842	-0.574	-0.829	-0.340
M_{heavy}	783.4	215.2	959.1	234.7	412.1	356.4	565.4	378.5
$\tilde{\lambda}$	-8.49	5.00	5.00	4.91	-0.65	4.11	3.03	4.68
Δ_V	-0.045	-0.003	-0.032	-0.003	-0.062	0.000	-0.028	0.000
Δ_t	-0.322	-0.080	-0.283	-0.075	-0.324	-0.014	-0.242	-0.006
Δ_b	-0.322	0.082	-0.283	0.069	-0.324	0.031	-0.242	0.049
Δ_τ	-0.322	0.082	0.219	-0.075	-0.324	0.031	0.228	-0.006
Δ_γ	-0.070	0.071	-0.041	0.082	-0.057	-0.004	-0.036	-0.002
$\Delta_\gamma^{\text{tot}}$	-0.037	0.131	-0.007	0.099	-0.052	0.000	-0.007	-0.001
$-2 \log \mathcal{L}$	28.8	29.7	27.2	29.8	28.9	30.8	27.1	30.7

Table 6. Best-fit parameter points for the general 2HDM with a variable single heavy Higgs mass M_{heavy} , computed for $\tan \beta < 1$ (top panel) and $\tan \beta > 1$ (down panel). Separate results are shown for a fully unconstrained fit (left columns) and after we include the theoretical and experimental bounds as fit priors (right columns).

no significant log-likelihood variation. Small shifts of the tree-level couplings always provide excellent agreement with the LHC results within given uncertainties. In the bottom panels of Figure 10 we examine the charged Higgs effect on Δ_γ by correlating it with Δ_V . While centered at $\Delta_V = 0$, the statistically preferred region spans the range $\Delta_\gamma = -0.5 \dots 0.1$ to 2σ , in particular for the type-I 2HDM. We also find a secondary solution around $\Delta_V = -2$ related to the sign shift in the top Yukawa. This solution is by definition absent in the hierarchical 2HDM.

The theoretical and experimental constraints described in Section 2.2, including electroweak precision and flavor observables, Higgs mass exclusion limits, perturbative unitarity and vacuum stability are accounted for in the right columns of Table 6. As anticipated, values of $\tan \beta \ll 1$ are ruled out by flavor observables, like $B_d^0 - \bar{B}_d^0$ mixing. The charged Higgs boson contribution to this process scales like $1/\tan^4 \beta$, common to all of the natural flavor conserving models. When we focus on the $\tan \beta < 1$ region this pushes the constrained best-fit solutions towards $\tan \beta \simeq 1$. Even in the $\tan \beta > 1$ region the preferred values are slightly shifted and now fall in the $\tan \beta \simeq 1.5$ ball-park. This is below the large $\tan \beta$ range which would lead to enhanced bottom and tau Yukawas in type-II, lepton-specific and flipped models, and which is severely limited $\text{BR}(b \rightarrow s\gamma)$. Similarly, the unitarity and the vacuum stability conditions do not feature. These flavor constraints unify the heavy Higgs mass M_{heavy} and self-coupling $\tilde{\lambda}$ ranges in the different setups. Electroweak precision constraints play no role as long as the model setup essentially respects the custodial symmetry. As a further consequence, the com-

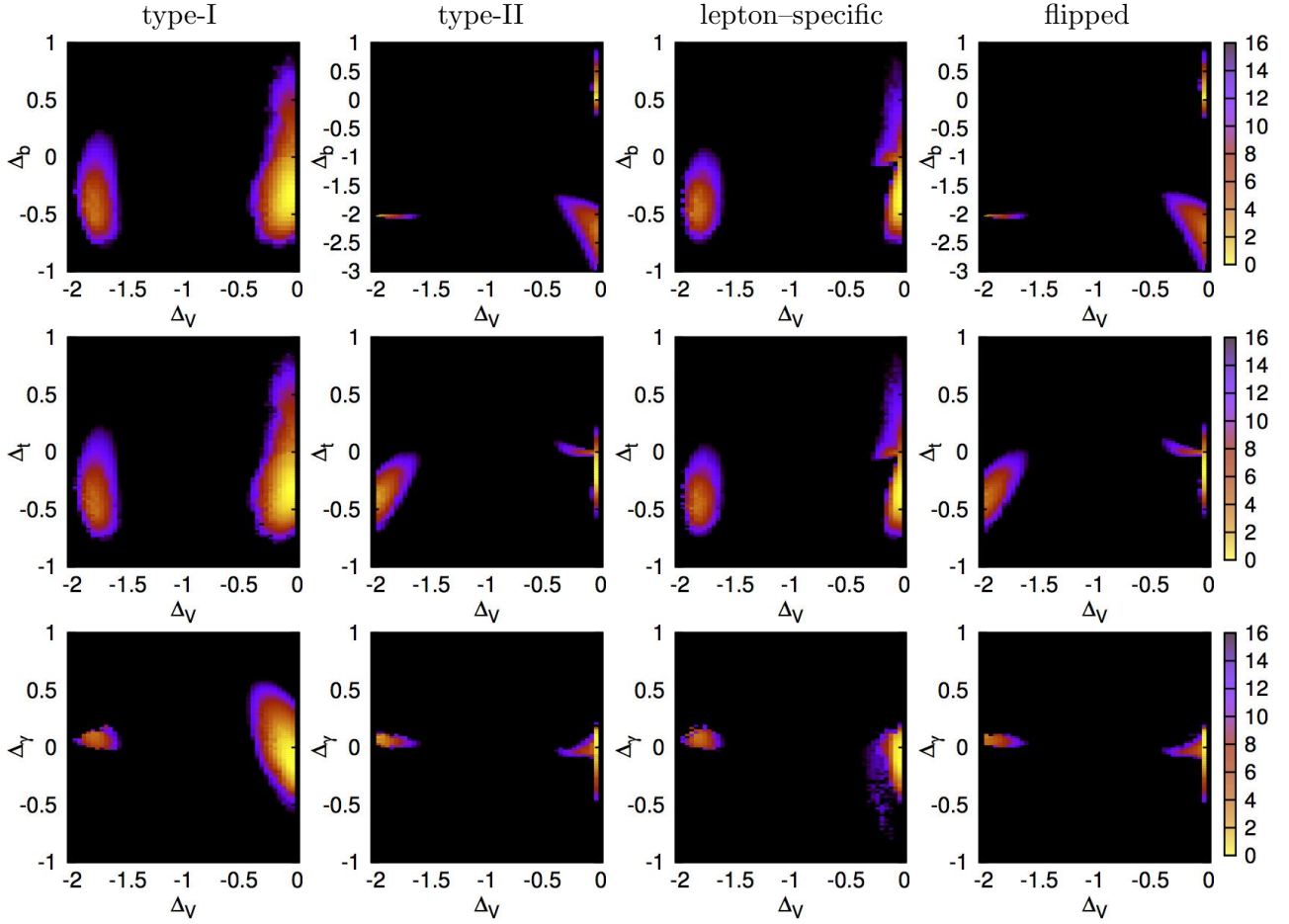


Figure 10. Correlated relative log-likelihood $-2\Delta \log \mathcal{L}$ for Δ_W vs Δ_b (top row), Δ_W vs Δ_t (center row), and Δ_W vs Δ_γ (bottom row) assuming a general 2HDM with natural flavor conservation.

patibility with all these additional constraints eliminates secondary solutions with sign-flipped quark Yukawas.

4.5 Yukawa-aligned 2HDM

The final step towards a fully independent Higgs couplings determination in a consistent 2HDM framework replaces the natural flavor conservation hypothesis with the more general Yukawa alignment described in Section 2.2. The third-generation Yukawas can now be shifted independently through the angles $\gamma_{b,\tau}$ defined in Table 10. The different Higgs couplings are functions of 6 independent model parameters, namely

$$\begin{aligned} \Delta_t(\tan \beta, \sin \alpha) & \quad \Delta_b(\tan \beta, \sin \alpha, \gamma_b) & \quad \Delta_\tau(\tan \beta, \sin \alpha, \gamma_\tau) \\ \Delta_V(\tan \beta, \sin \alpha) & \quad \Delta_\gamma(\tan \beta, \sin \alpha, m_{H^\pm}^2, \tilde{\lambda}, \gamma_b, \gamma_\tau) . \end{aligned} \quad (4.6)$$

The results of the corresponding fit to data are shown in Figure 11. We find broad allowed regions in the $\sin \alpha$ vs $\tan \beta$ plane, with a slight preference for low $\tan \beta$ values and $\sin \alpha < 0$. The log-likelihood profiles are relatively smooth under variations of $\gamma_{b,\tau}$. In the upper panels of Figure 11 the sign degeneracy in g_b and g_τ is clearly manifest as a twofold strip in the $\gamma_{b,\tau}$ vs $\tan \beta$ plane and a double-sided lobular area in the $\gamma_{b,\tau}$ vs $\sin \alpha$ plane. By the same token, we find corresponding excluded strips and oval-shaped areas for the parameter space regions with overly suppressed Yukawa interactions.

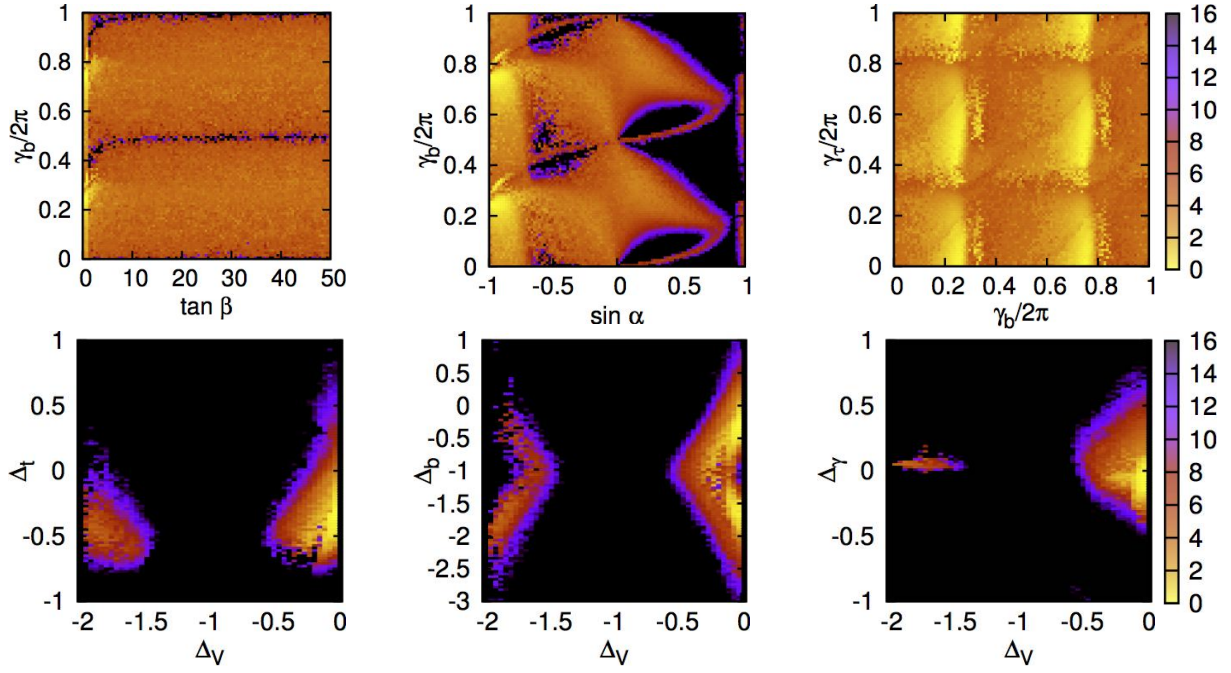


Figure 11. Correlated relative log-likelihood $-2\Delta \log \mathcal{L}$ for different pairs of parameters (top row) and coupling shifts (bottom row), assuming a 2HDM with Yukawa alignment.

In the lower panels of Figure 11 we illustrate multifarious deviations of the Yukawas with respect to the Standard Model, including enhancements, suppressions, and sign flips. Unlike for natural flavor conservation data now favors $\Delta_{b,t} \lesssim 0$, while the mild $\tau\tau$ excess points to $\Delta_\tau \gtrsim 0$.

For the effective Higgs coupling to photons our fit remains at $|\Delta_\gamma| \lesssim 0.2$. The correlation between Δ_γ and Δ_V in Figure 11 follows from an interplay of the interferences. The experimentally favored SM-like profile $\Delta_\gamma^{\text{tot}} \simeq 0$ can be realized in the general 2HDM in different ways: first, there can be

	unconstrained		constrained	
	$\tan \beta < 1$	$\tan \beta > 1$	$\tan \beta < 1$	$\tan \beta > 1$
$\tan \beta$	0.338	1.231	0.890	1.324
$\sin \alpha$	-0.977	-0.871	-0.900	-0.810
$\gamma_b/(2\pi)$	0.744	0.261	0.732	0.267
$\gamma_\tau/(2\pi)$	0.389	0.070	0.542	0.678
M_H	750.5	257.3	587.2	487.4
$\tilde{\lambda}$	-3.00	0.44	3.80	2.88
Δ_V	-0.006	-0.069	-0.038	-0.044
Δ_t	-0.332	-0.367	-0.345	-0.265
Δ_b	-0.298	-0.412	-0.281	-0.318
Δ_τ	0.176	0.107	0.099	-0.102
Δ_γ	-0.058	-0.045	-0.034	-0.031
$\Delta_\gamma^{\text{tot}}$	0.023	-0.036	0.009	-0.017
$-2 \log \mathcal{L}$	26.6	26.9	27.1	28.5

Table 7. Best-fit parameter points for the 2HDM with Yukawa alignment. Separate results are shown for a fully unconstrained fit (left columns) and after we include the theoretical and experimental bounds as fit priors (right columns).

consistently small deviations $\Delta_{f,V,\gamma} \simeq 0$, including a heavy and/or weakly coupled charged Higgs. Second, we can reduce Δ_W and Δ_t by similar finite amounts while keeping a negligible charged Higgs contribution. Third, we can slightly reduce g_t , preserve $\Delta_V \simeq 0$, and allow for a tempered charged Higgs contribution. Finally, we fix $\Delta_W \simeq -2$ together with a sign-flipped top Yukawa. These options are nicely visible in the log-likelihood correlation in the right lower panel of Figure 11, including the strip $\Delta_\gamma = -0.5 \dots +0.5$ with $\Delta_W \simeq 0$.

The best-fit central values for the coupling deviations in the Yukawa-aligned 2HDM are shown in Table 7. In line with the observations we have made for the natural flavor conserving 2HDM benchmarks, the constrained fit solutions shift the preferred $\tan \beta$ values upwards because the region $\tan \beta \simeq 0.1$ is in tension with $B_d^0 - \bar{B}_d^0$ mixing results. Once all the theoretical and phenomenological restrictions are included as fit priors, the preferred configurations feature $\tan \beta \simeq 1$, $\sin \alpha \simeq -1$, a wide range of Yukawa alignment angles $\gamma_{b,\tau}$, and heavy charged Higgs bosons, in particular for $\tan \beta < 1$. None of the coupling deviations is substantially altered with respect to the unconstrained fit. This result starts looking much more like a general coupling fit because the number of model parameters in the aligned 2HDM is identical to a general fit of all Standard Model coupling structures, with the exception of $\Delta_W = \Delta_Z$. We will show the direct comparison of the two approaches in the Summary.

4.6 Degenerate spectrum

So far, we have interpreted the LHC measurements in terms of models where only one state contributes to the observed Higgs resonance. We can depart from this hypothesis and entertain the possibility of two mass-degenerate CP-even states h^0, H^0 , both contributing to the same signal strength. Technically, we assume a very small splitting $m_{H^0} = m_{h^0} + \delta m$, to avoid the parameter space singularity at $m_{h^0} = m_{H^0}$ [100]. Away from this singular point, the two neutral CP-even mass-eigenstates and the respective mixing angle α are well defined. On the other hand, if δm is below the experimental resolution, both states can in practice be viewed as mass-degenerate. We begin by focusing our degenerate spectrum fits to the type-I and type-II natural flavor conserving 2HDMs, which we next compare to the more flexible Yukawa-aligned setup. The type-I setup, where the second Higgs scalar does not couple to fermions at all, can be viewed as an effective low-energy realization of the GUT-based extended Higgs sectors described in Section 2.5. The parameter regimes giving the best fit results are summarized in Tables 8-9. The relevant correlations among the model parameters are shown in Figure 12.

Type-I models exhibit a rather featureless log-likelihood spanning the entire $\tan \beta$ vs $\sin \alpha$ plane. Optimal agreement to data is achieved for two separate strips. One of them corresponds to $\sin \alpha \simeq 0$

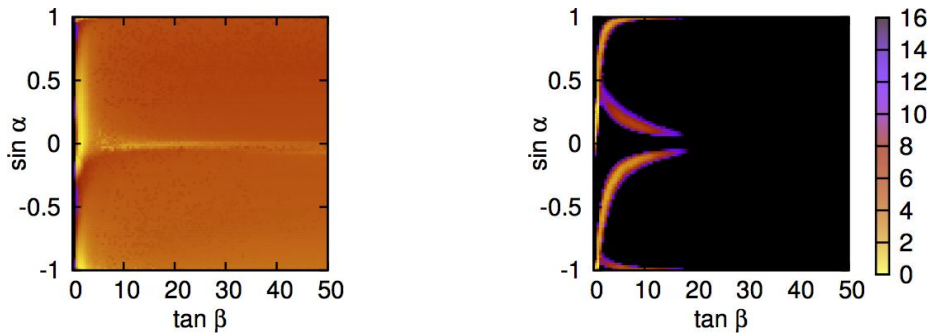


Figure 12. Correlated relative log-likelihood $-2\Delta \log \mathcal{L}$ for $\tan \beta$ vs $\sin \alpha$ ranges for a type-I 2HDM (left) and type-II 2HDM (right) with degenerate mass spectrum.

	type-I				type-II			
	unconstrained		constrained		unconstrained		constrained	
	$\tan \beta < 1$	$\tan \beta > 1$	$\tan \beta < 1$	$\tan \beta > 1$	$\tan \beta < 1$	$\tan \beta > 1$	$\tan \beta < 1$	$\tan \beta > 1$
$\tan \beta$	0.987	1.646	0.990	1.568	0.570	1.921	0.836	1.325
$\sin \alpha$	-0.139	-1.000	-0.783	0.014	0.303	-0.516	-0.806	0.774
M_H	364.4	545.7	646.8	622.5	200.0	226.4	608.2	570.2
$\tilde{\lambda}$	0.67	1.27	1.03	0.26	4.96	4.86	-1.86	0.81
$\Delta_V(h)$	-0.205	-0.471	-0.006	-0.165	-0.791	-0.002	-0.002	-0.960
$\Delta_t(h)$	0.409	-0.987	-0.115	0.186	0.924	-0.034	-0.077	-0.207
$\Delta_b(h)$	0.409	-0.987	-0.115	0.186	-1.348	0.118	0.051	-2.286
$\Delta_\tau(h)$	0.409	-0.987	-0.115	0.186	-1.348	0.118	0.051	-2.286
$\Delta_\gamma(h)$	-0.037	-0.022	-0.048	-0.042	0.133	0.097	-0.060	0.115
$\Delta_\gamma^{\text{tot}}(h)$	-0.405	-0.362	-0.025	-0.300	-0.871	0.105	-0.041	-0.818
$\Delta_V(H)$	-0.393	-1.849	-1.108	-0.450	-0.022	-1.062	-1.063	-0.001
$\Delta_t(H)$	-1.198	-2.170	-2.112	-0.983	-0.389	-1.582	-2.257	-0.031
$\Delta_b(H)$	-1.198	-2.170	-2.112	-0.983	0.097	0.855	-0.229	0.052
$\Delta_\tau(H)$	-1.198	-2.170	-2.112	-0.983	0.097	0.855	-0.229	0.052
$\Delta_\gamma(H)$	-0.028	0.040	0.005	-0.028	0.112	0.089	0.006	-0.048
$\Delta_\gamma^{\text{tot}}(H)$	-0.214	-0.261	-0.849	-0.343	0.190	-0.828	-0.739	-0.041
$-2 \log \mathcal{L}$	27.4	26.6	29.1	26.9	27.7	29.6	29.8	30.3

Table 8. Best-fit parameter points for the 2HDM with degenerate spectrum, considering type-I (left columns) and type-II Yukawa structures (right columns). Both sets of Δ_x are defined as deviations from the Standard Model couplings.

and extends to very large $\tan \beta$ values. It accommodates large variations in $\Delta_V(h^0) \sim \sin(\beta - \alpha)$. Large departures from the decoupling limit $\sin(\beta - \alpha) \rightarrow 1$ are protected by the unitarity sum rule $g_{VVh^0}^2 + g_{VVH^0}^2 = (g_{VVH}^{\text{SM}})^2$. In contrast, the Yukawas barely deviate from the Standard Model, because the additional Higgs field is by construction fermiophobic, $g_{ffH^0} \sim \sin \alpha / \sin \beta \sim 0$, as long as α is small.

A second favored configuration emerges at $\tan \beta \lesssim 1$ and either $\sin \alpha \simeq -1$ or $\sin \alpha = 0 \dots 0.5$. The absolute best fit point at maximal mixing $\sin \alpha = -1$ for $\tan \beta > 1$ is no longer allowed after all the model bounds are imposed. The constrained fit instead favors the small mixing angle regions. In the $\tan \beta < 1$ range the situation is the opposite; the best fit point mildly shifts towards $\tan \beta \simeq 1$ with a stronger mixing among the two Higgs doublets, $|\sin \alpha|$.

Again, we can switch from the analysis of the model parameters to the coupling shifts. In the upper panels of Figure 13 we display the correlated deviations in $\Delta_V(h^0)$ vs $\Delta_{t/b/\gamma}(h^0)$. Systematic suppressions in the h^0 couplings are balanced by H^0 , both contributing to the 126 GeV signal. The strongly correlated variations manifest as a thumb-print-shaped area, and can be tracked analytically by

$$(1 + \tan^2 \beta) \Delta_V^2(h^0) + 2(1 - \tan^2 \beta \Delta_{t/b}(h^0)) \Delta_V(h^0) + \tan^2 \beta \Delta_{t/b}^2(h^0) = 0, \quad (4.7)$$

which follows from the parameter dependencies of the coupling shifts $\Delta_{V,t/b}$ and the unitarity sum rules relating $\Delta(h^0)$ and $\Delta(H^0)$ (2.17). Two limiting cases are

$$\begin{aligned} \Delta_V^2(h^0) &\simeq -\frac{\Delta_f^2(h^0)}{2} && \text{for } \tan \beta \simeq 1 \\ \Delta_V(h^0) &\simeq \Delta_f(h^0) && \text{for } \tan \beta \gg 1. \end{aligned} \quad (4.8)$$

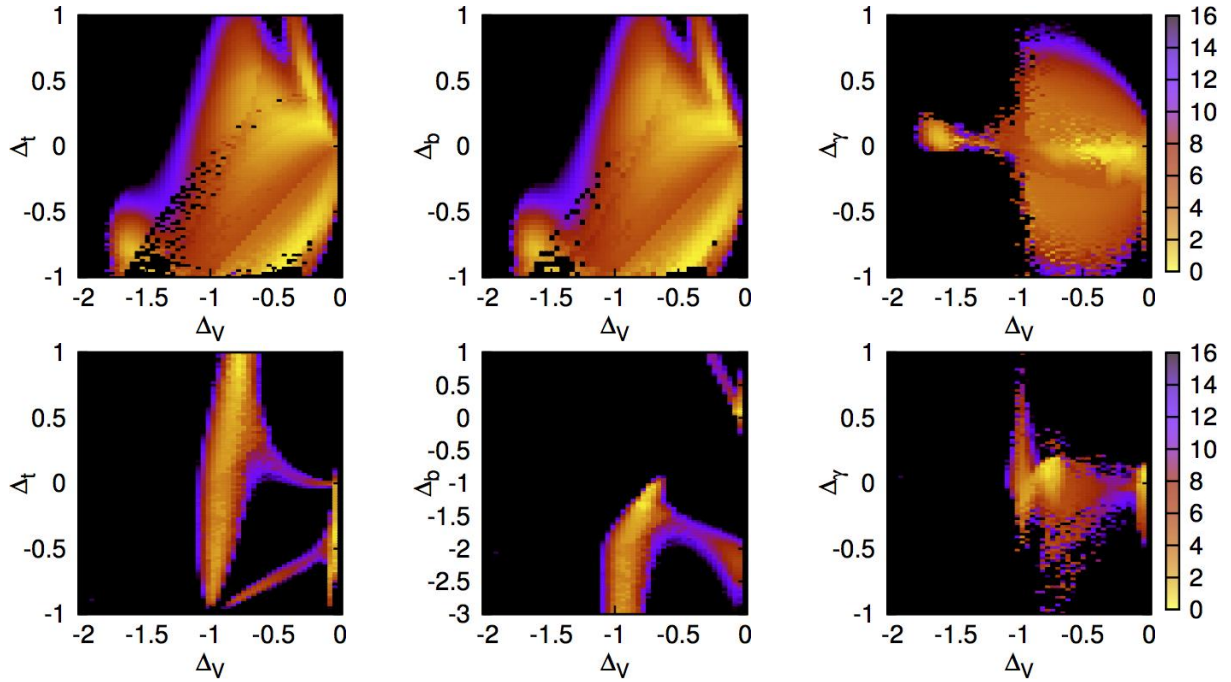


Figure 13. Correlated relative log-likelihood $-2\Delta \log \mathcal{L}$ for different pairs of assuming a type-I 2HDM (top row) and type-II 2HDM (bottom row) with degenerate mass spectrum.

The first relation describes an ellipse in the $\tan \beta$ vs $\sin \alpha$ plane, whereas the second relation corresponds to the diagonal line crossing the best fit area.

As for the Higgs–photon coupling we see charged Higgs–mediated contributions extending over a rather symmetric range $\Delta_\gamma(h^0) \simeq \pm 0.5$, with best fit configurations neatly peaking around $\Delta_\gamma(h^0) \simeq 0$, and well compatible with large departures from the decoupling limit.

Type-II models allow for separate shifts of the top and bottom Yukawa couplings to h^0 and H^0 . This typically leaves us with sharper log-likelihood profiles and more focused statistically preferred regions. Moreover, they may give rise to enhanced Yukawas which are severely limited by the LHC observation, as well as by the flavor constraints.

In terms of the model parameters, the best-fit solutions split into two separate classes, with interpolating areas in between. On the one hand we identify the usual $\sin^2 \alpha \simeq 1/(1 + \tan^2 \beta)$ pattern following the decoupling condition. The two-fold degeneracy stems from the sign ambiguity in the bottom and tau Yukawas. The narrow band around the no-mixing limit $\sin \alpha \simeq 0$ for $\tan \beta > 1$ would lead to an overly enhanced bottom quark Yukawa to the additional scalar field, $g_{bbH^0} \sim \cos \alpha / \cos \beta$. The $|\sin \alpha| \gtrsim 0.5$ areas for $\tan \beta \gtrsim 5$ would yield exceedingly large rates due to the combined contributions from both h^0, H^0 states. On the other hand, we find additional solutions for sizeable neutral Higgs mixing and away from the decoupling condition. They correspond to $|\sin \alpha| > 0.5$ and a more or less constrained $\tan \beta$ range — up to $\tan \beta \simeq 10$ for maximal mixing $\sin \alpha = \pm 1$.

When viewed as correlated coupling shifts, we recognize the SM-like profile $\Delta_V \simeq \Delta_f \simeq 0$ over the entire decoupling regime $\sin^2 \alpha \simeq 1/(1 + \tan^2 \beta)$. In addition, novel solutions departing from $\Delta_V \simeq 0$ lead to suppressed top Yukawas, $\cos \alpha / \sin \beta < 1$. For large $\tan \beta$ and $\sin \alpha$, these variations are linearly correlated, as shown in Eq.(4.8). Similarly, the different best fit $\sin \alpha$ vs $\tan \beta$ configurations away from

	Yukawa alignment			
	unconstrained		constrained	
	$\tan < 1$	$\tan \beta > 1$	$\tan \beta < 1$	$\tan \beta > 1$
$\tan \beta$	0.404	1.651	0.988	1.509
$\sin \alpha$	0.023	0.148	-0.961	-0.986
γ_b	0.149	0.275	0.218	0.752
γ_τ	0.959	0.137	0.180	0.120
M_H	425.6	390.2	661.7	397.0
$\tilde{\lambda}$	-1.35	3.79	-0.60	2.49
$\Delta_V(h)$	-0.647	-0.231	-0.122	-0.315
$\Delta_t(h)$	1.669	0.156	-0.606	-0.797
$\Delta_b(h)$	-0.067	0.307	-0.440	-0.814
$\Delta_\tau(h)$	-1.350	-0.336	-0.298	-0.145
$\Delta_\gamma(h)$	-0.039	-0.023	-0.047	-0.014
$\Delta_\gamma^{\text{tot}}(h)$	-0.685	-0.358	-0.042	-0.203
$\Delta_V(H)$	-0.064	-0.361	-1.478	-1.728
$\Delta_t(H)$	-0.938	-0.827	-2.367	-2.182
$\Delta_b(H)$	-0.283	-1.009	-2.063	-2.198
$\Delta_\tau(H)$	0.201	-0.235	-1.802	-1.569
$\Delta_\gamma(H)$	0.115	0.004	0.025	0.027
$\Delta_\gamma^{\text{tot}}(H)$	0.023	-0.236	-0.773	-0.407
$-2 \log \mathcal{L}$	25.7	26.0	26.8	26.1

Table 9. Best-fit parameter points for the 2HDM with degenerate spectrum, considering Yukawa-aligned Higgs couplings to fermions. Both sets of Δ_x are defined as deviations from the Standard Model couplings.

the decoupling limit trigger the multifarious bottom and tau Yukawa patterns displayed in Figure 13, which include enhanced, suppressed and sign-flipped interactions.

Solutions with a vector-phobic h^0 field $\Delta_V(h^0) \simeq -1$ or $\alpha \simeq \beta$ cover a wide range of coupling variations. They include maximal mixing solutions $\sin \alpha \simeq \pm 1$ for $\tan \beta \gg 1$ and no-mixing solutions $\sin \alpha \simeq 0$ for $\tan \beta \ll 1$. The former is characterized by enhanced (sign-reverted) bottom Yukawas with suppressed top interactions. Conversely, no-mixing solutions feature $\Delta_b(h^0) \simeq -1$ with enhanced top Yukawas. All of them are nicely visible in the lower panels of Figure 13.

The black voids in the Δ_V vs Δ_t and Δ_V vs Δ_b planes correspond to exceedingly large combined h^0, H^0 contributions to the relevant search channels. This is particularly apparent at moderate and large $\tan \beta$ for $|\sin \alpha| \gtrsim 0.5$. This implies enhanced bottom and tau Yukawas, a type-II structure hard to reconcile with the LHC observation.

Finally, for type-II models the best fit solutions at large $\sin \alpha$ survive after imposing the theoretical and experimental constraints. All we observe is a slight pull towards $\tan \beta \simeq 1$. The poor fit quality reflects the strong competition between the model constraints and the compatibility with the LHC measurements. The bulk of the phenomenologically viable parameter space fails to accommodate two roughly 126 GeV mass-degenerate states with SM-like couplings measurements. For example, the best fit for the constrained type-II model involves $\Delta_b \simeq -2.3$, *i.e.* a $\mathcal{O}(30)\%$ enhancement in the Yukawas $g_{bbh^0}/\tau\tau h^0$. This universal enhancement is reinforced by the contribution from the H^0 state with SM-like Yukawa interactions. In the view of LHC data, a type-I twin Higgs model is clearly more likely.

Yukawa-alignment completely disentangles the variations in the heavy fermion Yukawas. The corresponding best fit results are given in Table 9. As expected for a 2HDM setup with very large

flexibility, we find wide ranges of $\sin \alpha$, $\tan \beta$ and $\gamma_{b,\tau}$ to be compatible with data. The best agreement singles out $\tan \beta \simeq 1$ alongside with large mixing $|\sin \alpha| \gtrsim 0.7$, Yukawa structures not far from type-I $\gamma_b/2\pi = 0.25(0.75)$, and small charged Higgs contributions. The manifold coupling variations identified for type-I and type-II models, including sizable departures from $\Delta_V \simeq 0$ are recovered in this more general setup. In addition, we find broader parameter regimes with coexisting $\Delta_V(h^0) < 0$ and $\Delta_f(h^0) > 0$. This reflects how Yukawa-aligned structures unlink the fermion and the gauge boson coupling shifts.

5 Summary

In this paper we have studied extended Higgs sectors in the light of the 2011–2012 ATLAS and CMS measurements. Starting from the simple modifications of adding a dark singlet, not participating in electroweak symmetry breaking, we have looked at increasingly complex models.

As long as all our models include a decoupling limit we first confirm that all models are consistent with the observed data. The preferred parameter ranges depend on the model structure, in particular the different Yukawa couplings in type-I, type-II, lepton-specific, and flipped setups. In general, we find strong correlations between the VEV ratio $\tan \beta$ and the Higgs mixing parameters ξ or $\sin \alpha$. In Figure 14 we show the corresponding best-fit parameter points and error bars for some of the model parameters. The red curves show the expected limits from current data, assuming all LHC measurements right on the Standard Model parameter choices. The dark blue results from the actual data are fully consistent with the Standard Model limit, both in terms of the central values and in terms of the error bars. The results shown in light blue include the theoretical and phenomenological constraints on the respective models. They can be significantly different and most notably do not feature in the large- $\tan \beta$ panel, illustrating the considerable problems this parameter range has for example with flavor physics constraints.

The type-I 2HDM most naturally fits the observed Higgs rates, so it has the widest error bands. Segments close to the no-mixing point are excluded for those models where they overly suppress the bottom or tau Yukawas. For large $\tan \beta$ the decoupling condition $\sin(\beta - \alpha) \simeq 1$ strongly limits the allowed amount of mixing. Sign shifts in couplings are only attainable for $\tan \beta < 1$. Particularly interesting parameter regimes open when we allow for two mass-degenerate Higgs bosons to contribute to the observed resonance. The results shown in Figure 14 confirm our general conclusion that extended

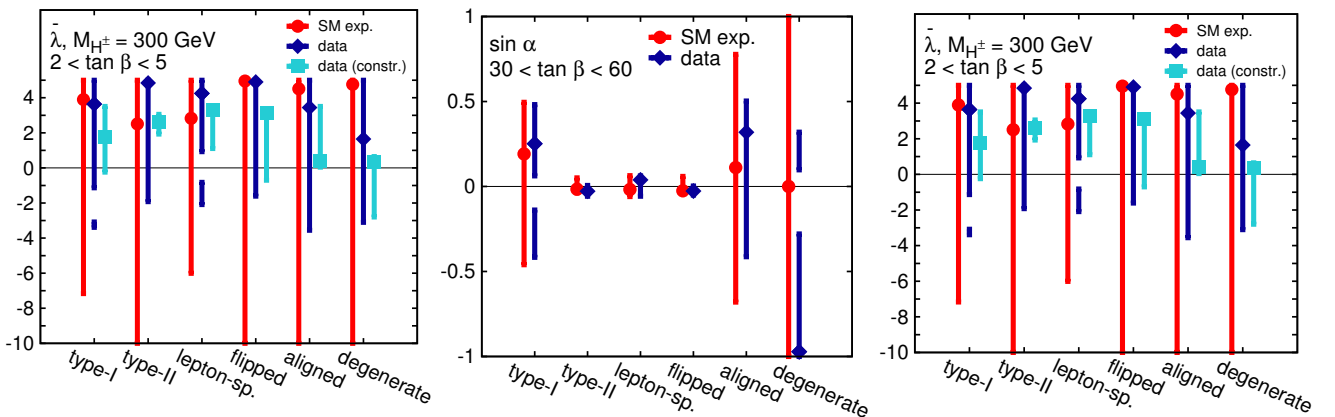


Figure 14. Extracted $\sin \alpha$ and $\tilde{\lambda}$ values and error bands for the different 2HDM benchmarks. The self couplings $\tilde{\lambda}$ is defined in Eq.(4.1). The variation of $\tan \beta$ is restricted to small (left and right panels) and large (center panel) values.

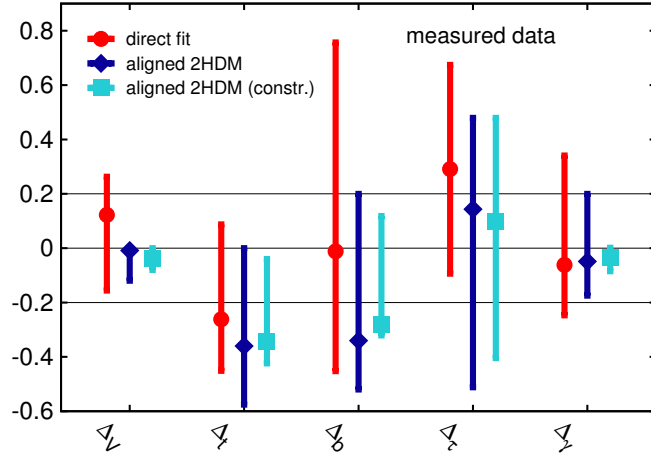


Figure 15. Extracted couplings and errors bars for the general fit of all Standard Model couplings and the Yukawa-aligned 2HDM fit. For the 2HDM we show the error bars without and with additional non-LHC constraints.

Higgs sectors are significantly constrained by current data, unless their structure is complex enough to resemble the full Standard Model Higgs Lagrangian in terms of degrees of freedom.

In addition, we target the question if the most general, Yukawa-aligned 2HDM can serve as a consistent model for a fully flexible fit of all Standard Model Higgs couplings. To begin with, deviations $\Delta_W \neq \Delta_Z$ and $\Delta_{W,Z} > 0$ can only be realized when we include quantum effects, as described in Section 3.2 and 3.3. In our current LHC fit we omit quantum corrections, because they are CPU-intensive and carry no numerical relevance; all we need to remember is that $\Delta_W \neq \Delta_Z$ as well as $\Delta_{W,Z} > 0$ can be achieved in principle. In the custodial limit $\Delta_W = \Delta_Z$ we compare the free SM-like couplings fit and the Yukawa-aligned 2HDM fit in Figure 15. The error bars of the actual Higgs couplings are indeed similar, as long as we ignore the experimental constraints on the 2HDM setup. The tree-level assumption $\Delta_V < 1$ explains the comparably larger downward shifts in the Higgs couplings to fermions, which compensate for the suppressed observed di-boson rates.

This numerical outcome confirms that once we fold in quantum effects we should indeed be able to structurally use an extended Higgs sector as the ultraviolet completion of a SM-like Higgs sector with free couplings. Obviously, this correspondence holds only when we ignore the model-specific non-LHC constraints for the 2HDM structure. In such a model electroweak quantum corrections can be computed for LHC and ILC observables and applied to the Higgs coupling measurement based on the renormalizable dimension-4 Lagrangian.

Acknowledgments

First of all, we would like to thank Berthold Stech for suggesting the degenerate spectrum setup and for the fruitful and enjoyable collaboration on this major part of our analysis. It is a pleasure to thank Dirk and Peter Zerwas for their help all along this analysis. Moreover, we would like to thank our SFITTER co-authors Markus Klute and Remi Lafaye for a fun, fruitful, and ongoing collaboration. TP would like to thank the CCPP at New York University for their hospitality while this paper was finalized. MR acknowledges partial support by the Deutsche Forschungsgemeinschaft via the Sonderforschungsbereich/Transregio SFB/TR-9 “Computational Particle Physics” and the Initiative and Networking Fund of the Helmholtz Association, contract HA-101 (“Physics at the Terascale”).

A Parameterizations

A.1 Additional singlet

Starting from the scalar potential defined by Eq.(2.3) and expanding the neutral component of the doublet field around its VEV $\Phi = (v + h_1^0)/\sqrt{2}$ we arrive at the mass-squared matrix

$$\begin{pmatrix} 2\lambda_1 v_1^2 & \lambda_3 v_1 v_2 \\ \lambda_3 v_1 v_2 & 2\lambda_2 v_2^2 \end{pmatrix}. \quad (\text{A.1})$$

Diagonalization in terms of $v_1 \equiv v = 246$ GeV and $v_2 = v \tan \beta$ returns the physical masses

$$\frac{m_{h^0, H^0}^2}{v^2} = \lambda_1 + \lambda_2 \tan^2 \beta \mp (\lambda_1 - \lambda_2 \tan^2 \beta) \sqrt{1 + \tan^2 2\theta}, \quad (\text{A.2})$$

and the mixing between the singlet and the doublet Higgs components

$$R(\theta) = \begin{pmatrix} \cos \theta & \sin \theta \\ -\sin \theta & \cos \theta \end{pmatrix} \quad \tan^2(2\theta) = \frac{\lambda_3^2 v_1^2 v_2^2}{(\lambda_1 v_1^2 - \lambda_2 v_2^2)^2}, \quad (\text{A.3})$$

We can invert these relations for the coupling parameters $\lambda_{1,2,3}$ as

$$\lambda_1 = \frac{m_{h^0}^2 \cos^2 \theta + m_{H^0}^2 \sin^2 \theta}{2v^2}; \quad \lambda_2 = \frac{m_{h^0}^2 \sin^2 \theta + m_{H^0}^2 \cos^2 \theta}{2v^2 \tan^2 \beta}; \quad \lambda_3 = \frac{\sin 2\theta}{\tan \beta} \frac{(m_{H^0}^2 - m_{h^0}^2)}{2v^2}. \quad (\text{A.4})$$

The singlet mixing reduces the coupling strength of the h^0 to all the Standard Model fields by $\cos \theta$. If kinematically allowed, the heavier scalar H^0 may decay into $h^0 h^0$ pairs at a rate

$$\Gamma(H^0 \rightarrow h^0 h^0) = \frac{|\lambda_{H^0 h^0 h^0}|^2}{32\pi m_{H^0}} \sqrt{1 - \frac{4m_{h^0}^2}{m_{H^0}^2}}. \quad (\text{A.5})$$

In the absence of a second VEV the dark singlet does not contribute to electroweak symmetry breaking and hence does not mix with the SM-like Higgs doublet. Notwithstanding, the portal interaction

$$\mathcal{L} \supset \lambda_3 (\Phi^\dagger \Phi) S^2, \quad (\text{A.6})$$

triggers a new hss triple coupling. If kinematically allowed, the corresponding decay mode

$$\Gamma(h \rightarrow ss) = \frac{\lambda_3^2 v^2}{32\pi m_h} \sqrt{1 - \frac{4m_s^2}{m_h^2}} \quad (\text{A.7})$$

will contribute to the invisible Higgs width.

A.2 Additional doublet

The 2HDM potential we refer to is given in Eq.(2.4). The Higgs mass-eigenstates require a set of rotations

$$\begin{pmatrix} H^0 \\ h^0 \end{pmatrix} = R(\alpha) \begin{pmatrix} h_1^0 \\ h_2^0 \end{pmatrix} \quad \begin{pmatrix} G^0 \\ A^0 \end{pmatrix} = R(\beta) \begin{pmatrix} a_1^0 \\ a_2^0 \end{pmatrix} \quad \begin{pmatrix} G^\pm \\ H^\pm \end{pmatrix} = R(\beta) \begin{pmatrix} h_1^\pm \\ h_2^\pm \end{pmatrix}, \quad (\text{A.8})$$

with $R(\theta)$ defined as a rotation matrix with a mixing angle θ . The VEVs $v_{1,2}$ associated with each of the doublets we write as $v_1 \equiv v \cos \beta$, $v_2 \equiv v \sin \beta$, such that $\tan \beta \equiv v_2/v_1$. Electroweak symmetry breaking requires $v_1^2 + v_2^2 = v^2$.

The mass parameters in the minimized Higgs potential Eq.(2.4) are

$$\begin{aligned} m_{11}^2 &= m_{12}^2 \tan \beta - \frac{v^2}{2} (\lambda_1 \cos^2 \beta + (\lambda_3 + \lambda_4 + \lambda_5) \sin^2 \beta + 3\lambda_6 \sin \beta \cos \beta + \lambda_7 \sin^2 \beta \tan \beta) \\ m_{22}^2 &= m_{12}^2 \cot \beta - \frac{v^2}{2} (\lambda_2 \sin^2 \beta + (\lambda_3 + \lambda_4 + \lambda_5) \cos^2 \beta + 3\lambda_7 \sin \beta \cos \beta + \lambda_6 \cos^3 \beta \sin \beta) . \end{aligned} \quad (\text{A.9})$$

The corresponding self-couplings read

$$\begin{aligned} \lambda_1 &= \frac{1}{v^2 \cos^2 \beta} \left[-m_{12}^2 \frac{\sin \beta}{\cos \beta} + m_{H^0}^2 \cos^2 \alpha + m_{h^0}^2 \sin^2 \alpha \right] \\ \lambda_2 &= \frac{1}{v^2 \sin^2 \beta} \left[-m_{12}^2 \frac{\cos \beta}{\sin \beta} + m_{H^0}^2 \sin^2 \alpha + m_{h^0}^2 \cos^2 \alpha \right] \\ \lambda_3 &= \frac{1}{v^2} \left[-\frac{m_{12}^2}{\sin \beta \cos \beta} + 2m_{H^\pm}^2 + (m_{H^0}^2 - m_{h^0}^2) \frac{\sin 2\alpha}{\sin 2\beta} \right] \\ \lambda_4 &= \frac{1}{v^2} \left[\frac{m_{12}^2}{\sin \beta \cos \beta} + m_{A^0}^2 - 2m_{H^\pm}^2 \right] ; \\ \lambda_5 &= \frac{1}{v^2} \left(\frac{m_{12}^2}{\sin \beta \cos \beta} - m_{A^0}^2 \right) - \lambda_6 \cot \beta - \lambda_7 \tan \beta . \end{aligned} \quad (\text{A.10})$$

For the physical masses of the five Higgs states we find

$$\begin{aligned} m_{H^\pm}^2 &= \frac{m_{12}^2}{\sin \beta \cos \beta} - \frac{v^2}{2} [\lambda_4 + \lambda_5 + \lambda_6 \cot \beta + \lambda_7 \tan \beta] \\ m_{A^0}^2 &= \frac{m_{12}^2}{\sin \beta \cos \beta} - \frac{v^2}{2} [2\lambda_5 + \lambda_6 \cot \beta + \lambda_7 \tan \beta] \\ m_{h^0, H^0}^2 &= \frac{1}{2} \left[A^2 + B^2 \mp \sqrt{(A^2 - B^2)^2 + 4C^4} \right] , \end{aligned} \quad (\text{A.11})$$

with A, B, C defined as

$$\begin{aligned} A^2 &= v^2 \left[\lambda_1 \cos^2 \beta + \frac{3}{2} \tan \beta \cos^2 \beta \lambda_6 - \tan \beta \sin^2 \beta \lambda_7 \right] + m_{12}^2 \frac{\sin \beta}{\cos \beta} \\ B^2 &= v^2 \left[\lambda_2 \sin^2 \beta + \frac{3}{2} \cot \beta \sin^2 \beta \lambda_7 - \cot \beta \cos^2 \beta \lambda_6 \right] + m_{12}^2 \frac{\cos \beta}{\sin \beta} \\ C^2 &= v^2 \left[\sin \beta \cos \beta (\lambda_3 + \lambda_4 + \lambda_5) + \frac{3}{2} (\lambda_6 \cos^2 \beta + \lambda_7 \sin^2 \beta) \right] - m_{12}^2 . \end{aligned} \quad (\text{A.12})$$

The general form of the couplings quoted in Table 10 with aligned Yukawa structures may be regarded as an interpolation between the canonical realizations of the 2HDM, *i.e.* featuring the natural flavor conservation hypothesis with the couplings modifications quoted in Table 11. The couplings and expressed in terms of Δ_x , defined by Eq.(1.1).

Finally, we need analytic expressions for the effective dimension 5 interactions. The light Higgs boson coupling to photons can be cast into

$$\Delta_\gamma = -\frac{m_W s_w}{e m_{H^\pm}^2} \lambda_{hH^+H^-} A_s(\tau_{H^\pm}); \quad (\text{A.13})$$

The usual loop function for a scalar contributing to this coupling is

$$A_s^H(x) = \frac{\arcsin^2 \sqrt{x} - x}{x^2} \quad (\text{A.14})$$

	h^0	H^0	A^0
$1 + \Delta_W$	$\sin(\beta - \alpha)$	$\cos(\beta - \alpha)$	0
$1 + \Delta_Z$	$\sin(\beta - \alpha)$	$\cos(\beta - \alpha)$	0
$1 + \Delta_t$	$\frac{\cos \alpha}{\sin \beta}$	$\frac{\sin \alpha}{\sin \beta}$	$\frac{1}{\tan \beta}$
$1 + \Delta_b$	$-\frac{\sin(\alpha - \gamma_b)}{\cos(\beta - \gamma_b)}$	$\frac{\cos(\alpha - \gamma_b)}{\cos(\beta - \gamma_b)}$	$\tan(\beta - \gamma_b)$
$1 + \Delta_\tau$	$-\frac{\sin(\alpha - \gamma_\tau)}{\cos(\beta - \gamma_\tau)}$	$\frac{\cos(\alpha - \gamma_\tau)}{\cos(\beta - \gamma_\tau)}$	$\tan(\beta - \gamma_\tau)$

Table 10. Neutral Higgs boson couplings to fermions and gauge bosons within a generic 2HDM. The flavor sector herewith we define according to the Yukawa alignment hypothesis.

in the low energy limit. The relevant trilinear interaction involving the light Higgs boson and the charged Higgs fields renders

$$\lambda_{h^0 H^+ H^-} = \frac{e}{2m_W s_w} \left[\sin(\beta - \alpha)(m_{h^0}^2 - 2m_{H^\pm}^2) - \frac{\cos(\alpha + \beta)}{\sin(2\beta)}(2m_{h^0}^2 - \tilde{\lambda}v^2) \right], \quad (\text{A.15})$$

with $\tilde{\lambda} = 2m_{12}^2/(v^2 \sin \beta \cos \beta)$. If we also entertain the possibility of the heavy neutral Higgs contributing to the overall signal strength we need to extract the corresponding coupling strength including the trilinear coupling

$$\lambda_{H^0 H^+ H^-} = \frac{e}{2m_W s_w} \left[\cos(\beta - \alpha)(m_{H^0}^2 - 2m_{H^\pm}^2) - \frac{\sin(\alpha + \beta)}{\sin(2\beta)}(2m_{H^0}^2 - \tilde{\lambda}v^2) \right]. \quad (\text{A.16})$$

The MSSM Higgs sector is a constrained 2HDM setup. Its main feature is the link between the Higgs masses and the Higgs couplings through the mixing angle α . The quartic couplings from the superpotential D -terms are gauge couplings, giving us

$$\lambda_1 = \lambda_2 = \frac{\pi \alpha_{em}}{s_w c_w} \quad \lambda_3 = \frac{\pi \alpha_{em}(c_w^2 - s_w^2)}{s_w^2 c_w^2} \quad \lambda_4 = -\frac{2\pi \alpha_{em}}{s_w^2} \quad \lambda_5 = 0. \quad (\text{A.17})$$

At tree level the entire Higgs sector is determined by two parameters, often chosen as m_{A^0} and $\tan \beta$. Typically, the MSSM Higgs sector shows a mass hierarchy $m_{h^0} \ll m_{H^0, A^0, H^\pm}$, in line with the generic hierarchical benchmark. Custodial symmetry and tree-level FCNC suppression are guaranteed. Dominant quantum corrections are due to third generation quarks and squarks. They rely on the corresponding soft-SUSY breaking parameters ($A_{t,b}, \mu, M_{\text{SUSY}}$) and have a sizable quantitative impact into the resulting Higgs mass spectrum and coupling pattern [120].

B Hierarchical 2HDM

The low-energy realization of the 2HDM with a large mass hierarchy corresponds to the case with one SM-like, weak-scale Higgs doublet, and a second heavier field with $M_{\text{heavy}} \gg v$. The underlying EW symmetry requires that scalar mass splittings within each of the doublets cannot be larger than $\mathcal{O}(v)$

	type-I	type-II	lepton-specific	flipped
	$\gamma_b = \pi/2$	$\gamma_b = 0$	$\gamma_b = \pi/2$	$\gamma_b = 0$
	$\gamma_\tau = \pi/2$	$\gamma_\tau = 0$	$\gamma_\tau = 0$	$\gamma_\tau = \pi/2$
$1 + \Delta_t(h^0)$	$\frac{\cos \alpha}{\sin \beta}$	$\frac{\cos \alpha}{\sin \beta}$	$\frac{\cos \alpha}{\sin \beta}$	$\frac{\cos \alpha}{\sin \beta}$
$1 + \Delta_b(h^0)$	$\frac{\cos \alpha}{\sin \beta}$	$-\frac{\sin \alpha}{\cos \beta}$	$\frac{\cos \alpha}{\sin \beta}$	$-\frac{\sin \alpha}{\cos \beta}$
$1 + \Delta_\tau(h^0)$	$\frac{\cos \alpha}{\sin \beta}$	$-\frac{\sin \alpha}{\cos \beta}$	$-\frac{\sin \alpha}{\cos \beta}$	$\frac{\cos \alpha}{\sin \beta}$
$1 + \Delta_t(H^0)$	$\frac{\sin \alpha}{\sin \beta}$	$\frac{\sin \alpha}{\sin \beta}$	$\frac{\sin \alpha}{\sin \beta}$	$\frac{\sin \alpha}{\sin \beta}$
$1 + \Delta_b(H^0)$	$\frac{\sin \alpha}{\sin \beta}$	$\frac{\cos \alpha}{\cos \beta}$	$\frac{\sin \alpha}{\sin \beta}$	$\frac{\cos \alpha}{\cos \beta}$
$1 + \Delta_\tau(H^0)$	$\frac{\sin \alpha}{\sin \beta}$	$\frac{\cos \alpha}{\cos \beta}$	$\frac{\cos \alpha}{\cos \beta}$	$\frac{\sin \alpha}{\sin \beta}$
$1 + \Delta_t(A^0)$	$\cot \beta$	$\cot \beta$	$\cot \beta$	$\cot \beta$
$1 + \Delta_b(A^0)$	$-\cot \beta$	$\tan \beta$	$-\cot \beta$	$\tan \beta$
$1 + \Delta_\tau(A^0)$	$-\cot \beta$	$\tan \beta$	$\tan \beta$	$-\cot \beta$

Table 11. Neutral Higgs boson couplings to fermions for the canonical realizations of the 2HDM featuring Natural Flavor Conservation.

for a weakly-coupled theory, which gives rise to the purported mass hierarchy between the light Higgs $m_{h^0} = \mathcal{O}(v)$ and its heavier companions $m_{H^0, H^\pm, A^0} \simeq \mathcal{O}(M_{\text{heavy}})$. If these are integrated out, we are left with an effective field theory description in terms of a single, SM-like Higgs field.

To construct this effective theory [47, 121] we start from the generic relations between the Higgs self-couplings, masses and mixing angles Eqs.(A.9) and (A.10),

$$\begin{aligned}
(\lambda_1 \cos^2 \beta - \lambda_2 \sin^2 \beta) v^2 &= M_{\text{heavy}}^2 \cos(2\beta) + (m_{H^0}^2 - m_{h^0}^2) \cos(2\alpha) \\
(\lambda_3 + \lambda_4 + \lambda_5) v^2 &= M_{\text{heavy}}^2 + (m_{H^0}^2 - m_{h^0}^2) \frac{\sin(2\alpha)}{\sin(2\beta)} - \lambda_6 \cot \beta - \lambda_7 \tan \beta .
\end{aligned} \tag{B.1}$$

For simplicity, we impose $\lambda_{6,7} = 0$ and define

$$\begin{aligned}
\hat{\lambda} v^2 &= (m_{H^0}^2 - m_{h^0}^2) \sin(\beta - \alpha) \cos(\beta - \alpha) \\
\hat{\lambda} &= \sin \beta \cos \beta (\lambda_1 \cos^2 \beta - \lambda_2 \sin^2 \beta - \lambda_{345} \cos(2\beta)) + \lambda_6 \cos \beta \cos 3\beta + \lambda_7 \sin \beta \sin 3\beta ,
\end{aligned} \tag{B.2}$$

with $\lambda_{345} \equiv \lambda_3 + \lambda_4 + \lambda_5$. The small parameter in the scale separation $m_{H^0, A^0, H^\pm}^2 \simeq M_{\text{heavy}}^2 \gg m_{h^0}^2$ can therefore be defined as

$$\xi = \hat{\lambda} \frac{v^2}{M_{\text{heavy}}^2} \ll 1 . \tag{B.3}$$

The fact that $\hat{\lambda}$ remains small rests on the assumption that the different Higgs self-couplings remain perturbative $\mathcal{O}(1)$ quantities. We are then left with the condition

$$\sin(\beta - \alpha) \cos(\beta - \alpha) \simeq \xi \ll 1 . \tag{B.4}$$

	h^0	H^0
$1 + \Delta_W$	$1 - \frac{\xi^2}{2}$	ξ
$1 + \Delta_Z$	$1 - \frac{\xi^2}{2}$	ξ
$1 + \Delta_t$	$1 + \cot \beta \xi - \frac{\xi^2}{2} + \mathcal{O}(\xi^3)$	$-\cot \beta + \xi + \cot \beta \frac{\xi^2}{2} + \mathcal{O}(\xi^3)$
$1 + \Delta_b$	$1 - \tan(\beta - \gamma_b) \xi - \frac{\xi^2}{2} + \mathcal{O}(\xi^3)$	$\tan(\beta - \gamma_b) + \xi - \tan(\beta - \gamma_b) \frac{\xi^2}{2} + \mathcal{O}(\xi^3)$
$1 + \Delta_\tau$	$1 - \tan(\beta - \gamma_\tau) \xi - \frac{\xi^2}{2} + \mathcal{O}(\xi^3)$	$\tan(\beta - \gamma_\tau) + \xi - \tan(\beta - \gamma_\tau) \frac{\xi^2}{2} + \mathcal{O}(\xi^3)$

Table 12. Effective light Higgs boson couplings to fermions and gauge bosons up to $\mathcal{O}(\xi^3)$ within the 2HDM with a large mass hierarchy. The flavor sector features a general Yukawa alignment structure. The different interactions are normalized to the Standard Model and expressed in terms of Δ_x as defined in Eq.(1.1).

By construction, the heavy Higgs mass follows $M_{\text{heavy}} \sim v^2/\xi$. For a hierarchical spectrum we need to assume a non-vanishing PQ soft-breaking term $m_{12}^2 \neq 0$ for a stable Higgs potential if $\lambda_{6,7} = 0$ [100].

If the low-energy effective field theory description of the 2HDM should approach the SM-like limit $\sin(\beta - \alpha) \rightarrow 1$, this limit requires

$$\cos(\beta - \alpha) \simeq \xi \ll 1 \quad \Leftrightarrow \quad \cos \beta \sim \sin \alpha . \quad (\text{B.5})$$

The correlation of the mixing angle is a key property of the hierarchical 2HDM. In the limit of large $\tan \beta$ we can derive the leading correlation between ξ and $\tan \beta$,

$$\sin^2 \alpha = \frac{1}{1 + \tan^2 \beta} \quad \text{or} \quad \xi = \frac{2 \tan \beta}{1 + \tan^2 \beta} . \quad (\text{B.6})$$

The relation $\cos(\beta - \alpha) = \xi \ll 1$ allows us to write the scale separation $v^2 \ll M_{\text{heavy}}^2$ in terms of 2HDM parameters. The effective theory can be implemented by imposing Eq.(B.5) on the conventional analytic expressions for the 2HDM couplings. For example, the type-II bottom Yukawa can be written as

$$\begin{aligned} g_b &= -\frac{\sin \alpha}{\cos \beta} = \sin(\beta - \alpha) - \tan \beta \cos(\beta - \alpha) \\ &= 1 - \tan \beta \cos(\beta - \alpha) - \frac{1}{2} \cos^2(\beta - \alpha) + \mathcal{O}(\cos^3(\beta - \alpha)) \\ &= 1 - \tan \beta \xi - \frac{1}{2} \xi^2 + \mathcal{O}(\xi^3) . \end{aligned} \quad (\text{B.7})$$

The complete set of effective light Higgs boson interactions to leading order in ξ (up to $\mathcal{O}(\xi)^3$ corrections we present in Table 12, again written in terms of the coupling shifts Δ_x defined in Eq.(1.1).

For the loop-induced Higgs interaction to photons we need to consistently expand the corresponding trilinear Higgs coupling to the charged Higgs bosons up to $\mathcal{O}(\xi^3)$ terms, reading

$$\lambda_{h^0 H^+ H^-} = \frac{-e}{2 m_W s_w} \left[\left(1 - \frac{\xi^2}{2} \right) (m_{h^0}^2 + 2m_H^{\pm 2} - \lambda v^2) + \frac{\xi}{2} (2m_{h^0}^2 - \tilde{\lambda} v^2) (\cot \beta - \tan \beta) \right] . \quad (\text{B.8})$$

The leading dependence in the decoupling limit,

$$\lambda_{h^0 H^+ H^-} = \lambda_{h^0 H^0 H^0} = \lambda_{h^0 A^0 A^0} = m_{h^0}^2 + 2M_{\text{heavy}}^2 - \tilde{\lambda} v^2 + \mathcal{O}(\xi) \quad (\text{B.9})$$

is common to all trilinear self-interactions involving the light Higgs boson and two heavy companions. Similarly, in this limit we find $\lambda_{h^0 h^0 H^0} = \mathcal{O}(\xi)$ and $\lambda_{h^0 h^0 h^0} = \lambda_{h^0 h^0 h^0}^{\text{SM}} = -3im_{h^0}^2/v^2$. Therefore, the condition

$$m_{h^0}^2 + 2M_{\text{heavy}}^2 - \tilde{\lambda} v^2 \simeq 0 \quad (\text{B.10})$$

ensures the consistent decoupling of the heavy fields in the $\xi \rightarrow 0$ limit, with dominant non-decoupling effects reading

$$\begin{aligned} \lambda_{h^0 HH}^{\text{non-dec}} &\simeq \frac{e}{4m_W s_w} \xi \tilde{\lambda} v^2 (\cot \beta - \tan \beta) \simeq \frac{e}{2m_W s_w} \xi M_{\text{heavy}}^2 (\cot \beta - \tan \beta) \\ &\simeq \frac{ev^2}{2m_W s_w} (\cot \beta - \tan \beta). \end{aligned} \quad (\text{B.11})$$

References

- [1] P. W. Higgs, Phys. Lett. **12**, 132 (1964); P. W. Higgs, Phys. Rev. Lett. **13**, 508 (1964); F. Englert and R. Brout, Phys. Rev. Lett. **13**, 321 (1964).
- [2] for pedagogical introductions see e.g. M. Spira and P. M. Zerwas, Lect. Notes Phys. **512**, 161 (1998); A. Djouadi, Phys. Rept. **457**, 1 (2008); T. Plehn, Lect. Notes Phys. **844**, 1 (2012).
- [3] G. Aad *et al.* [ATLAS Collaboration], Phys. Lett. B **716**, 1 (2012),
- [4] S. Chatrchyan *et al.* [CMS Collaboration], Phys. Lett. B **716**, 30 (2012), JHEP **06**, 081 (2013), CMS-NOTE-2012-006.
- [5] The ATLAS collaboration, ATLAS-CONF-2011-161; ATLAS-CONF-2012-015; ATLAS-CONF-2012-160; ATLAS-CONF-2012-161; ATLAS-CONF-2013-012; ATLAS-CONF-2013-013; ATLAS-CONF-2013-030. The CMS collaboration, Phys. Rev. Lett. **108**, 111804 (2012); CMS-PAS-HIG-12-044; CMS-PAS-HIG-13-001; CMS-PAS-HIG-13-002; CMS-PAS-HIG-13-003; CMS-PAS-HIG-13-004; CMS-PAS-HIG-13-012.
- [6] R. Lafaye, T. Plehn, M. Rauch, D. Zerwas and M. Dührssen, JHEP **0908**, 009 (2009); M. Klute, R. Lafaye, T. Plehn, M. Rauch and D. Zerwas, Phys. Rev. Lett. **109**, 101801 (2012); T. Plehn and M. Rauch, Europhys. Lett. **100**, 11002 (2012); and references therein.
- [7] A. Azatov, R. Contino and J. Galloway, JHEP **1204**, 127 (2012); A. Azatov, R. Contino, D. Del Re, J. Galloway, M. Grassi and S. Rahatlou, JHEP **1206**, 134 (2012).
- [8] for more or less constrained Higgs couplings analyses see e.g. F. Bonnet, M. B. Gavela, T. Ota and W. Winter, Phys. Rev. D **85**, 035016 (2012); P. P. Giardino, K. Kannike, M. Raidal and A. Strumia, Phys. Lett. B **718**, 469 (2012); J. Ellis and T. You, JHEP **1209**, 123 (2012); J. Ellis and T. You, JHEP **1306**, 103 (2013); J. R. Espinosa, C. Grojean, M. Mühlleitner and M. Trott, JHEP **1212**, 045 (2012); T. Corbett, O. J. P. Eboli, J. González-Fraile and M. C. González-García, Phys. Rev. D **86**, 075013 (2012) and Phys. Rev. D **87**, 015022 (2013); S. Banerjee, S. Mukhopadhyay and B. Mukhopadhyaya, JHEP **1210**, 062 (2012); N. Craig and S. Thomas, JHEP **1211**, 083 (2012); F. Bonnet, T. Ota, M. Rauch and W. Winter, Phys. Rev. D **86**, 093014 (2012); A. Djouadi, arXiv:1208.3436 [hep-ph]; B. A. Dobrescu and J. D. Lykken, JHEP **1302**, 073 (2013); E. Massó and V. Sanz, Phys. Rev. D **87**, 033001 (2013); G. Belanger, B. Dumont, U. Ellwanger, J. F. Gunion and S. Kraml, JHEP **1302**, 053 (2013); C. Cheung, S. D. McDermott and K. M. Zurek, JHEP **1304**, 074 (2013); K. Cheung, J. S. Lee and P. -Y. Tseng, JHEP **1305**, 134 (2013); P. P. Giardino, K. Kannike, I. Masina, M. Raidal and A. Strumia, arXiv:1303.3570 [hep-ph]; W. -F. Chang, W. -P. Pan, F. Xu and , arXiv:1303.7035 [hep-ph]; A. Djouadi and G. Moreau, arXiv:1303.6591 [hep-ph];

- [9] D. Carmi, A. Falkowski, E. Kuflik and T. Volansky, JHEP **1207**, 136 (2012); D. Carmi, A. Falkowski, E. Kuflik, T. Volansky and J. Zupan, JHEP **1210**, 196 (2012);
- [10] The ATLAS collaboration, ATLAS-CONF-2013-034; The CMS collaboration, CMS-PAS-HIG-13-005.
- [11] M. Dührssen, Czech. J. Phys. **55**, B145 (2005); M. Dührssen, Eur. Phys. J. C **33**, S686 (2004).
- [12] P. Bechtle, S. Heinemeyer, O. Stål, T. Stefaniak and G. Weiglein, arXiv:1305.1933 [hep-ph].
- [13] LHC Higgs Cross Section Working Group, A. David, A. Denner, M. Dührssen, M. Grazzini, C. Grojean, G. Passarino and M. Schumacher *et al.*, arXiv:1209.0040 [hep-ph].
- [14] G. Passarino, Nucl. Phys. B **868**, 416 (2013).
- [15] M. Klute, R. Lafaye, T. Plehn, M. Rauch and D. Zerwas, Europhys. Lett. **101**, 51001 (2013).
- [16] J. McDonald, Phys. Rev. D **50**, 3637 (1994); C. P. Burgess, M. Pospelov and T. ter Veldhuis, Nucl. Phys. B **619**, 709 (2001); S. Profumo, M. J. Ramsey-Musolf and G. Shaughnessy, JHEP **0708**, 010 (2007); E. Pontón and L. Randall, JHEP **0904**, 080 (2009); S. Das, P. J. Fox, A. Kumar and N. Weiner, JHEP **1011**, 108 (2010); S. Kanemura, S. Matsumoto, T. Nabeshima and N. Okada, Phys. Rev. D **82**, 055026 (2010); S. Andreas, C. Arina, T. Hambye, F. -S. Ling and M. H. G. Tytgat, Phys. Rev. D **82**, 043522 (2010); O. Lebedev and H. M. Lee, Eur. Phys. J. C **71**, 1821 (2011); B. Batell, S. Gori and L. -T. Wang, JHEP **1206**, 172 (2012); A. Biswas and D. Majumdar, Pramana **80**, 539 (2013); Y. Mambrini, Phys. Rev. D **84**, 115017 (2011); X. Chu, T. Hambye and M. H. G. Tytgat, JCAP **1205**, 034 (2012); L. López-Honorez, T. Schwetz and J. Zupan, Phys. Lett. B **716**, 179 (2012); I. Low, P. Schwaller, G. Shaughnessy and C. E. M. Wagner, Phys. Rev. D **85**, 015009 (2012); F. Bazzocchi and M. Fabbrichesi, Eur. Phys. J. C **73**, 2303 (2013).
- [17] M. Bowen, Y. Cui and J. D. Wells, JHEP **0703**, 036 (2007); S. Gopalakrishna, S. Jung and J. D. Wells, Phys. Rev. D **78**, 055002 (2008); C. Englert, T. Plehn, D. Zerwas and P. M. Zerwas, Phys. Lett. B **703**, 298 (2011); C. Englert, T. Plehn, M. Rauch, D. Zerwas and P. M. Zerwas, Phys. Lett. B **707**, 512 (2012).
- [18] J. C. Pati and A. Salam, Phys. Rev. D **10**, 275 (1974) [Erratum-ibid. D **11**, 703 (1975)].
- [19] F. Gurse, P. Ramond and P. Sikivie, Phys. Lett. B **60**, 177 (1976); Y. Achiman and B. Stech, Phys. Lett. B **77**, 389 (1978); Q. Shafi, Phys. Lett. B **79**, 301 (1978); R. Barbieri, D. V. Nanopoulos and A. Masiero, Phys. Lett. B **104**, 194 (1981).
- [20] H. Georgi, AIP Conf. Proc. **23**, 575 (1975); H. Fritzsch and P. Minkowski, Annals Phys. **93**, 193 (1975).
- [21] Y. Achiman and B. Stech, in *Advanced Summer Institute on New Phenomena in Lepton and Hadron Physics*, edited by D.E.C. Fries and J. Wess (Plenum, New York, 1979); S. L. Glashow, in *Fifth Workshop on Grand Unification*, edited by K. Kang, H. Fried, and P. Frampton (World Scientific, Singapore, 1984), p. 88; K. S. Babu, X. -G. He and S. Pakvasa, Phys. Rev. D **33**, 763 (1986).
- [22] B. Stech, Phys. Rev. D **86**, 055003 (2012).
- [23] B. Stech and Z. Tavartkiladze, Phys. Rev. D **77**, 076009 (2008). B. Stech, Fortsch. Phys. **58**, 692 (2010).
- [24] B. Stech, arXiv:1303.6931 [hep-ph].
- [25] R. Killick, K. Kumar and H. E. Logan, arXiv:1305.7236 [hep-ph].
- [26] P. Langacker, Phys. Rept. **72**, 185 (1981).
- [27] V. Barger, H. E. Logan and G. Shaughnessy, Phys. Rev. D **79**, 115018 (2009); S. Kanemura, M. Kikuchi and K. Yagyu, arXiv:1301.7303 [hep-ph].
- [28] H. Georgi and M. Machacek, Nucl. Phys. B **262**, 463 (1985); M. S. Chanowitz and M. Golden, Phys. Lett. B **165**, 105 (1985); J. F. Gunion, R. Vega and J. Wudka, Phys. Rev. D **42**, 1673 (1990); J. F. Gunion, R. Vega and J. Wudka, Phys. Rev. D **43**, 2322 (1991); M. Aoki and S. Kanemura, Phys. Rev. D **77**, 095009 (2008); H. E. Logan and M. -A. Roy, Phys. Rev. D **82**, 115011 (2010); C. Englert, E. Re and M. Spannowsky, Phys. Rev. D **87**, 095014 (2012).
- [29] J. Hisano and K. Tsumura, arXiv:1301.6455 [hep-ph].

- [30] S. Chpoi, S. Jung and P. Ko, arXiv:1307.3948 [hep-ph].
- [31] V. Silveira and A. Zee, Phys. Lett. B **161**, 136 (1985); M. J. G. Veltman and F. J. Ynduráin, Nucl. Phys. B **325**, 1 (1989). H. Davoudiasl, R. Kitano, T. Li and H. Murayama, Phys. Lett. B **609**, 117 (2005); O. Bahat-Treidel, Y. Grossman and Y. Rozen, JHEP **0705**, 022 (2007); D. O’Connell, M. J. Ramsey-Musolf and M. B. Wise, Phys. Rev. D **75**, 037701 (2007); V. Barger, P. Langacker, M. McCaskey, M. J. Ramsey-Musolf and G. Shaughnessy, Phys. Rev. D **77**, 035005 (2008). M. Gonderinger, Y. Li, H. Patel and M. J. Ramsey-Musolf, JHEP **1001**, 053 (2010); P. J. Fox, R. Harnik, J. Kopp and Y. Tsai, Phys. Rev. D **85**, 056011 (2012); E. Weihs and J. Zurita, JHEP **1202**, 041 (2012).
- [32] G. M. Pruna and T. Robens, arXiv:1303.1150 [hep-ph]; S. K. Kang and J. Park, arXiv:1306.6713 [hep-ph].
- [33] X. -G. He and J. Tandean, Phys. Rev. D **84**, 075018 (2011); A. Djouadi, O. Lebedev, Y. Mambrini and J. Quevillon, Phys. Lett. B **709**, 65 (2012).
- [34] The ATLAS collaboration, ATLAS-CONF-2013-011; The CMS collaboration, CMS-PAS-HIG-13-018.
- [35] G. Bélanger, B. Dumont, U. Ellwanger, J. F. Gunion and S. Kraml, Phys. Lett. B **723**, 340 (2013)
- [36] E. Komatsu *et al.* [WMAP Collaboration], Astrophys. J. Suppl. **192**, 18 (2011).
- [37] E. Aprile *et al.* [XENON100 Collaboration], Phys. Rev. Lett. **109**, 181301 (2012).
- [38] M. Ackermann *et al.* [Fermi-LAT Collaboration], Phys. Rev. Lett. **107**, 241302 (2011).
- [39] K. Cheung, Y. -L. S. Tsai, P. -Y. Tseng, T. -C. Yuan and A. Zee, JCAP **1210**, 042 (2012).
- [40] J. M. Cline, K. Kainulainen, P. Scott and C. Weniger, arXiv:1306.4710 [hep-ph].
- [41] B. Batell, D. McKeen and M. Pospelov, JHEP **1210**, 104 (2012).
- [42] A. Drozd, B. Grzadkowski and J. Wudka, JHEP **1204**, 006 (2012).
- [43] J. F. Gunion, H. E. Haber, G. L. Kane and S. Dawson, *The Higgs hunter’s guide*, Addison-Wesley, Menlo-Park, 1990; G. C. Branco, P. M. Ferreira, L. Lavoura, M. N. Rebelo, M. Sher and J. P. Silva, Phys. Rept. **516**, 1 (2012).
- [44] M. S. Carena and H. E. Haber, Prog. Part. Nucl. Phys. **50**, 63 (2003); A. Djouadi, Phys. Rept. **459**, 1 (2008).
- [45] D. B. Kaplan, H. Georgi and S. Dimopoulos, Phys. Lett. **B136**, 187 (1984); K. Agashe, R. Contino and A. Pomarol, Nucl. Phys. **B719**, 165–187 (2005); G. Burdman and C. E. F. Haluch, JHEP **12**, 038 (2011).
- [46] for a useful review see e.g. M. Schmaltz and D. Tucker-Smith, Ann. Rev. Nucl. Part. Sci. **55**, 229–270 (2005); M. Perelstein, Prog. Part. Nucl. Phys. **58**, 247–291 (2007).
- [47] for a useful review see e.g. J. F. Gunion and H. E. Haber, Phys. Rev. **D72**, 095002 (2005); P. M. Ferreira, H. E. Haber, M. Maniatis, O. Nachtmann and J. P. Silva, Int. J. Mod. Phys. **A26**, 769–808 (2011).
- [48] E. Ma, Phys. Rev. **D73**, 077301 (2006).
- [49] S. Kanemura, Y. Okada and E. Senaha, Phys. Lett. **B606**, 361–366 (2005); J. M. Cline, K. Kainulainen and M. Trott, JHEP **1111**, 089 (2011); A. Tranberg and B. Wu, JHEP **1207**, 087 (2012); G. C. Dorsch, S. J. Huber and J. M. No, arXiv:1305.6610 [hep-ph]; C. Cheung and Y. Zhang, arXiv:1306.4321 [hep-ph].
- [50] J. -O. Gong, H. M. Lee and S. K. Kang, JHEP **1204**, 128 (2012).
- [51] M. Aoki *et al.*, Phys. Rev. **D84**, 055028 (2011); S. Chang, J. A. Evans and M. A. Luty, Phys. Rev. **D84**, 095030 (2011); A. Arhrib, C. -W. Chiang, D. K. Ghosh and R. Santos, Phys. Rev. D **85**, 115003 (2012); S. Kanemura, K. Tsumura and H. Yokoya, Phys. Rev. D **85**, 095001 (2012); W. Mader, J. -h. Park, G. M. Pruna, D. Stöckinger and A. Straessner, JHEP **1209**, 125 (2012); K. Tsumura, arXiv:1305.1754 [hep-ph]; R. V. Harlander, S. Liebler and T. Zirke, arXiv:1307.8122 [hep-ph].

- [52] P. M. Ferreira, R. Santos, M. Sher and J. P. Silva, Phys. Rev. D **85**, 077703 (2012).
- [53] P. M. Ferreira, R. Santos, M. Sher and J. P. Silva, Phys. Rev. **D85**, 035020 (2012). J. Chang, K. Cheung, P. -Y. Tseng and T. -C. Yuan, Phys. Rev. D **87**, 035008 (2013). A. Drozd, B. Grzadkowski, J. F. Gunion and Y. Jiang, JHEP **1305**, 072 (2013). S. Chang, S. K. Kang, J. -P. Lee, K. Y. Lee, S. C. Park and J. Song, JHEP **1305**, 075 (2013).
- [54] G. Burdman, C. E. F. Haluch and R. D. Matheus, Phys. Rev. D **85**, 095016 (2012).
- [55] A. Azatov, S. Chang, N. Craig and J. Galloway, Phys. Rev. D **86**, 075033 (2012).
- [56] D. S. M. Alves, P. J. Fox and N. J. Weiner, arXiv:1207.5499 [hep-ph]; H. S. Cheon and S. K. Kang, arXiv:1207.1083 [hep-ph]; C. -W. Chiang and K. Yagyu, arXiv:1303.0168 [hep-ph]; B. Grinstein and P. Uttayarat, arXiv:1304.0028 [hep-ph]; M. Krawczyk, D. Sokolowska and B. Swiezewska, arXiv:1303.7102 [hep-ph]; A. Barroso, P. M. Ferreira, R. Santos, M. Sher and J. P. Silva, arXiv:1304.5225 [hep-ph]. B. Coleppa, F. Kling and S. Su, arXiv:1305.0002 [hep-ph]; C. -Y. Chen, S. Dawson and M. Sher, arXiv:1305.1624 [hep-ph]; O. Eberhardt, U. Nierste and M. Wiebusch, arXiv:1305.1649 [hep-ph];
- [57] C. -Y. Chen and S. Dawson, Phys. Rev. D **87**, 055016 (2013); N. Craig, J. Galloway and S. Thomas, arXiv:1305.2424 [hep-ph]; G. Bélanger, B. Dumont, U. Ellwanger, J. F. Gunion and S. Kraml, arXiv:1306.2941 [hep-ph].
- [58] Y. Bai, V. Barger, L. L. Everett and G. Shaughnessy, Phys. Rev. D **87**, 115013 (2013); V. Barger, L. L. Everett, H. E. Logan and G. Shaughnessy, arXiv:1308.0052 [hep-ph].
- [59] A. Celis, V. Ilisie and A. Pich, JHEP **1307**, 053 (2013).
- [60] W. Altmannshofer, S. Gori and G. D. Kribs, Phys. Rev. D **86**, 115009 (2012).
- [61] N. G. Deshpande and E. Ma, Phys. Rev. D **18**, 2574 (1978); R. Barbieri, L. J. Hall and V. S. Rychkov, Phys. Rev. D **74**, 015007 (2006).
- [62] D. Majumdar and A. Ghosal, Mod. Phys. Lett. A **23**, 2011 (2008); L. López Honorez, E. Nezri, J. F. Oliver and M. H. G. Tytgat, JCAP **0702**, 028 (2007); M. Gustafsson, E. Lundstrom, L. Bergstrom and J. Edsjo, Phys. Rev. Lett. **99**, 041301 (2007); P. Agrawal, E. M. Dolle and C. A. Krenke, Phys. Rev. D **79**, 015015 (2009); E. Nezri, M. H. G. Tytgat and G. Vertongen, JCAP **0904**, 014 (2009); E. M. Dolle and S. Su, Phys. Rev. D **80**, 055012 (2009); C. Arina, F. -S. Ling and M. H. G. Tytgat, JCAP **0910**, 018 (2009); L. López-Honorez, T. Schwetz and J. Zupan, Phys. Lett. B **716**, 179 (2012); A. Goudelis, B. Herrmann and O. Stal, arXiv:1303.3010 [hep-ph];
- [63] A. W. El Kaffas, P. Osland and O. M. Ogreid, Phys. Rev. D **76**, 095001 (2007).
- [64] S. Su and B. Thomas, Phys. Rev. D **79**, 095014 (2009); M. Aoki, S. Kanemura, K. Tsumura and K. Yagyu, Phys. Rev. D **80**, 015017 (2009); S. Kanemura, Y. Okada, H. Taniguchi and K. Tsumura, Phys. Lett. B **704**, 303 (2011); F. Mahmoudi and T. Hurth, arXiv:1211.2796 [hep-ph].
- [65] H. Neufeld, W. Grimus, G. Ecker and , Int. J. Mod. Phys. A **3**, 603 (1988).
- [66] I. P. Ivanov, Phys. Rev. D **75**, 035001 (2007) [Erratum-ibid. D **76**, 039902 (2007)]; P. M. Ferreira, H. E. Haber and J. P. Silva, Phys. Rev. D **79**, 116004 (2009).
- [67] M. J. G. Veltman, Acta Phys. Polon. B **8**, 475 (1977).
- [68] M. E. Peskin and T. Takeuchi, Phys. Rev. Lett. **65**, 964 (1990) and Phys. Rev. D **46**, 381 (1992).
- [69] D. Toussaint, Phys. Rev. D **18**, 1626 (1978); J. M. Frère and J. A. M. Vermaseren, Z. Phys. C **19**, 63 (1983); S. Bertolini, Nucl. Phys. **B272**, 77 (1986); W. Grimus, L. Lavoura, O. M. Ogreid and P. Osland, J. Phys. **G35**, 075001 (2008); W. Hollik, Z. Phys. C **32**, 291 (1986) and Z. Phys. C **37**, 569 (1988); C. D. Froggatt, R. G. Moorhouse and I. G. Knowles, Phys. Rev. **D45**, 2471–2481 (1992); H. -J. He, N. Polonsky and S. -f. Su, Phys. Rev. D **64**, 053004 (2001); W. Grimus, L. Lavoura, O. Ogreid and P. Osland, Nucl. Phys. **B801**, 81–96 (2008).
- [70] [ALEPH and CDF and D0 and DELPHI and L3 and OPAL and SLD and LEP Electroweak Working Group and Tevatron Electroweak Working Group and SLD Electroweak and Heavy Flavour Groups

- Collaborations], arXiv:1012.2367 [hep-ex]; M. Baak, M. Goebel, J. Haller, A. Hoecker, D. Ludwig, K. Moenig, M. Schott and J. Stelzer, Eur. Phys. J. C **72**, 2003 (2012); J. Beringer et al. (Particle Data Group Collaboration), Phys. Rev. D **86**, 010001 (2012).
- [71] LEP Electroweak Working Group, <http://lepewwg.web.cern.ch/LEPEWWG/>.
 - [72] S. L. Glashow and S. Weinberg, Phys. Rev. D **15**, 1958 (1977).
 - [73] G. D'Ambrosio, G. F. Giudice, G. Isidori and A. Strumia, Nucl. Phys. B **645**, 155 (2002).
 - [74] A. Dery, A. Efrati, G. Hiller, Y. Hochberg and Y. Nir, arXiv:1304.6727 [hep-ph].
 - [75] A. Pich and P. Tuzón, Phys. Rev. D **80**, 091702 (2009).
 - [76] S. Davidson and H. E. Haber, Phys. Rev. D **72**, 035004 (2005) [Erratum-ibid. D **72**, 099902 (2005)].
 - [77] B. Aubert *et al.* [BABAR Collaboration], Phys. Rev. D **77**, 051103 (2008); E. Barberio *et al.* [Heavy Flavor Averaging Group Collaboration], arXiv:0808.1297 [hep-ex].
 - [78] J. P. Leveille, Nucl. Phys. B **137**, 63 (1978); H. E. Haber, G. L. Kane and T. Sterling, Nucl. Phys. B **161**, 493 (1979); S. M. Barr and A. Zee, Phys. Rev. Lett. **65**, 21 (1990) [Erratum-ibid. **65**, 2920 (1990)]; M. Krawczyk and J. Zochowski, Phys. Rev. D **55**, 6968 (1997); A. Dedes and H. E. Haber, JHEP **0105**, 006 (2001); D. Chang, W. -F. Chang, C. -H. Chou and W. -Y. Keung, Phys. Rev. D **63**, 091301 (2001); K. Cheung and O. C. W. Kong, Phys. Rev. D **68**, 053003 (2003).
 - [79] S. Schael *et al.* [ALEPH and DELPHI and L3 and OPAL and LEP Working Group for Higgs Boson Searches Collaborations], Eur. Phys. J. C **47**, 547 (2006); V. M. Abazov *et al.* [D0 Collaboration], Phys. Rev. Lett. **88**, 151803 (2002); A. Abulencia *et al.* [CDF Collaboration], Phys. Rev. Lett. **96**, 042003 (2006); S. Chatrchyan *et al.* [CMS Collaboration], JHEP **1207**, 143 (2012); G. Aad *et al.* [ATLAS Collaboration], JHEP **1206**, 039 (2012); CMS-PAS-HIG-12-050; ATLAS-CONF-2012-094.
 - [80] D. Eriksson, J. Rathsmann and O. Stål, Comput. Phys. Commun. **181**, 189–205 (2010).
 - [81] P. Bechtle, O. Brein, S. Heinemeyer, G. Weiglein and K. E. Williams, Comput. Phys. Commun. **181**, 138–167 (2010); P. Bechtle, O. Brein, S. Heinemeyer, G. Weiglein and K. E. Williams, Comput. Phys. Commun. **182**, 2605–2631 (2011).
 - [82] F. Mahmoudi, Comput. Phys. Commun. **178**, 745–754 (2008); F. Mahmoudi, Comput. Phys. Commun. **180**, 1579–1613 (2009).
 - [83] for a useful review see e.g. M. Maniatis, Int. J. Mod. Phys. A **25**, 3505 (2010); U. Ellwanger, C. Hugonie and A. M. Teixeira, Phys. Rept. **496**, 1 (2010).
 - [84] J. C. Pati and A. Salam, Phys. Rev. D **10**, 275 (1974) [Erratum-ibid. D **11**, 703 (1975)]; R. N. Mohapatra and J. C. Pati, Phys. Rev. D **11**, 2558 (1975); G. Senjanovic and R. N. Mohapatra, Phys. Rev. D **12**, 1502 (1975).
 - [85] A. Delgado, G. Nardini and M. Quirós, JHEP **1307**, 054 (2013).
 - [86] M. Aoki, S. Kanemura, M. Kikuchi and K. Yagyu, Phys. Rev. D **87**, 015012 (2013).
 - [87] B. Stech, arXiv:1012.6028 [hep-ph].
 - [88] M. Heikinheimo, A. Racioppi, M. Raidal and C. Spethmann, arXiv:1307.7146 [hep-ph].
 - [89] J. F. Gunion, Y. Jiang and S. Kraml, Phys. Rev. Lett. **110**, 051801 (2013).
 - [90] P. M. Ferreira, R. Santos, H. E. Haber and J. P. Silva, Phys. Rev. D **87**, 055009 (2013).
 - [91] J. F. Gunion, Y. Jiang and S. Kraml, Phys. Rev. D **86**, 071702 (2012); Y. Grossman, Z. 'e. Surujon and J. Zupan, JHEP **1303**, 176 (2013).
 - [92] H. Hüffel and G. Pocsik, Z. Phys. C **8**, 13 (1981); R. A. Flores and M. Sher, Annals Phys. **148**, 95 (1983); A. Boviér and D. Wyler, Phys. Lett. B **154**, 43 (1985); J. Maalampi, J. Sirkka and I. Vilja, Phys. Lett. B **265**, 371 (1991); D. Kominis and R. S. Chivukula, Phys. Lett. B **304**, 152 (1993).

- [93] K. S. Babu and E. Ma, Phys. Rev. D **31**, 2861 (1985) [Erratum-ibid. D **33**, 3471 (1986)]; A. J. Davies and G. C. Joshi, Phys. Rev. Lett. **58**, 1919 (1987).
- [94] B. M. Kastening, hep-ph/9307224; J. Velhinho, R. Santos and A. Barroso, Phys. Lett. B **322**, 213 (1994); S. Nie and M. Sher, Phys. Lett. B **449**, 89 (1999); P. M. Ferreira, R. Santos and A. Barroso, Phys. Lett. B **603**, 219 (2004) [Erratum-ibid. B **629**, 114 (2005)]; M. Maniatis, A. von Manteuffel, O. Nachtmann and F. Nagel, Eur. Phys. J. C **48**, 805 (2006); P. M. Ferreira and D. R. T. Jones, JHEP **0908**, 069 (2009).
- [95] M. Lindner, Z. Phys. C **31**, 295 (1986). M. Sher, Phys. Rept. **179**, 273 (1989). G. Kreyerhoff and R. Rodenberg, Phys. Lett. B **226**, 323 (1989); J. Freund, G. Kreyerhoff and R. Rodenberg, Phys. Lett. B **280**, 267 (1992).
- [96] G. Isidori, V. S. Rychkov, A. Strumia and N. Tetradis, Phys. Rev. D **77**, 025034 (2008); J. Ellis, J. R. Espinosa, G. F. Giudice, A. Hoecker and A. Riotto, Phys. Lett. B **679**, 369 (2009); J. Elias-Miró, J. R. Espinosa, G. F. Giudice, G. Isidori, A. Riotto and A. Strumia, Phys. Lett. B **709**, 222 (2012); G. Degrandi, S. Di Vita, J. Elias-Miró, J. R. Espinosa, G. F. Giudice, G. Isidori and A. Strumia, JHEP **1208**, 098 (2012); S. Alekhin, A. Djouadi and S. Moch, Phys. Lett. B **716**, 214 (2012); D. Buttazzo, G. Degrandi, P. P. Giardino, G. F. Giudice, F. Sala, A. Salvio and A. Strumia, arXiv:1307.3536 [hep-ph]; V. Branchina and E. Messina, arXiv:1307.5193 [hep-ph].
- [97] B. W. Lee, C. Quigg and H. B. Thacker, Phys. Rev. D **16**, 1519 (1977); B. W. Lee, C. Quigg and H. B. Thacker, Phys. Rev. Lett. **38**, 883 (1977).
- [98] R. Casalbuoni, D. Dominici, R. Gatto and C. Giunti, Phys. Lett. B **178**, 235 (1986); R. Casalbuoni, D. Dominici, F. Feruglio and R. Gatto, Nucl. Phys. B **299**, 117 (1988).
- [99] A. G. Akeroyd, A. Arhrib and E. -M. Naimi, Phys. Lett. B **490**, 119 (2000). S. Kanemura, T. Kubota and E. Takasugi, Phys. Lett. **B313**, 155–160 (1993); J. Maalampi, J. Sirkka and I. Vilja, Phys. Lett. **B265**, 371–376 (1991); A. G. Akeroyd, A. Arhrib and E.-M. Naimi, Phys. Lett. **B490**, 119–124 (2000); I. F. Ginzburg and I. P. Ivanov, Phys. Rev. **D72**, 115010 (2005); P. Osland, P. N. Pandita and L. Selbuz, Phys. Rev. **D78**, 015003 (2008).
- [100] J. F. Gunion and H. E. Haber, Phys. Rev. D **67**, 075019 (2003).
- [101] J. M. Cornwall, D. N. Levin and G. Tiktopoulos, Phys. Rev. Lett. **30**, 1268 (1973) [Erratum-ibid. **31**, 572 (1973)]; J. M. Cornwall, D. N. Levin and G. Tiktopoulos, Phys. Rev. D **10**, 1145 (1974) [Erratum-ibid. D **11**, 972 (1975)]; C. H. Llewellyn Smith, Phys. Lett. B **46**, 233 (1973); H. A. Weldon, Phys. Lett. B **146**, 59 (1984) and Phys. Rev. D **30**, 1547 (1984); J. F. Gunion, H. E. Haber and J. Wudka, Phys. Rev. D **43**, 904 (1991).
- [102] S. Kanemura, T. Kasai and Y. Okada, Phys. Lett. B **471**, 182 (1999).
- [103] T. P. Cheng, E. Eichten and L. -F. Li, Phys. Rev. D **9**, 2259 (1974); M. E. Machacek and M. T. Vaughn, Nucl. Phys. B **249**, 70 (1985); H. E. Haber and R. Hempfling, Phys. Rev. D **48**, 4280 (1993).
- [104] P. M. Ferreira and D. R. T. Jones, JHEP **0908**, 069 (2009).
- [105] G. D. Kribs, T. Plehn, M. Spannowsky and T. M. P. Tait, Phys. Rev. D **76**, 075016 (2007).
- [106] G. Ferrera, J. Guasch, D. López-Val and J. Solà, Phys. Lett. **B659**, 297–307 (2008), A. Arhrib, R. Benbrik and C.-W. Chiang, Phys. Rev. **D77**, 115013 (2008); R. N. Hodgkinson, D. López-Val and J. Solà, Phys. Lett. **B673**, 47–56 (2009); F. Cornet and W. Hollik, Phys. Lett. **B669**, 58–61 (2008); E. Asakawa, D. Harada, S. Kanemura, Y. Okada and K. Tsumura, Phys. Lett. **B672**, 354–360 (2009); N. Bernal, D. López-Val and J. Solà, Phys. Lett. **B677**, 39–47 (2009); A. Arhrib, R. Benbrik, C.-H. Chen and R. Santos, Phys. Rev. **D80**, 015010 (2009); D. López-Val, J. Solà and N. Bernal, Phys. Rev. **D81**, 113005 (2010); E. Asakawa, D. Harada, S. Kanemura, Y. Okada and K. Tsumura, Phys. Rev. **D82**, 115002 (2010); J. Solà and D. López-Val, Fortsch. Phys. **58**, 660–664 (2010); D. López-Val and J. Solà, Phys. Lett. **B702**, 246–255 (2011); D. López-Val and J. Solà, Eur. Phys. J. C **73**, 2393 (2013).
- [107] T. Appelquist and J. Carazzone, Phys. Rev. D **11**, 2856 (1975).

- [108] J. Elias-Miró, J. R. Espinosa, G. F. Giudice, H. M. Lee and A. Strumia, JHEP **1206**, 031 (2012).
- [109] A. Arhrib, W. Hollik, S. Peñaranda and M. Capdequi Peyranère, Phys. Lett. B **579**, 361 (2004); M. Malinsky and J. Horejsi, Eur. Phys. J. C **34**, 477 (2004); and Eur. Phys. J. C **40**, 137 (2005); S. Kanemura, S. Kiyoura, Y. Okada, E. Senaha and C. P. Yuan, Phys. Lett. B **558**, 157 (2003); M. Krawczyk and D. Temes, Eur. Phys. J. C **44**, 435 (2005); S. Kanemura, Y. Okada, E. Senaha and C. -P. Yuan, Phys. Rev. D **70**, 115002 (2004); S. Kanemura, Y. Okada and E. Senaha, Phys. Lett. B **606**, 361 (2005).
- [110] D. López-Val and J. Solà, Phys. Rev. D **81**, 033003 (2010).
- [111] T. Hahn, Comput. Phys. Commun. **140**, 418 (2001); T. Hahn and M. Pérez-Victoria, Comput. Phys. Commun. **118**, 153 (1999); T. Hahn and C. Schappacher, Comput. Phys. Commun. **143**, 54 (2002); T. Hahn and M. Rauch, Nucl. Phys. Proc. Suppl. **157**, 236 (2006).
- [112] S. Kanemura, S. Matsumoto, T. Nabeshima and H. Taniguchi, Phys. Lett. B **701**, 591 (2011); A. Djouadi, O. Lebedev, Y. Mambrini and J. Quevillon, Phys. Lett. B **709**, 65 (2012); S. K. Garg and C. S. Kim, arXiv:1305.4712 [hep-ph]; X. Chu, Y. Mambrini, Jrm. Quevillon and B. Zaldivar, arXiv:1306.4677 [hep-ph].
- [113] L. G. Almeida, E. Bertuzzo, P. A. N. Machado and R. Z. Funchal, JHEP **1211**, 085 (2012); A. Joglekar, P. Schwaller and C. E. M. Wagner, JHEP **1212**, 064 (2012); P. Schwaller, T. M. P. Tait and R. Vega-Morales, arXiv:1305.1108 [hep-ph].
- [114] A. Djouadi and A. Lenz, Phys. Lett. B **715**, 310 (2012); E. Kuflik, Y. Nir and T. Volansky, arXiv:1204.1975 [hep-ph]; O. Eberhardt, G. Herbert, H. Lacker, A. Lenz, A. Menzel, U. Nierste and M. Wiebusch, Phys. Rev. Lett. **109**, 241802 (2012).
- [115] L. J. Hall, R. Rattazzi and U. Sarid, Phys. Rev. D **50**, 7048 (1994); M. S. Carena, M. Olechowski, S. Pokorski and C. E. M. Wagner, Nucl. Phys. B **426**, 269 (1994).
- [116] M. S. Carena, D. Garcia, U. Nierste and C. E. M. Wagner, Nucl. Phys. B **577**, 88 (2000); M. S. Carena, D. Garcia, U. Nierste and C. E. M. Wagner, Phys. Lett. B **499**, 141 (2001).
- [117] R. Lafaye, T. Plehn, M. Rauch and D. Zerwas, Eur. Phys. J. C **54**, 617 (2008).
- [118] R. S. Gupta, H. Rzehak and J. D. Wells, Phys. Rev. D **86**, 095001 (2012).
- [119] B. Patt and F. Wilczek, hep-ph/0605188; R. Schabinger and J. D. Wells, Phys. Rev. D **72**, 093007 (2005); R. S. Gupta and J. D. Wells, Phys. Lett. B **710**, 154 (2012).
- [120] S. Heinemeyer, Int. J. Mod. Phys. A **21**, 2659 (2006); M. Frank, T. Hahn, S. Heinemeyer, W. Hollik, H. Rzehak and G. Weiglein, JHEP **0702**, 047 (2007).
- [121] L. Randall, JHEP **0802**, 084 (2008); K. Blum and R. T. D’Agnolo, Phys. Lett. B **714**, 66 (2012).